

**Molecular Characterisation of three Novel
Photosynthetic Proteins in *Arabidopsis
thaliana***

Dissertation

zur Erlangung des Doktorgrades der Fakultät für Biologie
der Ludwig-Maximilians-Universität München

Vorgelegt von
Ute Armbruster
aus Kleve

München
Mai 2008

Erstgutachter: Prof. Dr. Dario Leister
Zweitgutachter: Prof. Dr. Jörg Nickelsen
Tag der mündlichen Prüfung: 26.05.2008

Summary

Photosynthesis is the biological process, in which organisms utilize light energy in order to synthesize organic matter. In plants this process takes place in the chloroplast. Nuclear photosynthetic genes and nuclear genes involved in chloroplast gene expression are co-regulated at the transcriptional level. Therefore, the working hypothesis was put forth that the physiological function of genes with so-far unknown functions, which show a similar transcriptional regulation, resides in photosynthesis or chloroplast gene expression. To test this hypothesis, three co-regulated genes with so-far unknown physiological functions were analysed employing a reverse genetics strategy and biochemical analyses of the encoded proteins. Insertional mutants for the genes encoding the Putative Photosynthetic Protein 1 (PPP1), 4 (PPP4) and the Thylakoid Membrane Phosphoprotein of 14 kDa (TMP14) were characterised with respect to putative defects in the processes of photosynthesis or chloroplast gene expression. Both PPP4 and TMP14 belong to a novel, nucleus encoded and chloroplast targeted family of four membrane proteins in *Arabidopsis*. They functionally and physically interact in a previously unknown complex in the stromal lamellae of thylakoid membranes, which can be solubilised with the detergent digitonin. Several lines of biochemical evidence suggest that both proteins interact with other thylakoid proteins of unknown identity. Electron transport measurements of the single and the double mutants of *PPP4* and *TMP14* support that this new complex is indeed involved in the regulation of photosynthesis, especially under low light conditions. The assumed function for the stromal localised PPP1 as an RNA binding protein involved in chloroplast gene expression was investigated by analyses of plastid gene expression in *ppp1* mutant plants. Here, decreased levels of chloroplast proteins and changes in plastid translation rate could be demonstrated. This was accompanied by alterations in the photosynthetic electron transport. Additionally, it was shown that plants lacking PPP1 show delayed germination in response to the exogenous application of the phytohormone ABA, which indicates a function of this protein in the ABA signalling network.

Zusammenfassung

Photosynthese beschreibt den biologischen Prozess der Umwandlung von Licht in chemische Energie, und deren Nutzung zur Synthese organischen Materials. Bei Pflanzen findet dieser Prozess im Chloroplasten statt. Nukleäre Gene, welche Komponenten der Photosynthese oder der plastidären Genexpression kodieren, werden auf transkriptioneller Ebene ko-reguliert. Daher wurden drei als unbekannt annotierte Gene mit ähnlicher transkriptioneller Regulation und ihre Genprodukte, „Putative Photosynthetic Protein“ 1 (PPP1) und 4 (PPP4) und „Thylakoidmembran Phosphoprotein 14 kDa“ (TMP14) auf eine mögliche Funktion in der Photosynthese und der plastidären Genexpression hin untersucht. Die Charakterisierung dieser putativen neuen Photosynthese-Komponenten erfolgte mittels reverser Genetik und biochemischer Analysen. PPP4 und TMP14 gehören zu einer kernkodierten und chloroplastidär lokalisierten Familie von Membranproteinen mit vier Mitgliedern in *Arabidopsis*. Beide Proteine interagieren in einem bislang unbekanntem Komplex in den stromalen Lamellen der Thylakoidmembran sowohl auf Proteinebene als auch funktionell. Mehrere unabhängige biochemische Untersuchungen implizieren, dass PPP4 und TMP14 mit weiteren Thylakoidproteinen bislang unbekannter Identität interagieren. Messungen des photosynthetischen Elektronentransports bei Einfach- und Doppelmutanten weisen vor allem unter niedrigen Lichtbedingungen auf eine Funktion dieses neuen Komplexes in der Photosynthese hin. Das dritte Protein PPP1 ist im Stroma lokalisiert und wurde mittels Analyse der plastidären Genexpression in der *ppp1* Mutante auf eine putative Funktion in diesem Prozess hin untersucht. Dabei konnte gezeigt werden, dass die Mutanten verringerte Mengen an Chloroplasten-Proteinen und veränderte plastidäre Translationsraten aufweisen. Damit einhergehend weisen die *ppp1* Mutanten Veränderungen im photosynthetischen Elektronenfluss auf. Zusätzlich konnte gezeigt werden, dass bei exogener Zugabe des Phytohormons ABA die *ppp1* Mutanten verzögerte Keimung aufweisen, welches auf eine Funktion des Proteins in dem ABA Signal-Netzwerk hindeutet.

Contents

| | |
|--|-----------|
| Summary | i |
| Zusammenfassung | ii |
| Contents | iii |
| Abbreviations | vii |
| 1 Introduction..... | 1 |
| 1.1 Photosynthesis..... | 1 |
| 1.1.1 Photosynthetic electron transport | 1 |
| 1.1.1.1 Linear electron transport | 1 |
| 1.1.1.2 Cyclic electron transport around PSI..... | 2 |
| 1.1.1.3 Physical measurements of electron transport | 4 |
| 1.1.2 Carbon fixation..... | 4 |
| 1.1.3 The thylakoid membrane..... | 5 |
| 1.1.3.1 The thylakoid polypeptide composition | 6 |
| 1.1.4 Regulation of photosynthetic processes | 8 |
| 1.1.4.1 Energisation dependent non-photochemical quenching (qE)..... | 8 |
| 1.1.4.2 State transitions | 9 |
| 1.2 Expression of photosynthetic genes | 9 |
| 1.2.1 Nuclear gene expression..... | 10 |
| 1.2.1 Chloroplast gene expression..... | 11 |
| 1.3 Abscisic acid (ABA) biosynthesis in plants | 11 |
| 1.4 Aims of thesis | 12 |
| 2 Materials and Methods | 14 |
| 2.1 Materials..... | 14 |
| 2.1.1 Chemicals | 14 |
| 2.1.2 Antibiotics | 14 |
| 2.1.3 Enzymes, kits and biochemical agents | 14 |
| 2.1.4 Membranes | 14 |
| 2.1.5 Antibodies | 14 |
| 2.2 Methods | 15 |
| 2.2.1 Plant lines and propagation | 15 |

| | |
|--|----|
| 2.2.2 Nucleic acid analysis..... | 15 |
| 2.2.2.1 DNA analysis | 15 |
| 2.2.2.2 RNA analysis..... | 17 |
| 2.2.2.3 Analysis of mRNAs associated with polysomes..... | 17 |
| 2.2.2.4 Transcript end mapping of <i>rbcL</i> using circular RT-PCR..... | 18 |
| 2.2.3 Transformation of <i>Arabidopsis</i> | 18 |
| 2.2.3.1. Bacterial strains | 18 |
| 2.2.3.2 Agrobacterium binary vectors | 18 |
| 2.2.3.3 <i>Agrobacterium</i> -mediated transformation of <i>A. thaliana</i> | 19 |
| 2.2.4 Biochemical Analysis..... | 19 |
| 2.2.4.1 Antibody production..... | 19 |
| 2.2.4.2 SDS-PAGE..... | 19 |
| 2.2.4.3 Immunoblot analysis | 19 |
| 2.2.4.4 Total protein isolation | 20 |
| 2.2.4.5 Isolation of intact chloroplasts | 20 |
| 2.2.4.6 Fractionation of chloroplasts..... | 20 |
| 2.2.4.7 Preparation of thylakoid membranes..... | 20 |
| 2.2.4.8 Fractionation of thylakoids..... | 21 |
| 2.2.4.9 PSI isolation | 21 |
| 2.2.4.10 Blue native and second dimension gels..... | 21 |
| 2.2.4.11 Bis (Sulfosuccinimidyl) suberate (BS ³) crosslinking..... | 22 |
| 2.2.4.12 Co-Immunoprecipitation | 22 |
| 2.2.4.13 Salt treatment of thylakoid membranes..... | 22 |
| 2.2.4.14 Trypsin treatment of thylakoid membranes..... | 23 |
| 2.2.4.15 <i>In vivo</i> labelling with ³⁵ S-Methionine | 23 |
| 2.2.5 Mass spectrometry..... | 23 |
| 2.2.5.1 Tryptic in gel digestion of proteins | 23 |
| 2.2.5.2 LC-ESI MS/MS..... | 24 |
| 2.2.5.3 Protein identification | 24 |
| 2.2.6 Pigment analysis..... | 24 |
| 2.2.7 Database analysis, Digital Northern, prediction of subcellular targeting and protein modelling..... | 25 |
| 2.2.8 Intracellular localization of dsRED fusions | 25 |

| | |
|---|-----------|
| 2.2.9 Germination assay | 26 |
| 2.2.10 Determination of photosynthetic parameters using the PAM fluorometer | 26 |
| 2.2.10.1 Chlorophyll fluorescence measurements..... | 26 |
| 2.2.10.2 Measurements of the redox state of P700 | 26 |
| 2.2.10.3 Cyclic electron flow measurements | 27 |
| 3 Results | 28 |
| 3.1 Characterisation of PPP4 and TMP14 | 28 |
| 3.1.1 Description of a novel protein family in photosynthetic organisms | 28 |
| 3.1.2 Localisation of PPP4 and TMP14 in the thylakoid membrane | 31 |
| 3.1.3 Knock-out mutants of <i>PPP4</i> and <i>TMP14</i> | 32 |
| 3.1.4 Localisation of PPP4 in BN-PAGE..... | 34 |
| 3.1.5 TMP14 protein levels are decreased in <i>ppp4</i> mutants..... | 37 |
| 3.1.6 Investigating the interaction between PPP4 and TMP14 | 37 |
| 3.1.6.1 Epitope tagging of PPP4..... | 37 |
| 3.1.6.2 Crosslinking..... | 38 |
| 3.1.6.3 Co-immunoprecipitation (Co-IP)..... | 41 |
| 3.1.7 TMP14 and PPP4 are not stably associated with any of the main photosynthetic complexes | 43 |
| 3.1.8 Photosynthetic parameter of WT, <i>ppp4</i> , <i>tmp14</i> , <i>ppp4 tmp14</i> and PPP4:c-myc overexpressors | 45 |
| 3.1.9 Topology of PPP4 and TMP14 | 49 |
| 3.1.10 Analysis of thylakoid protein composition | 52 |
| 3.1.11 Location of thylakoid proteins in WT and <i>ppp4 tmp14</i> | 53 |
| 3.1.12 Investigating phosphorylation of thylakoid proteins in WT and <i>ppp4 tmp14</i> | 55 |
| 3.1.13 Characterisation of PPP4-like and TMP14-like | 55 |
| 3.2 Characterisation of PPP1 | 58 |
| 3.2.1 Gene expression, protein structure and localisation..... | 58 |
| 3.2.2 Phenotypical analysis of knock-out mutants of <i>PPP1</i> and <i>CSP41</i> | 60 |
| 3.2.3 Leaf pigments and photosynthetic parameters | 62 |
| 3.2.4 Analysis of the abundance of photosynthetic proteins..... | 65 |
| 3.2.5 Chloroplast expression analysis | 67 |
| 3.2.6 Analysis of transcript processing | 68 |
| 3.2.7 Effect of the absence of photosynthetic complexes on PPP1 abundance..... | 70 |

| | |
|---|------------|
| 3.2.8 A PPP1:CFP fusion complements the <i>ppp1</i> mutant phenotype | 70 |
| 3.2.9 Germination assay | 71 |
| 4 Discussion | 73 |
| 4.1 PPP4/TMP14..... | 73 |
| 4.1.1 Novel family of chloroplast localised proteins..... | 73 |
| 4.1.2 A novel thylakoid complex predominantly localised in the stromal lamellae | 73 |
| 4.1.3 Phenotype of <i>ppp4</i> and <i>ppp4 tmp14</i> mutants in relation to specific processes of photosynthesis | 75 |
| 4.1.3.1 Linear electron flow | 75 |
| 4.1.3.2 Regulatory processes in photosynthesis..... | 76 |
| 4.1.3.3 Cyclic electron flow around PSI (CEF) | 77 |
| 4.1.3.3.1 In-depth analysis of CEF in <i>ppp4</i> and <i>ppp4 tmp14</i> mutants | 79 |
| 4.1.3.3.2 Speculation about an involvement of PPP4 and TMP14 in CEF processes..... | 80 |
| 4.1.4 Conclusions | 81 |
| 4.2 The putative RNA-binding protein PPP1 | 82 |
| 4.2.1 Physiological role: Chloroplast gene expression..... | 82 |
| 4.2.2 The homologue AtCSP41..... | 84 |
| 4.2.3 Involvement of PPP1 in ABA signalling | 84 |
| 5 References..... | 87 |
| 6 Supplementary Data..... | 101 |
| 6.1 Mass spectrometry fragmentation spectra..... | 101 |
| 6.1.1 PPP4 | 101 |
| 6.1.2 TMP14..... | 103 |
| 6.1.3 TMP14-like | 104 |
| 6.2 Plastome expression analysis of <i>ppp1</i> mutants..... | 105 |
| <i>Acknowledgements</i> | 106 |
| <i>Curriculum vitae</i> | 107 |
| Ehrenwörtliche Versicherung..... | 109 |

Abbreviations

| | |
|---------------------------|--|
| Φ_{II} | Effective quantum yield of PSII |
| °C | Degree celsius |
| ABA | Abscisic acid |
| ABI4 | ABA insensitive 4 |
| ATP | Adenine triphosphate |
| Auto | Autofluorescence |
| β -Car | β -carotene |
| β -DM | β -dodecylmaltoside |
| BN gel | Blue native gel |
| BS ³ | Bis (Sulfosuccinimidyl) suberate |
| C-terminus | Carboxy terminus |
| Ci | Curie |
| cDNA | Complementary deoxyribonucleic acid |
| CEF | Cyclic electron flow |
| CFP | Cyan fluorescent protein |
| Chl | Chlorophyll |
| Co-IP | Co-immunoprecipitation |
| Col-0 | <i>Arabidopsis</i> ecotype Columbia |
| CSP41 | Chloroplast stem loop binding protein 41 kDa |
| Cyt <i>b₆f</i> | Cytochrome <i>b₆f</i> complex |
| D | Dark |
| Da | Dalton |
| DNA | Deoxyribonucleic acid |
| EDTA | Ethylene diamine tetraacetic acid |
| EGTA | Ethylene glycol tetraacetic acid |
| ETR | Electron transport rate |
| Fd | Ferredoxin |
| FNR | Ferredoxin NADPH dehydrogenase |
| FR | Far-red light |
| HA | Hemagglutinin |
| HL | High light |
| g | Gram |
| <i>g</i> | Times the force of gravity |
| h | Hour |
| HEPES | 4-(2-hydroxyethyl)-1-piperazineethanesulfonic acid |
| HPLC | High performance liquid chromatography |
| IgG | Immunoglobulin G |
| k | Kilo |
| LB | left T-DNA border |
| LEF | Linear electron flow |
| <i>Ler</i> | <i>Arabidopsis</i> ecotype Landsberg <i>erecta</i> |
| LHC | Light harvesting complex |
| LL | Low light |
| μ | Micro |
| m | Meter |
| M | Mole(s) per litre |
| min | Minute(s) |

| | |
|------------------|---|
| mol | Mole |
| MS | Mass spectrometry |
| N-terminus | Amino terminus |
| NADP(H) | Nicotinamide adenine dinucleotide phosphate |
| NDH | NAD(P)H dehydrogenase complex |
| No-0 | <i>Arabidopsis</i> ecotype Noessen-0 |
| NPQ | Non-photochemical quenching |
| Nx | Neoxanthin |
| P680 | Reaction center of PSII |
| P700 | Reaction center of PSI |
| PAGE | Polyacrylamide gel electrophoresis |
| PAM | Pulse amplitude modulation |
| PAR | Photosynthetic active radiation |
| PCR | Polymerase chain reaction |
| pers. com. | Personal communication |
| PGR5 | Proton gradient defective 5 |
| PGRL1 | PGR5 like 1 |
| PMSF | Phenylmethanesulphonylfluoride |
| PPP1/4 | Putative photosynthetic protein 1/4 |
| PSI | Photosystem I |
| PSII | Photosystem II |
| PQ | Plastoquinone |
| PQH ₂ | Plastohydroquinone |
| PVDF | Polyvinylidene difluoride |
| qE | Δ pH-dependent NPQ |
| qP | Photochemical quenching |
| RB | Right T-DNA border |
| RFP | Red fluorescent protein |
| RNA | Ribonucleic acid |
| Rubisco | Ribulose biphosphate carboxylase/ oxygenase |
| r.u. | Relative units |
| s | Second(s) |
| SD | Standard deviation |
| SDR | Short chain dehydrogenase reductase |
| SDS | Sodium dodecyl sulphate |
| TMP14 | Thylakoid membrane protein 14 kDa |
| Tris | Tris(hydroxymethyl)-aminomethane |
| v/v | Volume per volume |
| VAZ | Violaxanthin, antheraxanthin, zeaxanthin (Xanthophyll cycle pigments) |
| VDE | Violaxanthin-deepoxidase |
| w/v | Weight per volume |
| WS | <i>Arabidopsis</i> ecotype wassilewskija |
| WT | Wild-type |
| ZEP | Zeaxanthin epoxidase |

1 Introduction

1.1 Photosynthesis

During photosynthesis light energy is transformed into chemical energy in form of NADPH and ATP, which are then employed by the Calvin-Benson cycle to incorporate atmospheric carbon into the biosphere. The highly optimised light reaction of photosynthesis, as it has evolved in plants, takes place in the thylakoid membranes of the chloroplast. The concerted action of four large membrane complexes, the Photosystems I and II (PSI and PSII), the Cytochrome *b₆f* complex (Cyt *b₆f*) and an ATP-synthase to conduct the transformation of light into chemical energy has been studied thoroughly by spectroscopy, molecular genetics, biochemistry and structural analyses (reviewed by Jensen *et al.*, 2007; Dekker and Boekema, 2005; Richter *et al.*, 2005). Important for optimal photosynthetic activity are the spatial organisation of the photosynthetic apparatus and various regulatory processes fine-tuning and adjusting this process.

1.1.1 Photosynthetic electron transport

Electron flow from water to the final electron acceptor NADPH is referred to as linear electron transport. This process also leads to the phosphorylation of ADP to ATP via the generation of a proton gradient across the thylakoid membrane. The cyclic electron flow around PSI, which generates ATP without accumulation of the final electron acceptor NADPH can adjust the ATP:NADPH ratio according to the requirements of the Calvin-Benson cycle and other chloroplast localised physiological processes for.

1.1.1.1 Linear electron transport

The primary step in oxygenic photosynthesis consists of light driven charge separations, which are catalysed by two large transmembrane protein complexes, PSI and PSII. These two photosystems synergistically interact by a number of redox components including plastoquinone, the Cyt *b₆f* complex and plastocyanin. Thereby, light energy is converted into chemical energy in form of NADPH and ATP. Synthesis of the latter occurs by the ATP-synthase, which employs physical energy conserved by the transmembrane proton gradient, a product of light driven proton electron symport. Linear electron flow from PSII to PSI occurs according to the so-called Z-scheme, which refers to the midpoint redox potentials of the redox carriers within this electron transport chain (**Figure 1.1**). In detail, light-induced charge separations in PSII, which acts as a water-plastoquinone oxidoreductase (Renger and Govindjee, 1985), cause the reduction of a stromal side

bound quinone acceptors (Q_A) via rapid oxido-reductions of a phaeophytin molecule. The resulting electron gaps in the reaction centre special pair chlorophylls lead to the oxidation of H_2O molecules by the luminal oxygen evolving complex producing molecular oxygen and protons as by-products (Cruz *et al.*, 2005). Two electrons from the PSII acceptor Q_A and two stromal localised protons are then transferred to a free membrane soluble plastoquinone molecule (PQ) to form plastohydroquinol (PQH_2). Electron flow from the PQH_2 pool to PSI occurs via the Cyt b_6f complex by reduction of the Rieske iron-sulphur protein of this complex and release of protons into the lumen (Joliot and Joliot, 1986). Optimisation of proton translocation occurs via the Cyt b_6f localised Q-cycle, in which one electron from PQH_2 is employed to again reduce a molecule of PQ on the stromal side of the Cyt b_6f complex (Joliot and Joliot, 1994). The second electron is transported to the lumen-localised electron carrier plastocyanin, which then transfers the electrons to the stromal acceptor site of PSI. Here, light energy drives a further charge separation that leads to the reduction of ferredoxin and then, catalysed by the ferredoxin: NADPH oxidoreductase (FNR), of $NADP^+$ to NADPH (Taiz and Zeiger, 1998).

1.1.1.2 Cyclic electron transport around PSI

In this pathway stromal electron acceptors from PSI are employed to reduce plastoquinone resulting in the generation of ΔpH without the accumulation of NADPH (dashed line, **Figure 1.1**; reviewed by Shikanai, 2007). There are two pathways carrying out this process: the antimycin A sensitive, which requires PGR5 and PGRL1 (Munekage *et al.*, 2002; DalCorso *et al.*, 2008) and the NADH dehydrogenase (NDH) complex dependent one. Cyclic electron flow (CEF) participates in regulatory processes of photosynthesis, which require additional acidification of the lumen or ATP by this pathway. The activation of the Calvin-Benson cycle enzymes by ATP after a dark period for example is accelerated by CEF (Joliot and Joliot, 2002). The extent of non-photochemical quenching (NPQ) of excess light energy also depends on additional acidification of the lumen by cyclic electron transport. Both processes, as measured by the NPQ capacity of the plant under the respective conditions, are impaired in the *pgr5* and *pgrl1* mutants (Munekage *et al.*, 2002; Dal Corso *et al.*, 2008). However, cyclic electron flow around PSI might not be restricted to carry out fine-tuning functions, because if plants lack both the PGR5/ PGRL1 and NDH dependent pathways, they are severely affected in growth and photosynthetic parameters in all conditions tested. This led to the assumption that CEF is mandatory for plant fitness (Munekage *et al.*, 2004), probably because the ATP:NADPH ratio produced by linear electron flow does not meet the requirements for carbon fixation by the Benson-Calvin-cycle and other chloroplast localised physiological processes. The antimycin A sensitive CEF seems to carry out the majority of Fd-PQ

reduction, because mutants in this pathway contrary to those impaired in NDH activity, show significant changes in photosynthetic parameters (Munekage *et al.*, 2002; DalCorso *et al.*, 2008; Muraoka *et al.*, 2006; Munshi *et al.*, 2006; Kamruzzaman *et al.*, 2005). However, the executing components of the antimycin A sensitive pathway are not completely deciphered, as the involved proteins lack binding domains for electron transferring co-factors (DalCorso *et al.*, 2008).

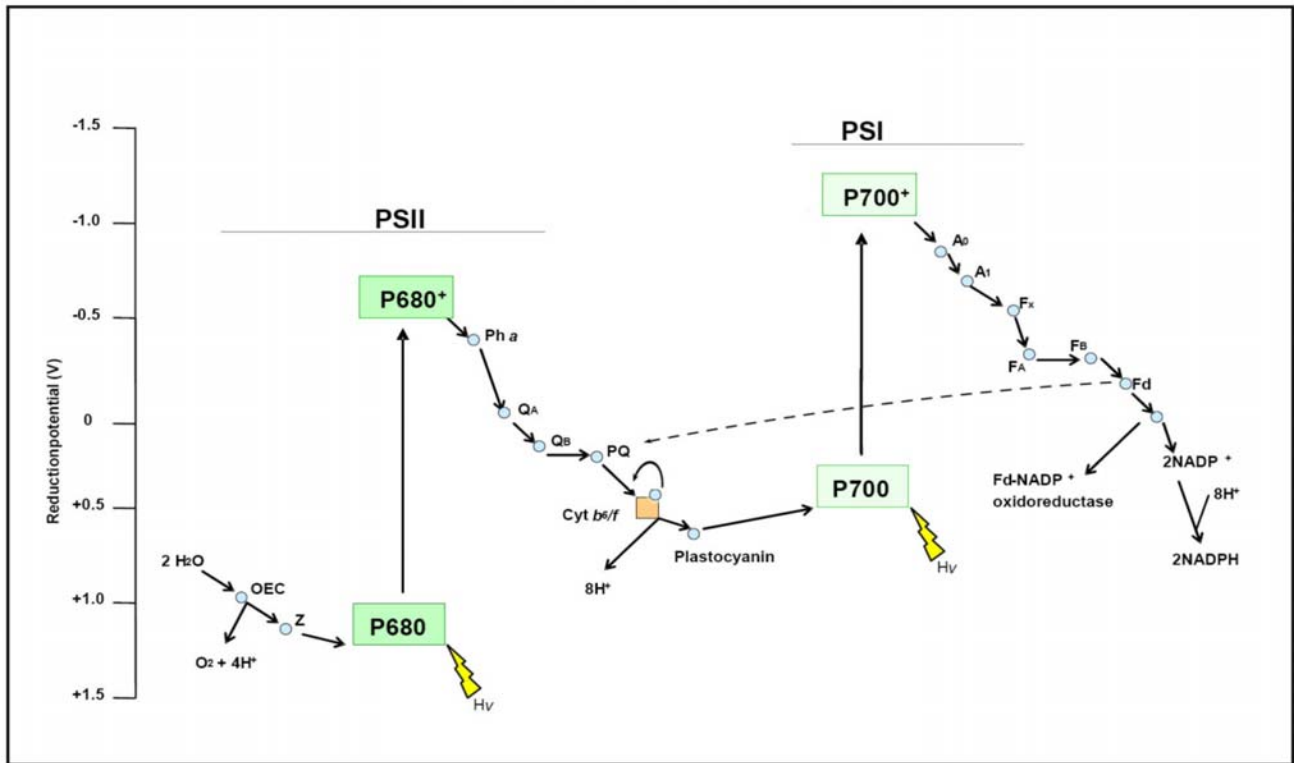


Fig. 1.1 Z-scheme of linear electron flow in oxygenic photosynthesis

Redox carriers are placed at their midpoint redox potentials (at pH 7). The vertical arrows display the light induced decrease of redoxpotential of the reaction centre chlorophylls. Z, electron donor to P680; Ph *a*, pheophytin *a*, electron acceptor of P680; QA, plastoquinone tightly bound to PSII; QB, pool made up of PQ and PQH₂; A₀, chlorophyll *a*, the primary electron acceptor of PSI; A₁, phyloquinone; F_x, F_B and F_A, iron sulphur clusters; Fd, soluble ferredoxin; NADP⁺, oxidised nicotinamide adenine dinucleotide phosphate. Dashed line indicates cyclic electron flow around PSI (CEF).

Because both linear electron flow (LEF) and the CEF around PSI employ identical components except for PGR5 and PGRL1 (Munekage *et al.*, 2002; DalCorso *et al.*, 2008), the specific dissection of both pathways remains difficult to achieve (Breyton *et al.*, 2006). Different models of the mode of action and regulation of CEF have been postulated, which are in part supported by experimental evidences (Okegawa *et al.*, 2005; Joliot and Joliot, 2002; DalCorso *et al.*, 2008). Highly controversial remains the question whether Fd directly reduces PQ or indirectly through reduction of component of the Cyt *b₆f* complex. The FNR has been found associated with the Cyt *b₆f* complex in flowering plants and is thought to reduce Fd in order to activate CEF via the Q-cycle of this complex (Zhang *et al.*, 2001; Joliot and Joliot, 2002). However Okegawa and co-workers showed that an impaired Q-cycle does not interfere with PGR5 mediated CEF (2005). The latest results

stem from the identification of PGRL1 as a mandatory component of CEF, which interacts with PSI, Cyt *b₆f*, FNR and Fd and is indispensable for the accumulation of PGR5 (DalCorso *et al.*, 2008).

Whereas in the process of CEF around PSI, where electrons fed into the PQ pool are then employed for reduction of PSI, they can also be used to reduce oxygen in a process referred to as chloro-respiration, which is postulated to occur especially at higher light intensities and to function as a safety valve to prevent over-reduction of the stroma (Rosso *et al.*, 2006).

1.1.1.3 Physical measurements of electron transport

Chlorophyll *a* (Chl *a*) fluorescence is widely used as an indicator for light-driven electron transport. Because the oxidised state of the reaction centre of PSI (P700⁺) is much longer lived than that of PSII (P680⁺), with the oxidised states of the photosystems being quenchers of excitons, most measurable fluorescence is coming from the PSII associated Chl *a* molecules. The energy of the light induced excitation states of chlorophyll molecules can be transferred to three competing pathways, which are the photochemical charge separation, the release of heat and fluorescence. As such the efficiency of energy consumption by photochemistry and heat at a given state can be measured reciprocally by determining Chl *a* fluorescence (Clayton, 1980). Maximum fluorescence can be measured during a very strong light pulse that saturates reduction of PSII acceptors after dark adaption of the plant, as heat dissipation of energy is then negligible. Light induced changes in photochemistry and heat dissipation can then be estimated from measuring Chl *a* fluorescence during the application of further saturating light pulses to light adapted plants. To quantify this fluorescence, the Pulse Amplitude Modulation (PAM) fluorometer system has been designed (Schreiber *et al.*, 1986). This instrument can additionally be used for recording P700 oxidation (Schreiber *et al.*, 1988). Thereby, the activity of both photosystems as well as the reduction/oxidation state of inter-chain electron carriers and stromal acceptors can be estimated.

1.1.2 Carbon fixation

Carbon dioxide fixation occurs in the Calvin-Benson cycle, which consists of three stages, (i) the carboxylation of ribulose-1,5-bisphosphate, forming two molecules of 3-phosphoglycerate, (ii) their reduction to glyceraldehyde-3-phosphate, the carbohydrates forming module and (iii) the regeneration of ribulose-1,5-bisphosphate. In total, this reaction requires 2 NADPH and 3 ATP for the fixation of one carbon dioxide (Taiz and Zeiger, 1998). In C3 plants, the carboxylation step is catalysed by the enzyme ribulose biphosphate carboxylase/ oxygenase (Rubisco), which represents the most abundant enzyme on earth. The functional enzyme is composed of eight large subunits

encoded in the chloroplast genome and eight small subunits encoded by a small multigene (*RBCS*) family in the nucleus (Allahverdiyeva *et al.*, 2005; Mizioroko and Lorimer, 1983). Besides the carboxylation of ribulose 1,5-bisphosphate, it also catalyses the oxygenation, a competing process, which especially predominates at high temperatures or low carbon dioxide concentrations.

1.1.3 The thylakoid membrane

The thylakoid membrane is composed of a lipid bilayer, which embeds a high amount of proteins. Besides representing the location of photosynthetic electron transport reactions, it leads to the separation of the aqueous content of the chloroplast into the external stroma and the enclosed lumen, this partitioning being required for the generation of the transmembrane proton gradient. The thylakoid membranes themselves are structurally heterogeneous. They consist of two main domains: the grana, which are stacks of thylakoids, and the stroma lamellae connecting the grana stacks (**Figure 1.2**; reviewed by Dekker and Boekema, 2005). Protein composition and biochemical properties differ in the two domains (Albertsson, 1990). The grana are enriched in Photosystem II (PSII), whereby the stacking of the grana membranes mainly originates from van-der-Waals attractive forces between chlorophylls of the PSII light-harvesting complex (LHCII) and the cation-mediated electric interaction of the proteins (Allen *et al.*, 1988; Chow *et al.*, 1981; Barber *et al.*, 1982). This tight packing of grana stacks leads to the exclusion of complexes with stromal side protrusions such as PSI and the ATPase, which are localised in the stromal lamellae (**Figure 1.2**). Whereas most experiments have located the Cyt *b₆f* complex in both grana and stromal lamellae (Anderson 1982, Vallon *et al.*, 1991), others have shown the existence of grana devoid of Cyt *b₆f* (van Roon *et al.*, 2000). It is disputed that under severe stacking conditions the Cyt *b₆f* complex might be displaced to the margins of PSII-LHCII supercomplexes, due to steric hindrances of the protruding loop of the subunit IV (Dekker and Boekema, 2005). The spatial organisation of the different photosynthetic complexes ensures sequential action of the linear electron transport, as it prevents spill over of excitation energy from PSII to PSI (Trissl and Wilhelm, 1993) and it has been proposed that it physically separates the cyclic from the linear electron flow (Joliot *et al.*, 2004). Moreover, the thylakoid membrane organization can also be rapidly and dynamically modified according to environmental cues, a process of which the major contributing effector is thought to be the phosphorylation of LHCII molecules (Pesaresi *et al.*, 2002).

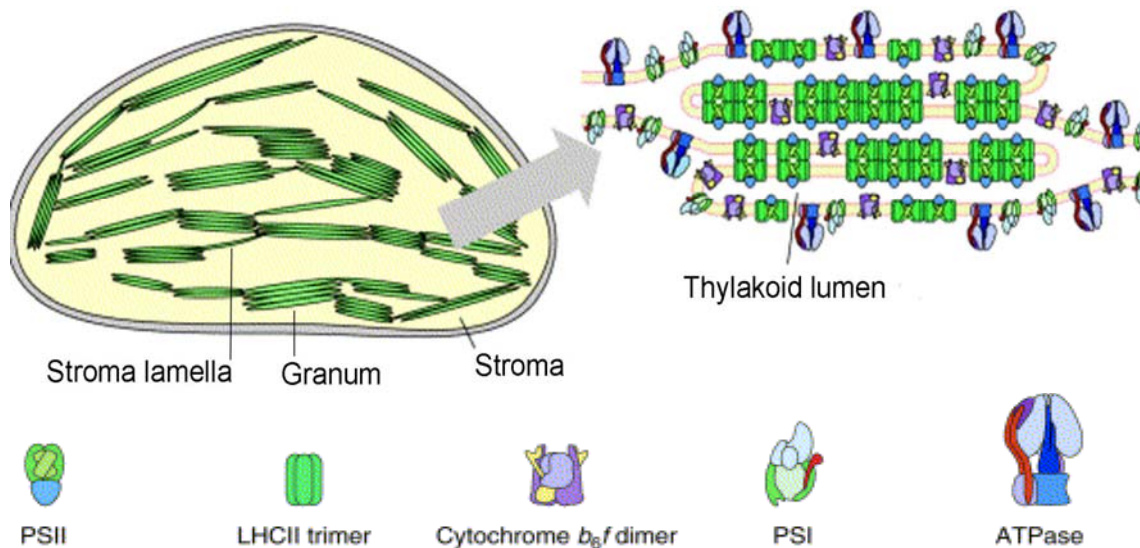


Fig 1.2 Compartmentalisation of the chloroplast and spatial arrangement of the thylakoid membrane

The chloroplast consists of the aqueous stroma enclosed by two lipid bilayers, the outer and the inner envelope. Imbedded in the stroma is an interconnected membrane system, the thylakoid membrane, which encloses the lumen. The thylakoid membrane is structured into stromal lamellae connecting stacks of thylakoid membranes, the grana. The distribution of thylakoid protein complexes is highly organised. ATPase and PSI are localised in the stromal lamellae and regions exposed to the stroma. PSII is mainly localised in the stacked thylakoids (adapted from Allen and Forsberg, 2001).

1.1.3.1 The thylakoid polypeptide composition

As the majority of processes performed by the thylakoid membrane relate to the harvesting and conversion of light energy, most components of the thylakoid proteome belong to one of the four large photosynthetic complexes or associate temporarily for regulatory purposes, as assembly or stability factors (reviewed by Nelson and Yocum, 2006). In flowering plants, the protein compositions of the four main photosynthetic complexes are principally understood. Crystallisation of the respective complexes and additional biochemical evidences lead to the allocation of 21 different subunits to PSII (Barber, 2006; Shi and Schröder, 2004), eight to Cyt b_6/f (Stroebel *et al.*, 2003), 16 to PSI (Jensen *et al.*, 2007) and nine to the ATPase (Seelert *et al.*, 2000). The functional units for the complexes are dimers for PSII and Cyt b_6/f and monomers for PSI and ATPase, but also the presence of supercomplexes comprising more functional entities of one or of different kinds have been reported (Boekema and Dekker, 2005). Association of antenna complexes to the two photosystems is prerequisite for efficient harvesting of light energy. The PSII antenna consists of six different subunits. Three Lhcb proteins, Lhcb4 (CP29), Lhcb5 (CP26), and Lhcb6 (CP24), which form the minor antenna, are monomeric and directly associated with PSII. They act in the transfer of excitation energy from the major light harvesting complex of PSII (LHCII) to the PSII core (Yakushevskaya *et al.*, 2001). The major light harvesting complex consists of three other Lhcb polypeptides, Lhcb1-3 and is in its functional state trimeric. The ratio of LHCII trimers to PSII

dimeric core complexes is about 8:1, but in *Arabidopsis* one PSII functional unit binds two to four trimers, which leaves the rest unbound or loosely bound (Kouril *et al.*, 2005). PSI light harvesting is carried out by a complex consisting of the four polypeptides Lhca1-4, which is stably associated with PSI. All light harvesting polypeptides bind carotenoids and chlorophyll a and b as prosthetic groups.

Both the nuclear and the plastid genome encode subunits of photosynthetic complexes, but all essential core subunits of PSII and PSI binding the cofactors necessary for electron transport are encoded by the plastome. **Figure 1.3** depicts the location of the subunit encoding genes. Plastid encoded subunits are coloured in green and nucleus encoded ones in red.

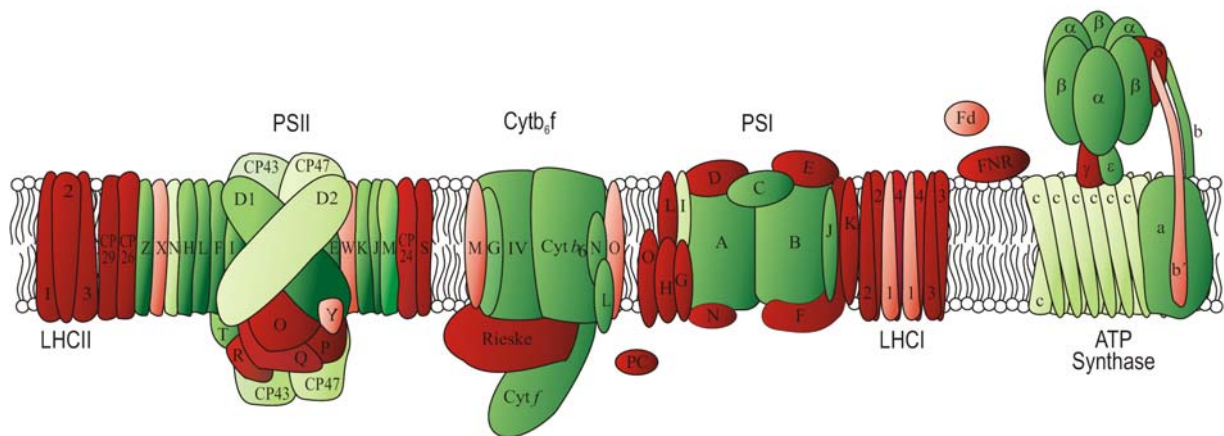


Figure 1.3 Schematic view of the thylakoid polypeptide composition in flowering plants

PSII, photosystem II; Cyt *b₆/f*, cytochrome *b₆/f*; PSI, photosystem I; LHCI/ LHCII, light harvesting complex I/II, PC plastocyanin, FD, Ferredoxin, FNR, Ferredoxin NADP Reductase. Nuclear encoded subunits are depicted in red, plastome encoded subunits in green. Those subunits, of which knock-out mutants have been characterised are coloured in a darker shade (from Leister, 2003).

However, knowledge about the thylakoid polypeptide composition remains incomplete. Therefore, the quest for novel photosynthetic proteins persists and extensive research is carried out in order to identify the function of previously undescribed subunits. In the past two years, knock-out mutants of the plastid-encoded low molecular weight subunits PetL,-N and G of the Cyt *b₆/f* complex, and, PsbM and -I of PSII have been characterised in tobacco (Schwenkert *et al.*, 2007; Umate *et al.*, 2007; Schwenkert *et al.*, 2006) and phenotypes of *Arabidopsis* mutants lacking the nuclear encoded PSII minor antenna Lhcb6 (Kovacs *et al.*, 2006) and the small subunits PsbQ and -R (Yi *et al.*, 2006; Suorsa *et al.*, 2006) have been published. Even previously unknown components of photosystems have been identified by proteomic approaches. The Thylakoid Membrane Phosphoprotein of 14 kDa (TMP14), has been designated a novel subunit of PSI (PsaP), on the basis that it

co-migrates with PSI in Blue native gels and because PSI accumulation is prerequisite for its stability. Additionally, it was demonstrated that PsaP abundance depends on the presence of the PSI subunits L, H and G (Khrouchtchova *et al.*, 2005). Another approach to identify novel photosynthetic components is the characterisation of unknown proteins, of which the encoding genes are co-regulated on transcriptional level with nuclear photosynthetic genes. With this method PGRL1 has been identified, which represents an indispensable component of cyclic electron flow around PSI (Chapter 1.1.1.2; DalCorso *et al.*, 2008). The basis to this approach will further be described in Chapter 1.2.1.

1.1.4 Regulation of photosynthetic processes

Photosynthesis is not a static situation, as the adjustment of physiological processes to environmental conditions is crucial for survival and fitness of the plant, due to its sessile nature. Therefore modes of regulation of photosynthesis have evolved in plants in order to cope with environmental changes. Here those will be described, which adapt the plant to changing light conditions by either protecting them from an excess of highly energetic intermediates produced by the absorption of light energy, or by ensuring optimum photosynthetic performance in a variety of conditions. Regulatory processes as short term responses include the dissipation of excess light energy (qE; Holt *et al.*, 2004) and the balancing of excitation energy between the two photosystems by the mechanism of state transitions (qT; Wollman, 2001; Allen and Forsberg, 2001). These two components and photoinhibition (qI) amount for the short-term response process of non-photochemical quenching as measured by quenching of Chl *a* fluorescence.

1.1.4.1 Energisation dependent non-photochemical quenching (qE)

The majority of NPQ stems from the dissipation of excess light energy as heat by the rapidly inducible non-photochemical quenching (qE). Exciton pressure is thereby diverted from PSII protecting it from photoinactivation. This process is also known as feed-back de-excitation, because the thermal dissipation of energy is stimulated by the light driven proton translocation into the lumen (Szabo *et al.*, 2005). The resulting low luminal pH has two roles in the induction of qE. One role is the activation of the violaxanthin de-epoxidase (VDE), the enzyme that catalyses the conversion of violaxanthin to antheraxanthin and zeaxanthin, the latter being the pigment required for qE realisation (Demmig-Adams and Adams 1993, Niyogi *et al.*, 1999). The second role is the protonation of PSII proteins involved in this process (Ruban *et al.*, 1992). In addition to de-epoxidised xanthophylls and protonation of specific proteins, the Lhcb-related PsbS protein is required for qE (Niyogi *et al.*, 2005). If light energy exceeds the capacity of qE, reactive oxygen

species originating from the un-funnelled transfer of light energy to oxygen, damage PSII proteins, thus leading to the inhibition of PSII activity, a process also referred to as photoinhibition (Nishiyama *et al.*, 2006).

1.1.4.2 State transitions

To avoid a preferential excitation of one of the two photosystems, plants can adjust the size of their relative PSI and PSII antenna accordingly by state transitions. This regulatory mechanism occurs, because of the different light absorption properties of the PSI and PSII light harvesting systems. Whereas the PSI antenna preferentially absorbs light of 700 nm, the PSII antenna has an optimum at 650 nm (Rochaix, 2007). The sensor for an imbalance in excitation energy between the two photosystems is the reduction state of the plastoquinone pool and the balance restoration is executed by a mobile pool of LHCII (Larsson *et al.*, 1983; Kyle *et al.*, 1984).

If the rate of charge separation is increased in PSII as compared to PSI, the plastoquinone reduction state increases. This leads to the occupancy of the Q₀ site on the luminal side of the Cyt *b₆f* complex with plastoquinol, an event that activates the LHCII kinase (Zito *et al.*, 1999). The kinase STN7 has been shown to be obligatory for the phosphorylation of LHCII (Bellafiore *et al.*, 2005; Bonardi *et al.*, 2005). However, a direct interaction between STN7 and LHCII has not been demonstrated and therefore the presence of one or more further kinases downstream of STN7 cannot be excluded. At higher light intensities, when LHCII is required at PSII for non-photochemical quenching, the kinase is deactivated and the dephosphorylated mobile LHCII pool re-associates with PSII (Rintamäki *et al.*, 2000). A persisting imbalance of excitation energy between the two photosystems can be counteracted by changes in plastid gene expression resulting in the alteration of the PSII/PSI ratio (Allen, 1995; Pfannschmidt *et al.*, 2001). This long-term acclimation is impaired in *stn7* mutants, indicating a function not only in the short term response of state transitions but also in the signalling process, which subsequently leads to the changes in PSI and PSII stoichiometry (Bonardi *et al.*, 2005).

1.2 Expression of photosynthetic genes

Prerequisite for the acclimation of plants to long-term changes in growth conditions are adjustments in the amounts and stoichiometries of photosynthetic components. Respective regulatory mechanisms occur by changes in gene expression in both the chloroplast and the nucleus. During the co-evolution of chloroplasts and their host cells a co-ordination of gene expression had to be achieved in order to synchronise these adaptive changes, but also to accommodate the chloroplast in its functional state within the cell. This required the development of mutual communication

pathways resulting in the control of gene expression by mediated signals. Both, plastid and nuclear gene expressions respond to the redox state of the chloroplast as an intrinsic marker for photosynthetic performances. The pools of reduced plastoquinone, thioredoxin and glutathione, but also the levels of reactive oxygen species (Pfannschmidt *et al.*, 2003) amount for redox state signals, which act within the chloroplast, but are also mediated to the nucleus. Additionally, tetrapyrrole derivatives and organellar gene expression are implicated in the chloroplast to nucleus (retrograde) signalling pathways influencing the expression of nuclear organelle genes (reviewed by Pesaresi *et al.*, 2007). Recent evidence indicates that the transcriptional repressor ABI4 (Abscisic Acid Insensitive 4) is involved in the nuclear execution of chloroplast deriving signals (Koussevitzky *et al.*, 2007).

1.2.1 Nuclear gene expression

Most nuclear chloroplast genes are the final outcome of complex events, following the initial endosymbiosis of a cyanobacterial-like prokaryote by a eukaryotic cell and subsequent gene transfer to the host nucleus. Several thousands of genes of the endosymbiont were gradually relocated during this process (Timmis *et al.*, 2004). Additionally, nuclear encoded proteins evolved with new, plant specific functions in the chloroplast. The control of photosynthetic gene expression results from the integration of light, developmental, plastidial, redox and carbohydrate signals (Terzaghi and Cashmore, 1995; Smeekens, 2000; Rolland *et al.*, 2002; Pfannschmidt, 2003; Strand, 2004). All of these signals affect nuclear gene expression in a highly organised regulatory pattern. This was demonstrated by analysing the expression of 3292 nuclear genes encoding chloroplast proteins under 101 different genetic or environmental conditions (Richly *et al.*, 2003, Biehl *et al.*, 2005). Firstly, a “master switch” acting in a binary mode by either inducing or repressing sets of genes encoding chloroplast proteins was observed in more than half of the conditions tested. Secondly, a “mixed response”, with about the same amount of up- and down-regulated genes was induced by the other half of conditions. Mutants involved in retrograde signalling pathways acted in a binary mode, indicating a global effect on the expression of analysed genes (Richly *et al.*, 2003; Biehl *et al.*, 2005). Two of the 23 groups of co-regulated genes (regulons), containing mostly genes coding for proteins involved in photosynthesis or plastome gene expression, escaped these two responses (Biehl *et al.*, 2005). The expressional control especially of these two subsets of chloroplast proteins indicates a co-ordination of the expression of plastome- and nucleus-encoded proteins involved in photosynthesis. Some genes of unknown function are also present in these two regulons, which suggests a putative photosynthetic function of the respective gene products.

1.2.1 Chloroplast gene expression

As expected from the eubacterial origin of the chloroplast, the structure of its genes and the expressing apparatus principally resemble those of eubacteria. This includes the organisation of genes in operons, their polycistronic expression and posttranscriptional processing (reviewed by Lopez-Juez and Pyke, 2005). Contrary to bacteria, some chloroplast genes include introns and also editing of the encoded RNA takes place. Accordingly, both inherited and newly acquired characteristics of the chloroplast expressional apparatus require regulatory proteins. These proteins are encoded by the nucleus and thus enable nuclear regulation of chloroplast gene expression, which is primarily regulated at post-transcriptional level (Deng *et al.*, 1989). However, transcription of chloroplast genes also involves nuclear encoded gene products. One RNA-polymerase is nuclear encoded (nuclear encoded RNA-polymerase; NEP) (Barkan and Goldschmidt-Clermont, 2000) and the other one (plastid encoded RNA-polymerase; PEP) requires assembly with nuclear encoded sigma factors to gain promoter specificity (reviewed by Kanamaru and Tanaka, 2004). Concomitantly, the chloroplast translational process requires nuclear factors as the chloroplast ribosome consists of subunits encoded by the chloroplast as well as by the nucleus (Yamaguchi *et al.*, 2003). Another characteristic of the nuclear control of chloroplast gene expression is the evolution and divergence of the eukaryotic pentatricopeptide repeat (PPR) family of proteins. These are involved in multiple gene expressional processes of the chloroplast (Shikanai, 2006). The formation of 3'- stem loops is one characteristic of bacterial transcripts preserved in the chloroplast, where they are critical for stability by impeding degradation by exonucleases (Drager *et al.*, 1996). Additionally, targeted cleavage of the stem loop is assumed to be a mechanism of regulating mRNA accumulation (Monde *et al.*, 2000). One protein implicated in this mechanism is CSP41, which was first described as a component binding the 3'- stem loop of the *petD* transcript in spinach (Yang *et al.*, 1995). It was shown that it acts as an endonuclease and specifically cleaves the 3'- stem loop common to chloroplast transcripts (Yang *et al.*, 1997, Bollenbach and Stern, 2003).

1.3 Abscisic acid (ABA) biosynthesis in plants

The plant hormone ABA is synthesized in the cytosol from carotenoid precursors stemming from the chloroplast and is involved in many plant regulatory pathways, such as onset of seed dormancy and acquisition of desiccation tolerance in seeds as well as the response to drought and high salinity conditions in vegetative tissue (Seo and Koshiba, 2002). The biosynthesis of the C15 compound ABA occurs in multiple enzymatic steps from the C5 compound isopentenyl pyrophosphate via the C40 carotenoids zeaxanthin, antheraxanthin, violaxanthin (xanthophyll-cycle pigments) and neoxanthin (**Figure 1.4**; Seo and Koshiba, 2002). Some genes encoding photosynthetic components

respond to ABA (Seki *et al.*, 2002) and it has been demonstrated that sugar and ABA responsiveness of a minimal RBCS light-responsive unit is mediated by direct binding of ABI4 (Acevedo-Hernandez *et al.*, 2005). Recently, this ABA induced repressor ABI4 has been implicated in the execution of chloroplast originating (retrograde) signals in the nucleus (Koussevitzky *et al.*, 2007). Additionally, it is known that manipulation of enzymes involved in carotenoid biosynthesis can influence ABA levels in the plant (Estevez *et al.*, 2001, Frey *et al.*, 1999, Lindgren *et al.*, 2003). Several environmental stress conditions either modulate the activity of enzymes involved in the xanthophyll cycle (Golding and Johnson 2003) or increase the amount of these pigments in the chloroplast (Demmig-Adams and Adams, 1993).

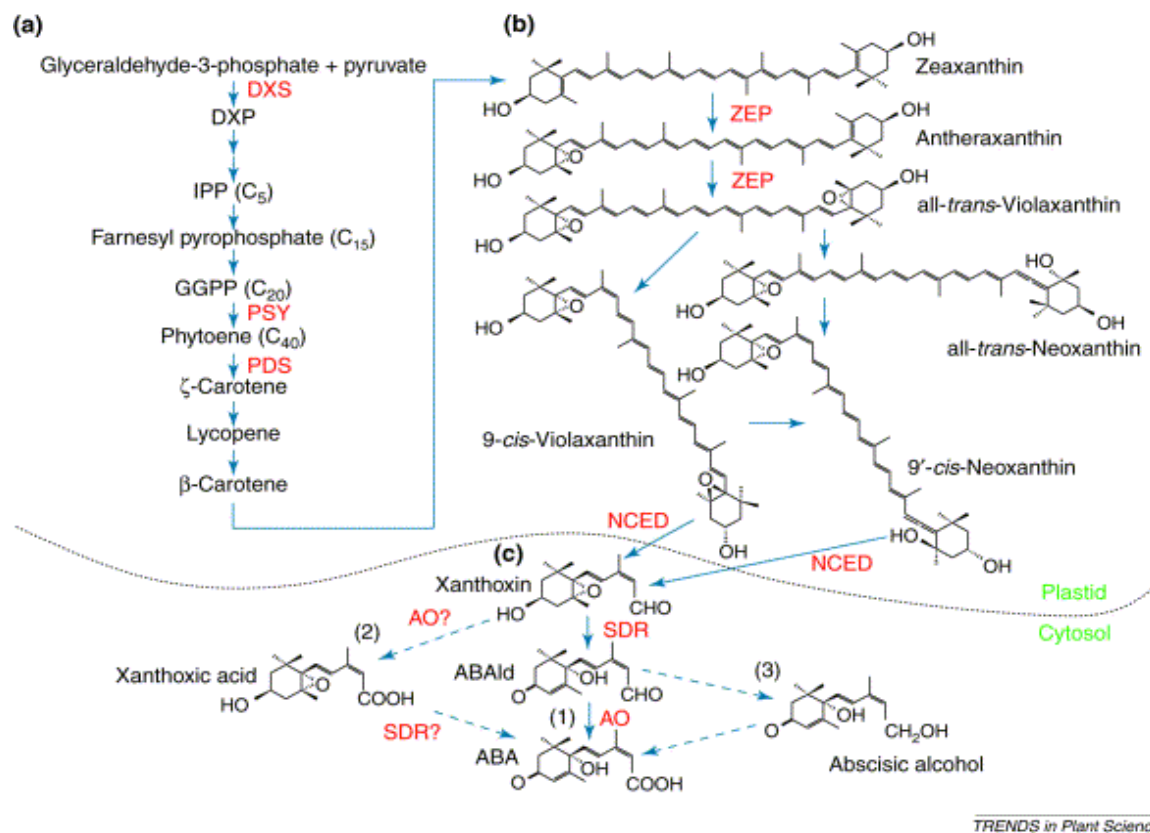


Fig 1.4 Biosynthetic pathway of ABA in the chloroplast and cytosol (Seo and Koshiba, 2002)

(a) Pathway leading to the synthesis of β -Carotene. (b) Xanthophyll-cycle pigments and neoxanthin, which are bound to the thylakoid light harvesting complexes. (c) Cytosolic pathways leading to the synthesis of ABA. Zeaxanthin epoxidase (ZEP), 1-deoxy-D-xylolose-5-phosphate synthetase (DXS), phytoene synthetase (PSY), phytoene desaturase (PDS) 9-cis-epoxycarotenoid dioxygenase (NCED), short-chain-dehydrogenase/ reductase (SDR), aldehyde oxidase (AO). Over-expression of the enzymes DXS, ZEP and PSY leads to higher endogenous ABA levels within the plant (Estevez *et al.*, 2001; Frey *et al.*, 1999; Lindgren *et al.*, 2003).

1.4 Aims of thesis

The basic idea to this thesis relies on the hypothesis that unknown genes co-regulated tightly with genes encoding components involved in a specific physiological activity likely code for proteins, of which the function also resides in this process (guilt by association; Walker *et al.*, 1999). Here, the

physiological process is photosynthesis (Biehl *et al.*, 2005) and the identification of the function of three unknown proteins was approached in the scope of this thesis. The characterisation of the Putative Photosynthetic Proteins 1, 4 and 5 (PPP1, PPP4, PPP5) was approached by reverse genetics combined with physiological dissection of knock-out plants employing physical measurements of electron transport and biochemical analyses. The as unknown annotated protein PPP5 was shown to be phosphorylated and therefore was termed Thylakoid Membrane Phospho protein of 14 kDa (TMP14; Hansson and Vener, 2002). Subsequently, this protein will be referred to by this name.

2 Materials and Methods

2.1 Materials

2.1.1 Chemicals

All chemicals were purchased from Sigma-Aldrich (Munich, Germany), Roth (Karlsruhe, Germany), Applichem (Darmstadt, Germany), Merck (Darmstadt, Germany), Serva (Heidelberg, Germany) and Biomol (Hamburg, Germany), except were stated otherwise. All chemicals were analytical grade.

2.1.2 Antibiotics

Antibiotics were provided by Duchefa (Haarlem, Netherlands) and by Sigma-Aldrich (Munich, Germany).

2.1.3 Enzymes, kits and biochemical agents

Enzymes used for cloning were obtained from New England Biolabs (Frankfurt, Germany), Roche (Penzberg, Germany) and Qiagen (Hildesheim, Germany). Those enzymes employed for the synthesis of cDNA were purchased from Invitrogen (Karlsruhe, Germany). For DNA purifications kits from Qiagen (Hildesheim, Germany) were used. Western-detection was carried out with the Enhanced Chemiluminescence kit (ECL; Pierce, Rockford, USA). Immunopure[®] Protein-A Agarose and BS³ were purchased from Pierce (Rockford, USA).

2.1.4 Membranes

Nitrocellulose membranes were acquired from Millipore (Eschborn, Germany) and positively charged Nylon membranes from Roche (Penzberg, Germany).

2.1.5 Antibodies

Peptide synthesis, generation of antibodies in rabbits and their monospecific purification was performed by Biogenes (Berlin, Germany). Commercially available primary antibodies against photosynthetic polypeptides were purchased from Agrisera (Vänås, Sweden). Tag antibodies were obtained from Sigma (c-myc, HA), Roche (c-myc) and Invitrogen (GFP), Actin antibodies from Dianova (Hamburg, Germany), Phospho-threonine antibodies from New England Biolabs (Frankfurt, Germany) and secondary antibodies from GE Healthcare and Sigma- Aldrich (both Munich, Germany). AtpD antibody was kindly provided by J. Meurer (Department of Botany, LMU, Munich), Rieske antibody by F. Ossenbühl (Department of Botany, LMU, Munich), antibodies against FNR, PsaD, PsaF by V. Scheller (Copenhagen, Denmark), TIC 110 by U. Voithknecht (Department of Botany, LMU, Munich), PsbS by K. Niyogi (Berkeley, USA).

2.2 Methods

2.2.1 Plant lines and propagation

Arabidopsis seeds were stratified for 2 days at 2-5°C in the dark to break dormancy and then sown out on plastic trays with soil. Plants were grown in a growth chamber illuminated with a 12h-light (20°C)/12h-dark (18°C) cycle with a PFD of 120 $\mu\text{mol photons m}^{-2}\text{s}^{-1}$ or under controlled greenhouse conditions (PDF 70-90 $\mu\text{mol photons m}^{-2}\text{s}^{-1}$, 16h light/ 8h dark cycles). Fertilisation with “Osmocote Plus” (Scotts Deutschland GMBH, Hildesheim, Germany) was performed according to manufacturer’s instructions.

The insertion mutant lines carried either T-DNA insertions or *Dissociation* (*Ds*) element insertions and were identified by searching the insertion flanking database SIGNAL (http://signal.salk.edu/cgi-bin/tdna_express). The *ppp1-1* and the *tmp14-like* mutants derive from the SALK T-DNA collection (<http://signal.salk.edu/>; Alonso *et al.*, 2003), the *ppp1-2* mutant from the GABI-KAT collection (Li *et al.*, 2003) and the *ppp4-like* from the SAIL collection (Session *et al.*, 2002), with all four of them in the Columbia-0 (Col-0) background. The *tmp14-2* mutant originates from the FLAG collection of T-DNA insertion lines in the Wassilevskija (WS) background (Samson *et al.*, 2002). *Dissociation* (*Ds*) element insertions are the *ppp4-1* mutant from IMA (Parinov *et al.*, 1999), the *ppp4-2* mutant from the Exotic collection (Exotic Handbook by J. Clarke 2000), both in Landsberg *erecta* (*Ler*) background and *tmp14-1* from the RIKEN collection in Noessen (No-0) background.

2.2.2 Nucleic acid analysis

2.2.2.1 DNA analysis

Arabidopsis DNA was isolated by disruption of leaf material frozen in liquid nitrogen with metal beads and addition of isolation buffer (200 mM Tris/ HCl pH 7.5, 250 mM NaCl, 25 mM EDTA, 0.5% SDS). DNA in the supernatant was precipitated by addition of 0.8 volumes of isopropanol and centrifugation at 16000g, RT for 20 min. The insertion flanking sites were identified by sequencing after PCR-amplifications using a combination of gene- and insertion-specific primers. T-DNA primers specific for ROK2 (SALK-collection) were LBa1 and RBb1; for Ac106 (GABI-KAT collection) LbGK1 and o2588; for CSA110 (SAIL-collection) LB1 and RB1, for GKB5 (FLAG-collection) TAG5 and TAG3, for IMA-DS *Ds3'-1* and *Ds5'-1*; for Exotic-DS *Ds3'-1* and *Ds5'-3* and for the Koncz collection Fish1 (**Table 2.1**).

| Oligonucleotides | Sequence 5'-3' |
|------------------|---------------------------|
| At1g09340-1176s | AGAAGTTGAGCCCATACTAGA |
| At1g09340-1851as | CAGTCAGTGGGTCCC TATAA |
| At1g09340-2281s | TCGGTCACGTTAAGGTCAGT |
| At1g09340-2779as | TTACCTGATCACGGAAAGGG |
| At3g63140--114s | GCGACCGTTGGATGTTGTTA |
| At3g63140-581as | AAGCAGACCTAACAGTATCCA |
| At4g01150--154s | AACACCACTGAGTTGGATTTC |
| At4g01150-410as | GACGAGGTCTCTTCTGAAGAA |
| At4g01150--25s | AAGAAGAAGTTCTCGGCGTG |
| At4g01150-916as | CTCAGCCAATTCCTTTCTGC |
| At2g46820--222s | ACTCCAAGATCGTCTCTACG |
| At2g46820-521as: | GGGTTCTGCTGGAATGATT |
| At2g46820-950s | TGGTTCACCTACAAGAACCTG |
| At2g46820-1427as | CATGCATGGTTAGCTTAGCTT |
| At1g52220-20s | CAACTTTCCTTCGCCATTGT |
| At1g52220-817as | CTGGCCAAGTATATCCGCTA |
| At4g38100-10s | TGCACCAGGTCTACCACAAT |
| At4g38100-530as | TTGAGTTTCCTCATCTTCAGC |
| Lba1 | TGGTTCACGTAGTGGGCCATCG |
| Rbb1 | TCAGTGACAACGTCGAGCAC |
| LbGK1 | CCCATTGGACGTGAATGTAGACAC |
| o2588 | CGCCAGGGTTTTCCAGTCACGACG |
| Lb1 | CTATTGGTAATAGGACACTGG |
| Rb1 | GTAAAACTGCCTGGCAC |
| Ds3'-1 | CGATTACCGTATTTATCCCGTTCCG |
| Ds5'-1 | CCGTTTACCGTTTTGTATATCCCG |
| Ds5'-3 | CGGTTCGGTACGGGATTTTCC |
| Fish1 | CTGGGAATGGCGAAATCAAGGCATC |
| TAG5 | CTACAAATTGCCTTTTCTTATCGAC |
| TAG3 | CTGATACCAGACGTTGCCCGCATAA |

Table 2.1 Oligonucleotides employed for identification of gene insertion lines

Primers specific for confirmation of the knock-out allele *ppp1-1* were At1g09340-1176s and At1g09340-1851as, for *ppp1-2* At1g09340-2281s and At1g09340-2779as; for *atcsp41* At3g63140-

114s and At3g63140-581as, for *ppp4-1* At4g01150--154s, and At4g01150-410as, for *ppp4-2* At4g01150--25s and At4g01150-916as, for *tmp14-1* At2g46820--222s and At2g46820-521as, for *tmp14-2* At2g46820-950s and At2g46820-1427as, for *tmp14-like* At1g52220-20s and At1g52220-817as, for *ppp4-like* At4g38100-10s and At4g38100-530as (**Table 2.1**).

2.2.2.2 RNA analysis

For RNA analysis, total leaf RNA was extracted from fresh tissue using the TRIzol reagent (Invitrogen, Karlsruhe, Germany). Reverse transcriptase-mediated PCRs (RT-PCR) were carried out by synthesizing first-strand cDNA using the SuperScriptTM Reverse Transcriptase (Invitrogen, Karlsruhe, Germany) and dT oligomers, followed by PCR with specific primers for *TMP14-like* (upstream of insertion: 5'-CAACTTTGCCTTCGCCATTGT-3', 5'-GCTGCTAGGGTTTCGAGTAA-3'; downstream of insertion: 5'-TGGGCATCATTGAATCTCATC-3', 5'-CTGGC CAAGTATATCCGCTA-3'), *PPP4-like* (upstream of insertion: 5'-TGCACCAGGTCTACCA CAAT-3', 5'-GCAACA ACTACTCCATCAGC-3'; downstream of insertion: 5'-CTCGAATAGTG AAGCTCCTC-3', 5'-CACTCACTATCAGACCCAAG-3'), *AtCSP41* (upstream of insertion: 5'-A TGGCGGCTTTATCATCCTC-3', 5'-TTTCACCTCCGACCACATTG-3') and *ACTIN1* (5'-TGC GACAATGGA ACTGGAATG-3'; 5'-GGATAGCATGTGGAAGTGCATACC-3') as control. Northern analyses were performed under stringent conditions, according to Sambrook *et al.* (1989). Probes complementary to nuclear and chloroplast genes were used for the hybridizations. **Table 2.2** lists the genes analyzed and the primers used to amplify the probes. All the probes were cDNA fragments labeled with ³²P. Signals were quantified by using a phosphoimager (Storm 860; Molecular Dynamics) and the program IMAGE QUANT for Macintosh (version 1.2; Molecular Dynamics).

| Genes | Forward primer (5'-3') | Reverse primer (5'-3') |
|---------------|------------------------|--------------------------|
| <i>ACTIN1</i> | TGCGACAATGGA ACTGGAATG | GGATAGCATGTGGAAGTGCATACC |
| <i>psbA</i> | TGCATCCGTTGATGAATGGC | TCGGCCAAAATAACCGTGAG |
| <i>psaA</i> | GATTATTCGTTCCGCCGAAC | TGGAGCTGCTTTGTGATAATG |
| <i>rbcL</i> | CGTTGGAGAGACCGTTTCTT | CAAAGCCCAAAGTTGACTCC |

Table 2.2 Oligonucleotides employed for Northern probe generation

2.2.2.3 Analysis of mRNAs associated with polysomes

Polysomes were isolated as described by Barkan (1988). Leaf tissue (200 mg) was ground with mortar and pestle in liquid nitrogen. Subsequently, the microsomal membranes were solubilized

with 1% Triton X-100 and 0.5% sodium deoxycholate. The solubilized material was layered onto 15 to 55% step sucrose gradients and centrifuged in a Beckman L7-55 ultracentrifuge (Kontron TST 60.4 rotor) at 45000 rpm for 65 min at 4 °C. The sucrose gradient was fractionated and the mRNA associated with polysomes was then extracted with phenol/chloroform/isoamyl alcohol (25:24:1) followed by precipitation at room temperature with 95% ethanol. All samples were then subjected to Northern analyses.

2.2.2.4 Transcript end mapping of *rbcL* using circular RT-PCR

Transcripts were ligated using T4 RNA ligase and cDNA synthesis of *rbcL* transcript ends was performed using primers 5'-CGATCAAGGCTGGTAAGC-3' and 5'-TCACTACCTGGTGTTCTGC-3' followed by nested PCR using primers 5'-CTTGCTTTAGTCTCTGTTTGTGGTG A-3' and 5'-GACGTGATCTTGCAGTCGAG-3'. PCR products were separated by agarose gel, excised and sequenced (Perrin *et al.*, 2004). This experiment was performed in collaboration with Agata Kazmierczak (Department of Botany, LMU, Munich).

2.2.3 Transformation of *Arabidopsis*

2.2.3.1. Bacterial strains

The bacterial strains used were: *E. coli* DH5 α (Bethesda Res. Lab., 1986) and *Agrobacterium tumefaciens* GV3101 (pMP90RK) (Koncz *et al.*, 1990).

2.2.3.2 Agrobacterium binary vectors

For expression of C-terminal tagged *PPP4* cDNAs in plants the vectors pPCV812 Δ *NotI*-Pily (*Hemagglutinin; HA*) and pPCV812 Δ *NotI*-Lola (*c-myc*) were used (kindly provided by C. Koncz, Max-Planck Institute for Plant Breeding Research, Germany). Both vectors derive from the same binary backbone vector (pPCV812), which carries a double 35S promoter upstream of the multiple cloning site and contains a β -lactamase gene conferring resistance of bacteria to ampicillin/carbenicillin and a hygromycin resistance gene for plant selection. The complete coding region of *PPP4* (primers: PPP4:c-myc-s: CGTCCCGGGATGGCGATATCA; PPP4:c-myc-as: GCCAGATCTTTCGCTTCCTGC) was ligated into both vectors using the *Bgl*III and *Sma*I restriction enzyme sites. For complementation of the *ppp1-1* mutant, plants were transformed with *AtCSP41b:CFP*-pBA002, which carries the complete *PPP1* coding region upstream of a CFP encoding sequence (kindly provided by S. Hoth, University of Erlangen- Nürnberg; Raab *et al.*, 2006).

2.2.3.3 *Agrobacterium*-mediated transformation of *A. thaliana*

Arabidopsis mutant plants were transformed as reported (Clough and Bent, 1998). Budding plants were dipped for 15 s in an *Agrobacterium* suspension containing 2.5% sucrose and the surfactant Silwet L-77 (0.02%). After dipping, plants were covered with clear plastic for two days to sustain high humidity levels, which facilitates transformation. Subsequently the plants were transferred to the greenhouse and grown to full maturity until seeds could be harvested.

2.2.4 Biochemical Analysis

2.2.4.1 Antibody production

Antibodies against epitopes of PPP1, PPP4 and TMP14 were produced in rabbits. Epitope synthesis, injection into rabbits, collection of serum and subsequent monospecific purification of Igs was carried out by Biogenes (Berlin, Germany). The epitopes ranging in size from 11 to 14 amino acids were designed in such way that they were specific for the respective proteins (fasta search: www.arabidopsis.org/cgi-bin/fasta/nph-TAIRfasta.pl) and covered a hydrophile stretch of amino acids with high antigenicity. For analysis of hydrophility the hydrophobicity plot of Clone manager was employed. To evaluate antigenicity the JaMBW Chapter 3.1.7 plot was used (<http://bioinformatics.org/JaMBW/3/1/7/>). The amino acid sequences of the epitopes in one letter code were KILHLKGDRKDYDF for PPP1, VKTAQEAWKVDK for TMP14 and LITDLKEKWDG for PPP4.

2.2.4.2 SDS-PAGE

Identical amounts of proteins equivalent to 2- 5 µg of chlorophylls calculated as described in Porra *et al.* (2002) were solubilised in SDS loading buffer (50 mM Tris/ HCl pH 6.8, 4% w/v SDS, 12% v/v glycerol, 50 mM DTT, 0.01% bromophenol blue), loaded and separated by SDS-PAGE (10% - 16% acrylamide) as described by Schägger and von Jagow (1987). After an overnight run at 30 mA per gel (150 mm x 180 mm x 15 mm separating gel; anode buffer: 0.2 M Tris/ HCl (pH 8.9), cathode buffer: 0.1 M Tris, 0.1 M Tricine, 0.1% SDS), Gels were either stained with silver or Coomassie Brilliant Blue to visualise proteins according to standard protocols or specific proteins were detected using the method of immunoblot analysis.

2.2.4.3 Immunoblot analysis

Proteins separated by native or SDS-PAGE were transferred to polyvinylidene difluoride (PVDF) membranes according to Towbin *et al.* (1979) by a semi-dry blotting system using a current

corresponding to 1 mA cm^{-2} in transfer buffer (96 mM glycine, 10 mM Tris, 10% (v/v) methanol). Replica filters were incubated with antibodies specific for the proteins of interest. Signals were detected using the Enhanced Chemiluminescence Western Blotting Kit (Pierce, Rockford, USA).

2.2.4.4 Total protein isolation

Leaves were disrupted in the presence of liquid nitrogen and total proteins were isolated by adding extraction buffer (100 mM Tris/ HCl pH 8.0, 50 mM EDTA pH 8.0, 0.25 M NaCl, and 1 mM DTT, 0.75% (w/v) SDS) and incubation at 68°C for 10 min. After centrifugation at $15000g$ for 10 min, the chlorophyll concentration of the supernatant was determined as described in Porra *et al.*, (2002) and total protein according to $5 \mu\text{g}$ of chlorophyll were loaded onto an SDS gel.

2.2.4.5 Isolation of intact chloroplasts

Leaves of 4- to 5- week-old plants were homogenized in homogenization buffer (330 mM sorbitol, 50 mM HEPES/ KOH pH 7.6, 20 mM EDTA) and the filtrate was collected after passing through two layers of Miracloth (Calbiochem through VWR International GmbH, Darmstadt, Germany). Chloroplasts were collected by centrifugation for 5 min at $2000g$, 4°C . The pellet was carefully resuspended in the homogenization buffer. Chloroplasts were loaded on a two step Percoll gradient as described in Aronsson and Jarvis (2002). Intact chloroplasts at the interface between the two Percoll phases were broken by incubation for 30 min on ice in four volumes lysis buffer (20 mM HEPES/ KOH pH 7.5, 10 mM EDTA). To separate thylakoids and stroma phases, ruptured chloroplasts were centrifuged at $42000g$, 30 min at 4°C .

2.2.4.6 Fractionation of chloroplasts

Intact chloroplasts were re-suspended in TE buffer (10 mM Tris/ HCl pH 8.0, 1 mM EDTA pH 8.0) at a chlorophyll concentration of 2 mg/ml chlorophyll and loaded onto a three step sucrose gradient consisting of, from the bottom to the top, 1.2 M, 1 M, and 0.46 M sucrose in TE. After centrifugation for 2 h at $30000g$, 4°C , the upper phase containing the stroma, the two interphases containing inner and outer envelopes and the pellet consisting of thylakoids were collected, the three membrane fractions were washed with TE and proteins were separated by SDS-PAGE.

2.2.4.7 Preparation of thylakoid membranes

Leaves from 4-week-old plants were harvested in the middle of the light period and thylakoids were prepared as described by Bassi *et al.* (1985). In detail, leaf material was homogenized in ice-cold buffer containing 0.4 M sorbitol, 0.1 M Tricine/ KOH pH 7.8 and 1 mM PMSF, the resulting homogenate was filtered through nylon mesh and centrifuged at 4°C , $3000g$ for 10 min.

Subsequently, chloroplast were broken in 20 mM HEPES/ KOH pH 7.8, 10 mM EDTA pH 8.0 and thylakoids were collected by centrifugation at 12000g for 10 min and resuspended in a buffer containing 50% glycerol, 10 mM HEPES/ KOH pH 7.5, 1 mM EDTA pH 8.0).

2.2.4.8 Fractionation of thylakoids

Isolated chloroplasts were lysed in 25 mM HEPES/ KOH pH 7.5, 5 mM MgCl₂ and thylakoids were fractionated into grana, intermediate membranes and stroma lamellae by digitonin treatment followed by differential centrifugation as modified from Ossenbuehl *et al.* (2002). In brief, thylakoid membranes were incubated with 0.2% digitonin in 15 mM Tricine/ KOH pH 7.9, 0.1 M sorbitol, 10 mM NaCl, 5 mM MgCl₂, for 1 min at room temperature. The incubation was stopped by 10 fold dilution in the same buffer. The suspension was centrifuged four times at 4 °C. Each supernatant was used for the next centrifugation step. The relative acceleration rates were 1000g for 10 min, 10000g for 30 min, 40000g for 60 min and 150000 g for 90 min. The different pellets grana thylakoids (10000g), intermediate membranes (40000g) and stroma thylakoids (150000g) according to 5 µg of chlorophyll were loaded onto an SDS gel.

2.2.4.9 PSI isolation

Thylakoids were prepared as described, then washed twice with 5 mM EDTA (pH 7.8) and diluted in the same solution to a chlorophyll concentration of 2 mg/ml. Solubilisation of membrane complexes was carried out by addition of 2% n-dodecyl-β-D-maltoside (β-DM) and incubation on ice for 10 min. Afterwards, centrifugation at 16000g for 5 min at 4°C was performed in order to remove un-solubilised membranes. The supernatant was loaded onto a sucrose gradient, originating from a freeze-thawing cycle of a 0.4 M sucrose, 20 mM Tricine/ KOH (pH 7.5) and 0.06% (w/v) β-DM containing solution, followed by centrifugation at 191000g for 21 h at 4°C. The PSI migrated as a distinct green band at the bottom of the centrifuge tube. The purity of the PSI isolation was analysed by separation of the proteins in a 16% to 23% acrylamide Tris-Glycine SDS-PAGE following standard protocols (Sambrook *et al.*, 1989).

2.2.4.10 Blue native and second dimension gels

Leaves from 4- to 5-week-old plants were harvested and thylakoids were prepared as already described (Bassi *et al.*, 1985). For the native PAGE analysis, protein amounts equivalent to 100 µg of chlorophyll were washed twice with 20 mM HEPES/ KOH pH 7.8, 10 mM EDTA pH 8.0, and subsequently solubilised in 750 mM ε-aminocaproic acid, 50 mM Bis-Tris/ HCl pH 7.0, 5 mM EDTA pH 7.0, 50 mM NaCl for 1 h with 2.8% (w/v) digitonin at 4°C on a wheel, or for 20 min

with 1.25% (w/v) n-dodecyl- β -D-maltoside (β -DM) on ice. Solubilised protein complexes were separated from unsolubilised by centrifugation for 1 h at 16000g, 4°C (digitonin) or for 20 min (β -DM). The supernatant was supplemented with 5% (w/v) Coomassie Brilliant Blue in 750 mM aminocaproic acid, and loaded onto polyacrylamides gel (4-12% acrylamide). One-dimensional BN-PAGE and 2D BN/SDS-PAGE were carried out as described by Schägger and von Jagow (1991)

2.2.4.11 Bis (Sulfosuccinimidyl) suberate (BS³) crosslinking

Isolated thylakoids were washed 5 times with 20 mM HEPES/ KOH pH 7.5 to remove the EDTA of the lysis buffer. Crosslinking was carried out with a thylakoid suspension containing 30 μ g/ml chlorophyll by adding 400 μ M BS³ and subsequent incubation for 1h on ice. The reaction was quenched by the addition of 150 mM Tris/ HCl pH 7.5.

2.2.4.12 Co-Immunoprecipitation

Isolated thylakoids were washed twice in 20 mM HEPES/ KOH pH 7.8, 10 mM EDTA pH 8.0 and then resuspended in Co-IP buffer (50 mM HEPES/ KOH pH 8.0, 330 mM sorbitol, 150 mM NaCl, 0.5% (w/v) BSA, 1 mM PMSF) at a chlorophyll concentration of 1.5 mg/ml. ProteinA-agarose was washed five times in Co-IP buffer, specific antibodies (1/6 volume) were added and the binding reaction was carried out for 2 h on a wheel at 4°C. Afterwards, beads were washed five times in Co-IP buffer to remove unbound antibodies. Meanwhile, solubilisation of thylakoid protein complexes was carried out by adding 2.5% digitonin to the thylakoid suspension and subsequent incubation for 30 min on a wheel at 4°C. Solubilised complexes were separated from unsolubilised thylakoid membrane by centrifugation for 30 min at 16000g, 4°C. Solubilised thylakoid membranes were diluted 1:5 in Co-IP buffer and subsequently combined with the antibody binding agarose beads. The immune-reaction was carried out on a wheel over night at 4°C. Subsequently the beads were collected by centrifugation for 2 min at 3000g and washed six times with the Co-IP buffer containing 0.5% digitonin. Samples were kept on ice at all times. Proteins were eluted from the matrix by incubation with SDS loading dye buffer for 10 min at 60°C, beads were pelleted by centrifugation for 5 min at 3000g, RT.

2.2.4.13 Salt treatment of thylakoid membranes

According to Karnauhov *et al.* (1997) isolated thylakoids were resuspended in 50 mM HEPES/ KOH pH 7.5 at a chlorophyll concentration of 0.5 mg/ml. Salts were added to a final concentration of 2 M NaCl, 0.1 M Na₂CO₃, 2 M NaSCN and 0.1 M NaOH. Extraction was carried out for 30 min

on ice, soluble and membrane proteins were separated by centrifugation for 10 min at 10000g, 4°C and Western analysis was performed on both fractions using specific antibodies.

2.2.4.14 Trypsin treatment of thylakoid membranes

Thylakoid membranes were isolated as described omitting the addition of PMSF and then resuspended in 50 mM HEPES/ KOH pH 8, 300 mM sorbitol at a chlorophyll concentration of 1 mg/ml. Trypsin was added to a concentration of 10 µg/ml. Samples were taken at 0, 10 and 20 min after the addition of trypsin, proteins were precipitated with 10 volumes of 100% acetone and resuspended in SDS loading dye containing 5 mM of the serine endopeptidase inhibitor PMSF.

2.2.4.15 *In vivo* labelling with ³⁵S-Methionine

For the radioactive labelling of chloroplast proteins according to Pesaresi *et al.* (2001), leaves of 3-week-old Arabidopsis WT and *ppp1-1* plants grown in the greenhouse were vacuum-infiltrated in a syringe containing 1 mCi of ³⁵S-L-methionine in 10 ml of 1 mM KH₂PO₄ (pH 6.3), 0.1% Tween-20 and illuminated with 50 µmol photons m⁻²s⁻¹ for 1h. Afterwards, leaves were disrupted in the presence of 10 mM Tris/ HCl pH 6.8, 10 mM MgCl₂ and 20 mM KCl and soluble protein was separated from membrane protein by centrifugation at 7500g, 4°C for 10 min. Both fractions were loaded onto an SDS-PAGE, which was subsequently dried and signals were quantified by using a phosphoimager (FLA 3000; FujiFilm Europe GMBH, Düsseldorf, Germany).

2.2.5 Mass spectrometry

Mass spectrometry analyses of protein samples were carried out in collaboration with B. Müller (Department of Botany, LMU, Munich).

2.2.5.1 Tryptic in gel digestion of proteins

The desired protein containing gel slice was excised and washed twice in ddH₂O for 10 min. Digestion was then carried out with trypsin in a basic buffer (100 mM NH₄HCO₃). The peptides were eluted by shrinking the gel with one volume of CH₃CN. After short centrifugation the peptide containing supernatant was supplemented with one quarter volume of H₂CO₂ to stop digestion. Peptides were dried and then resuspended in solvents used for analysis.

2.2.5.2 LC-ESI MS/MS

A quaternary HPLC pump (Flux, Basel, Switzerland) including a CTC auto sampler was connected to a Thermo Fisher Scientific LTQ-Orbitrap mass spectrometer (linear quadrupole ion trap coupled to a FT-analyzer) (Thermo Electron Corp., San Jose, CA).

The LTQ-Orbitrap was operated via Instrument Method files of Xcalibur to acquire a full high resolution MS scan between 400 and 2000 m/z (resolution was set to 7500) followed by full MS/MS scans of the six most intensive ions from the preceding MS scan. The heated desolvation capillary was set to 200°C. The relative collision energy for collision induced dissociation was set to 35%, dynamic exclusion was enabled with a repeat count of two, a repeat duration of 0.5 min, and a three minutes exclusion duration window. Samples were loaded onto a 10 cm fused silica column.

The fritless 100 µm capillary was packed in house with ProntoSIL C18 ace-EPS (ProntoSIL C18 ace-EPS, Bischoff Analysentechnik und -geräte GmbH, Leonberg, Germany). The column flow rate was set to 0.15-0.25 µL / min and a spray voltage of 1.3 kV was used. The buffer solutions for chromatography were 5% ACN (acetonitrile); 0.1% formic acid, 80% ACN; 0.1% formic acid. After equilibration for 5 min with buffer A, a linear gradient was generated within 80 min.

2.2.5.3 Protein identification

The SEQUEST algorithm was used to interpret MS/MS spectra. Results were interpreted on the basis of a conservative criteria set, i.e. only results with dCn (delta normalized correlation) scores greater than 0.2 were accepted, all fragments had to be at least partially tryptic and the cross-correlation scores (Xcorr) of single charged, double charged or triple charged ions had to be greater than 2, 2.8, or 3.5. Spectra were manually evaluated to match the following criteria: Distinct peaks with signals clearly above noise levels, differences of fragment ion masses in the mass range of amino acids, and fulfilment of consecutive b and y ion series.

2.2.6 Pigment analysis

Pigments were analyzed by reverse-phase HPLC as described previously by Färber *et al.* (1997). For pigment extraction, leaf discs were frozen in liquid nitrogen and disrupted with beads in microcentrifuge tubes in the presence of acetone. After a short centrifugation, pigment extracts were filtered through a 0.2 µm membrane filter and either used directly for HPLC analysis or stored for up to 2 days at -20°C (the pigment analysis was performed in collaboration with Peter Jahns, Düsseldorf, Germany).

2.2.7 Database analysis, Digital Northern, prediction of subcellular targeting and protein modelling

For the analysis of gene models and their coverage by full-length mRNAs or ESTs, the NCBI (www.ncbi.nlm.nih.gov), MIPS (<http://mips.gsf.de/proj/thal/db/index.html>), and TAIR (www.arabidopsis.org) databases were used. To identify orthologues, the protein sequences were blasted against the non-redundant protein sequence (nr) database using NCBI blastp (www.ncbi.nlm.nih.gov/blast/Blast.cgi). For the confirmation of *Chlamydomonas reinhardtii* and cyanobacterial homologues, the JGI Chlamy v2.0 Blast (<http://genome.jgi-psf.org/cgi-bin>) and the Cyanobase similarity search (<http://bacteria.kazusa.or.jp/cyano/cgi-bin>) online programs were applied.

Digital Northern analyses were performed by using the Geneinvestigator site (www.geneinvestigator.ethz.ch; Zimmermann *et al.*, 2004). Sequence data were analysed with Clone Manager 5. Amino acid sequences were aligned using the CLUSTAL-W program (www.ebi.ac.uk/clustalw/; Chenna *et al.*, 2003) and alignments were shaded according to sequence similarity using the Boxshade server 3.21 (www.ch.embnet.org/software/BOX_form.html). Sequence identities and similarities were calculated using NCBI Blast 2 sequences (Tatusova and Madden, 1999). Chloroplast transit peptide predictions were done using the programs TargetP (version 1.1; <http://www.cbs.dtu.dk/services/TargetP/>; Emanuelsson *et al.*, 2000) and ChloroP (version 1.1; <http://www.cbs.dtu.dk/services/ChloroP/>; Emanuelsson *et al.*, 1999). Protein molecular weights were calculated using Protparam (<http://www.expasy.org/tools/protparam.html>) and transmembrane domains were predicted using the TMHMM Server v. 2.0 (www.cbs.dtu.dk/services/TMHMM-2.0). Protein structures were calculated using the 3D-Jigsaw server (www.bmm.icnet.uk/~3djigsaw) and protein models were visualised by Swiss PDB Viewer (<http://expasy.org/spdbv>)

2.2.8 Intracellular localization of dsRED fusions

The red fluorescent protein from the reef coral *Discosoma* (dsRED) (Jach *et al.*, 2001) was used as a reporter to determine the intracellular localization of TMP14-like and PPP4-like in transient gene expression assays. The coding regions of the analyzed genes were amplified using primers 5'-CGCCATGGCTTCAATTTCTGCA-3' and 5'-CGCCATGGCCTGGCCAAGTATATCC-3' for *TMP14-like*, 5'-CGCCATGGAGCTCTGCACCA-3' and 5'-CGCCATGGCCTCACTATCAGACC-3' for *PPP4-like* and cloned upstream of the dsRed sequence using the *NcoI* restriction enzyme site. Sterile cotyledons of 2 week-old plants (ecotype ColGl-1) were cut into small pieces and incubated for 16 h at 24°C in the dark in a protoplasting solution (10 mM MES, 20 mM CaCl₂, 0.5

M mannitol pH 5.8, 0.1 g/ml macerozyme (Duchefa), 0.1 g/ml cellulase (Duchefa)) followed by the isolation of protoplasts as described in Dovzhenko *et al.* (2003). Plasmid DNA (40 µg) was introduced into protoplasts by PEG transfection as previously described (Koop *et al.*, 1996). Microscopy analysis (with Fluorescence Axio Imager microscope in ApoTome mode (Zeiss)) was conducted after 16 h of incubation at 23°C in the dark. Fluorescence was excited with the X-Cite Series 120 fluorescence lamp (EXFO) and images were collected in the 565–620 nm (dsRED fluorescence) and 670–750 nm (chlorophyll autofluorescence) ranges.

2.2.9 Germination assay

Seeds from identically grown WT and mutant plants were surface sterilised with 7.5% (v/v) hypochloride and 0.5% (v/v) Triton-X and grown on MS plates containing 1% sucrose and various concentration of abscisic acid (ABA). Seeds were stratified for 4 days at 4°C, then plates were transferred to 16 h/ 8 h light dark cycle at 22°C and amount of germinated seedlings was monitored after 48, 60, 72 and 96 h after the shift. The germination assay was performed in collaboration with Sabine Raab (University of Erlangen, Germany).

2.2.10 Determination of photosynthetic parameters using the PAM fluorometer

2.2.10.1 Chlorophyll fluorescence measurements

In vivo chlorophyll *a* fluorescence of single leaves was measured using either the Pulse Amplitude Modulation 101/103 (PAM 101/103) as already described in Varotto *et al.* (2000) or the Dual-PAM-100 fluorometer (Walz, Effeltrich, Germany). Plants were dark adapted for 30 min and minimal fluorescence (F_0) was measured. Then pulses (0.8 s) of white light ($5000 \mu\text{mol photons m}^{-2} \text{s}^{-1}$) were used to determine the maximum fluorescence (F_m) and the ratio $(F_m - F_0)/F_m = F_v/F_m$ (maximum quantum yield of PSII) was calculated. A 15 min illumination with actinic light of varying intensities was supplied to drive electron transport between PSII and PSI. Then firstly steady state fluorescence (F_s) and then by further saturation pulses (0.8 s, $5000 \mu\text{mol photons m}^{-2} \text{s}^{-1}$) F_m' were determined and the effective quantum yield of PSII (Φ_{II}) was calculated as $(F_m' - F_s)/F_m'$. Additionally the photosynthetic parameters qP (photo-chemical quenching $(F_m' - F_s)/(F_m' - F_0)$) and NPQ (non-photochemical quenching $(F_m - F_m')/F_m'$) were determined.

2.2.10.2 Measurements of the redox state of P700

Redox changes in P700 were measured by monitoring the absorbance at 810 nm and 860 nm with a PAM 101/103 chlorophyll fluorometer (Walz) connected to a Dual Wavelength ED_P700DW emitter detector unit as described by Schreiber *et al.* 1988. Oxidised P700 level (ΔA) was recorded

in vivo during actinic light illumination at different light intensities (from 70 to 1200 $\mu\text{mol photons m}^{-2}\text{s}^{-1}$). The maximum level of oxidised P700 (ΔA_{max}) was determined with far red light (720 nm, 50 $\mu\text{mol photons m}^{-2}\text{s}^{-1}$) illumination. The P700 oxidation state was then calculated as ($\Delta A/\Delta A_{\text{max}}$).

2.2.10.3 Cyclic electron flow measurements

Ferredoxin-dependent plastoquinone reduction was measured in ruptured chloroplasts diluted in lysis buffer (see Chapter 2.2.4.5) to 10 $\mu\text{g chlorophyll ml}^{-1}$ and immediately used for the measurements of chlorophyll fluorescence with a PAM fluorometer 101/103 (Walz, Germany). The fluorescence increase after the addition of 5 μM spinach ferredoxin (Sigma) and 0.25 mM NADPH (Sigma) was recorded under measuring light corresponding to 1 $\mu\text{mol photons m}^{-2}\text{s}^{-1}$.

3 Results

3.1 Characterisation of PPP4 and TMP14

The presented work is based on a macroarray analysis, which was conducted in order to uncover the transcriptional regulation of nuclear genes encoding chloroplast proteins (Biehl *et al.*, 2005). Here, the *Arabidopsis thaliana* (*Arabidopsis*) genes encoding the Putative Photosynthetic Protein 4 (PPP4, At4g01150) and the Thylakoid Membrane Phosphoprotein of 14 kDa (TMP14, At2g46820; Hansson and Vener, 2003) were found to be co-regulated with groups enriched with photosynthetic genes and therefore were assumed to be involved in photosynthesis. TMP14 has been described as a novel subunit of PSI, probably interacting with the LHCII binding interface of this complex (Khrouchtchova *et al.*, 2005). The proteins encoded by *PPP4* and *TMP14* show sequence similarities, also with two other *Arabidopsis* proteins and their functional interaction has been investigated in this work.

3.1.1 Description of a novel protein family in photosynthetic organisms

Expression analysis of *PPP4* and *TMP14* with Genevestigator (www.genevestigator.ethz.ch; Zimmermann *et al.*, 2004) underlines their putative involvement in photosynthesis as both genes are preferentially expressed in green tissue and in response to light. *PPP4* encodes a protein of 164 amino acids, of which the N-terminal 62 amino acids are predicted by ChloroP to be a chloroplast targeting sequence (cTP). The resulting mature protein is calculated to have a molecular weight of 11.4 kDa. *TMP14* encodes a protein of 174 amino acids, of which the first 49 are predicted to be a cTP. The calculated molecular weight of TMP 14 is 13.9 kDa. Both proteins are predicted by the TMHMM server (www.cbs.dtu.dk/services/TMHMM-2.0) and most other computer programs for prediction of protein secondary structure (www.expasy.org) to contain two transmembrane helices (TMHMM: PPP4: amino acids 91-113 and 123-142; TMP14: amino acids 103-125 and 130-52). Within these two transmembrane regions they exhibit their highest sequence similarity (**Figure 3.1.1**; 40% identity and 66% similarity of mature protein sequences, as calculated by NCBI Blast 2 sequences).

Further two proteins of *Arabidopsis* exhibit sequence similarities to PPP4 and TMP14. One of the two proteins shows a higher homology to TMP14 and is thus named TMP14-like (At1g52220; 50% identity, 70% similarity to TMP14, 36% identity, 61% similarity to PPP4; sequences without cTP). The other one shows higher homology to PPP4 and is thus named PPP4-like (At4g38100; 45% identity, 68% similarity to PPP4, 34% identity, 56% similarity to TMP14; sequences without cTP).

Both of these proteins are also predicted by the TMHMM server to contain two transmembrane helices each (TMP14-like: amino acids 85-107 and 112-134; PPP4-like: amino acids 118-140 and 150-169).



Fig 3.1.1 Sequence comparison of mature proteins of all four homologous *Arabidopsis* proteins

Sequences of PPP4, TMP14, PPP4-like and TMP14-like without cTP were aligned using ClustalW (Thompson *et al.*, 1994) and Boxshade. Conserved amino acids are highlighted by black boxes, whereas grey ones indicate closely related amino acids.

To investigate orthologous proteins of this protein family in other plant species, the mature PPP4 amino acid sequence was blasted against the non-redundant protein sequence (nr) database of NCBI (Chapter 2.2.7). This showed that proteins of this novel *Arabidopsis* family are conserved in all photosynthetic organisms. The protein sequences of the resulting homologous proteins from grapevine (*Vitis vinifera*), populus (*Populus trichocarpa*), rice (*Oryza sativa*), the moss *Physcomitrella patens*, the alga *Chlamydomonas reinhardtii* and cyanobacteria (*Nostoc sp. PCC 7120* and *Synechocystis sp. PCC 6803*) were aligned using ClustalW (default settings, gap extension: 1). An unrooted phylogram was built from the C-terminal 120 amino acids of each protein, which show highest similarity, in order to avoid unspecific comparison of amino acids. For this the programs Phylip version 3.67, Protmlk (default settings; <http://evolution.genetics.washington.edu/phylip.html>) and Phylodraw version 0.8 (<http://pearl.cs.pusan.ac.kr/phylodraw>) were employed. As demonstrated in **Figure 3.1.2** depicting the resulting phylogram, five major branches can be distinguished, with four of them containing one of the *Arabidopsis* homologous proteins: (i) PPP4 orthologues, (ii) PPP4-like orthologues, (iii) TMP14 orthologues, (iv) TMP14-like orthologues and (v) cyanobacterial proteins. This suggests that all four eukaryotic proteins are ancient and have evolved from one cyanobacterial ancestor. Some interesting aspects are put forth by this bioinformatical analysis. Firstly, the PPP4 clade contains the highest number of orthologues, with a lower level of divergence of the flowering plant proteins as compared to the other clades. Moreover, the only alga homologue also clusters with PPP4. The moss *Physcomitrella* has one

PPP4 orthologue a well, but interestingly its proteome contains three different proteins most homologous to TMP14-like.

For TMP14 a sequence alignment with orthologues has been published (Hansson and Vener, 2003) and the alignment of the PPP4 orthologues is depicted in **Figure 3.1.3**.

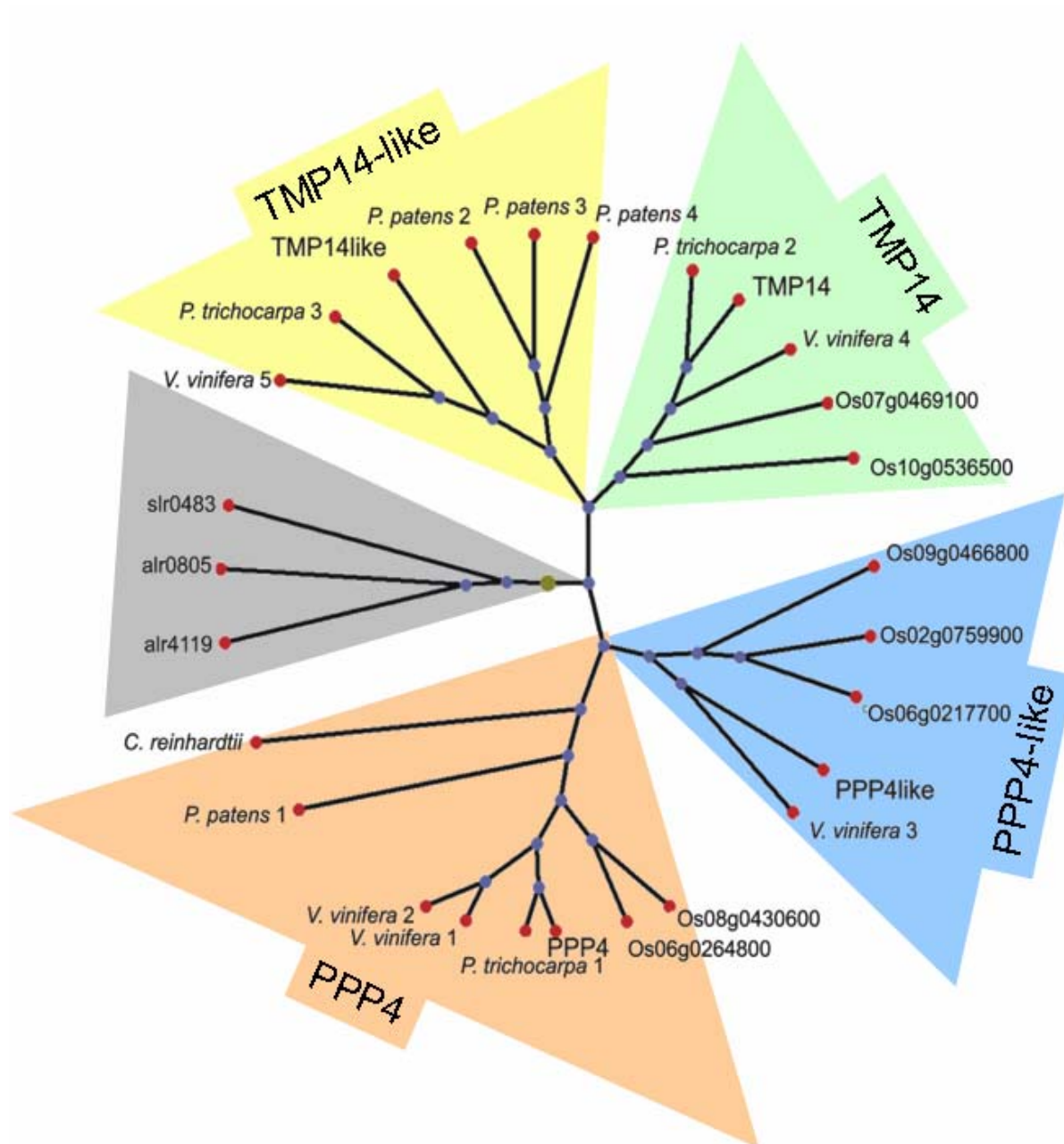


Fig 3.1.2 Unrooted Phylogram of the PPP4/TMP14 family of proteins

Protein sequences from *Arabidopsis*, grape-wine (*Vitis vinifera*), populus (*Populus trichocarpa*), rice (*Oryza sativa*), *Physcomitrella patens*, *Chlamydomonas reinhardtii* and cyanobacteria (*Nostoc sp. PCC 7120* and *Synechocystis sp. PCC 6803*) were obtained from the non-redundant (nr) protein database of NCBI (www.ncbi.nlm.nih.gov) and aligned using ClustalW (default settings; gap extensions:1; Thompson *et al.*, 1994). The unrooted Phylogram was built from the C-terminal 120 amino acids of each mature protein using the programs phylip version 3.67, Protmlk (default settings; <http://evolution.genetics.washington.edu/phylip.html>) and Phylodraw version 0.8 (<http://pearl.cs.pusan.ac.kr/phylodraw>).



Fig 3.1.3 Sequence comparison of the mature PPP4 proteins in *Arabidopsis*, *Oryza*, *Vitis*, *Populus*, *Physcomitrella* and *Chlamydomonas*

The mature amino acid sequence without cTP of the *Arabidopsis thaliana* PPP4 (At4g01150) was compared with related sequences from *Oryza sativa* (Os08g0430600, Os06g0264800), *Vitis vinifera* (IDs GI:147805130, GI:157349856), *Populus trichocarpa* (ID GI:118487811), *Physcomitrella patens* (ID GI:168048886) and *Chlamydomonas reinhardtii* (ID 1860020) using ClustalW (Thompson *et al.*, 1994) and Boxshade. Black boxes indicate strictly conserved amino acids, and gray boxes closely related ones. Sequences were obtained from NCBI (www.ncbi.nlm.nih.gov and <http://genome.jgi-psf.org/cgi-bin>).

3.1.2 Localisation of PPP4 and TMP14 in the thylakoid membrane

Analysis of the *Arabidopsis* chloroplast proteome (Kleffmann *et al.*, 2004), indicated that PPP4 and TMP14 are localised in the chloroplast and also the analyses of the thylakoid (Friso *et al.*, 2004) and the envelope (Fröhlich *et al.*, 2003) proteome found these proteins in the respective fractions. To verify the localisation within the chloroplast, *Arabidopsis* chloroplasts were isolated and then fractionated with a sucrose density gradient into thylakoids, stroma and two envelope containing fractions. Immuno-detection using specific antibodies against PPP4 and TMP14 (Chapter 2.2.4.1) demonstrated that both proteins are enriched in the thylakoid membrane (**Figure 3.1.4A**). A weak signal of the TMP14 antibody can be found in the envelope fractions, but the detected protein seems to have a slightly higher molecular weight, which indicates that the obtained signals is unspecific. To verify the transmembrane prediction of the TMHMM server, WT thylakoid membranes were treated with solutions of chaotropic salts and alkaline pH and the resulting fractions were assayed with Western analysis in order to obtain information about the stability of membrane protein interactions (Karnauchov *et al.*, 1997). After treatment with NaCl and Na₂CO₃, which extract membrane associated proteins, as seen with the stromal exposed β -subunit of the ATPase, both PPP4 and TMP14 can be found in the membrane fraction, which verifies the bioinformatically predicted transmembrane topology (**Figure 3.1.4B**). However, despite their similar protein sequence, anchorage in the membrane differs. Whereas only slight amounts of PPP4 are extracted by NaSCN and NaOH, most TMP14 protein can be found in the soluble fraction. The release of

TMP14 with NaOH (pH 13) indicates that the majority of interactions anchoring the protein are of electrostatic nature (Karnauchov *et al.*, 1997) and thus executed by other proteins. That electrostatics might play an important role for TMP14 interaction with other proteins, is supported by the amino acid sequence of the N-terminal sequence of the mature TMP14 protein, which contains one third (19/57) charged amino acids (5 lysines, 3 arginines, 8 glutamic acids and 2 aspartic acids). Whereas the very N-terminus contains 5 basic amino acids, the following stretch before the predicted transmembrane helices contains all 10 acidic amino acids. In the acidic amino acid stretch there are also 8 threonines, of which at least one is phosphorylated (T65, T66; Hansson and Vener, 2003), adding to the negativity of this stretch. The extraction of TMP14 by 2 M NaSCN, a salt which at this concentration destroys the integrity of the membrane, but not by 2 M NaCl suggests that extraction of the TMP14 protein by chaotropic salts, which disrupt hydrophobic interactions, can only take place under conditions in which the integrity of the thylakoids is destroyed.

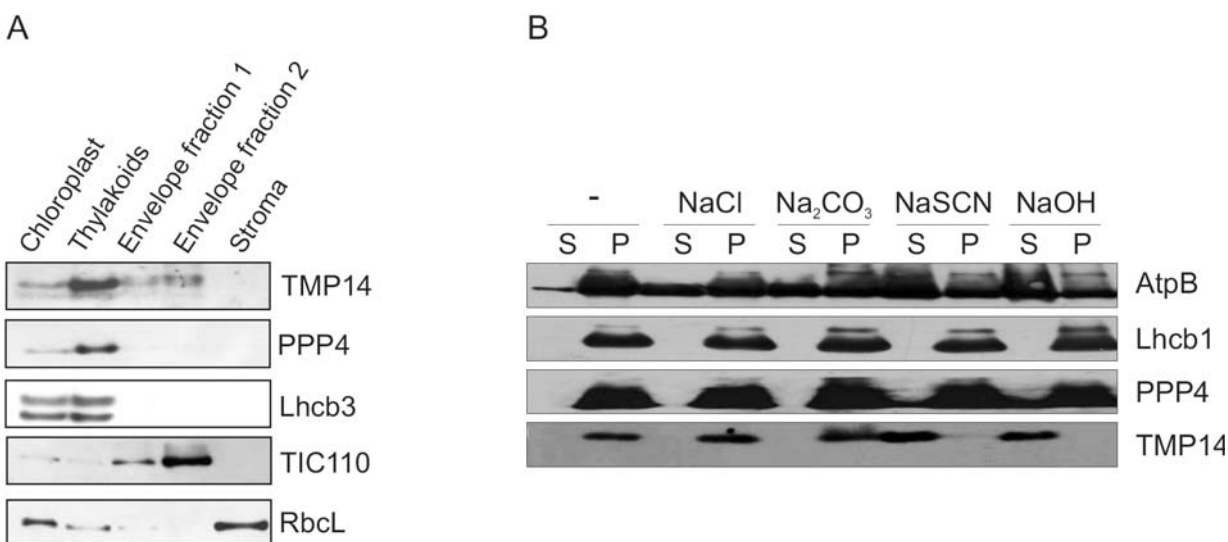


Fig 3.1.4 Localisation and topology of PPP4 and TMP14

(A) Fractionation of chloroplasts. Chloroplasts were isolated via Percoll gradient and after lysis further fractionated on a sucrose gradient. Phases were collected and proteins of half of the two envelope fractions and 1/10th of the stroma were precipitated with TCA. Chloroplasts corresponding to 2.5 μ g and thylakoids corresponding to 5 μ g of chlorophyll and precipitated fractions were loaded onto SDS-PAGE, transferred to PDVF membrane and immunodetection was carried out using antibodies against fraction specific proteins, Lhcb3 (thylakoids), Tic 110 (envelope), RbcL (stroma) as well as PPP4 and TMP14. (B) Extraction of PPP4 and TMP14 by solutions of chaotropic salts or alkaline pH. Isolated *Arabidopsis* thylakoids were resuspended at 0.5 mg chlorophyll/ml in buffer (10 mM HEPES/ KOH, pH 7.5) containing either 2 M NaCl, 2 M NaSCN, 0.1 M Na₂CO₃, 0.1 M NaOH or no additive. After incubation for 30 min on ice, the assays were separated into membrane fractions (P) and supernatants (S), proteins were separated by SDS-PAGE and immuno-labelling was carried out with specific antibodies against AtpB as control for membrane associated proteins, Lhcb1 as control for membrane integral proteins, PPP4 and TMP14.

3.1.3 Knock-out mutants of *PPP4* and *TMP14*

Gene structures of *PPP4* and *TMP14* are depicted in **Figure 3.1.5A**. The predicted intron-exon organizations were confirmed by RT-PCR for both genes and the sequences obtained were

compared with the coding sequences available on public websites (MIPS: <http://mips.gsf.de/proj/plant/jsf/athal/searchjsp/index.jsp> and TAIR: <http://www.arabidopsis.org>). For *TMP14* only the coding sequence annotated as *At2g46820.1* could be supported. Insertion lines for *PPP4* and *TMP14* were identified by searching T-DNA insertion flanking databases. The presence of the insertion and the exact insertion point were confirmed by PCR with gene and T-DNA border specific primers and subsequent sequencing of the amplified product. For each, *PPP4* and *TMP14* two independent knock-out alleles were obtained and analysed. Both *ppp4* alleles are in the Landsberg *erecta* (*Ler*) ecotype, whereas *tmp14-1* is an insertion in Noessen (No-0) and *tmp14-2* in Wassilewskija (*WS*) background. The lack of PPP4 and TMP14 proteins in the respective mutants was confirmed by Western analysis of total leaf protein extract using monospecific epitope antibodies (**Figure 3.1.5B**). However, no significant growth phenotype could be observed in the mutants neither under greenhouse nor under climate chamber conditions.

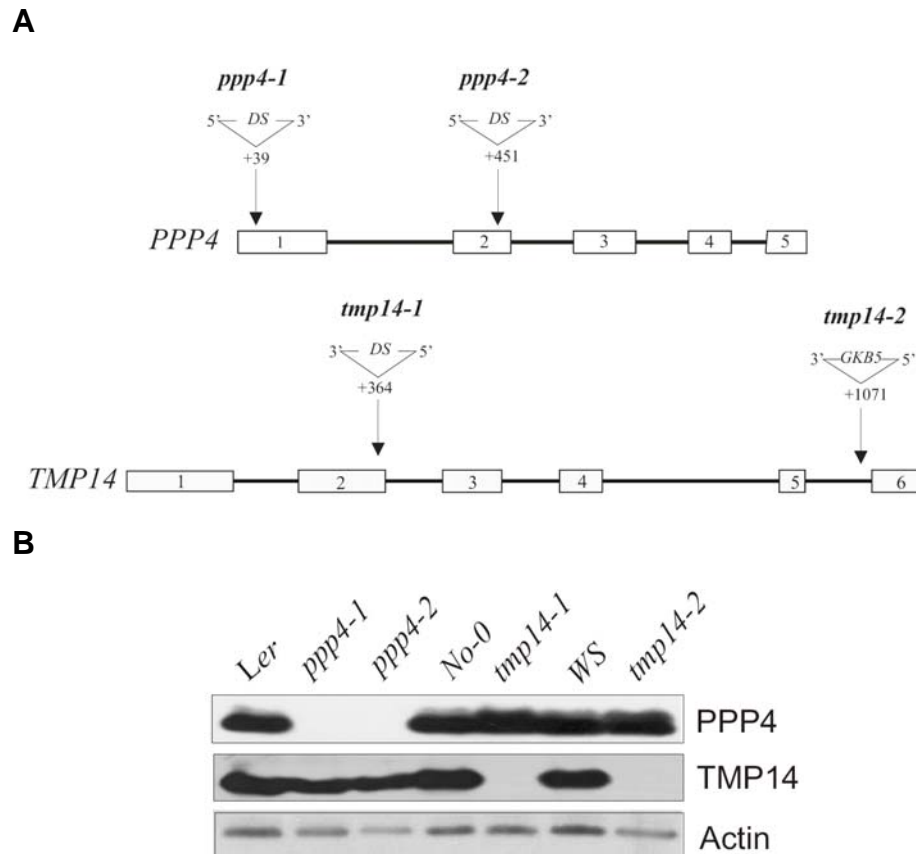


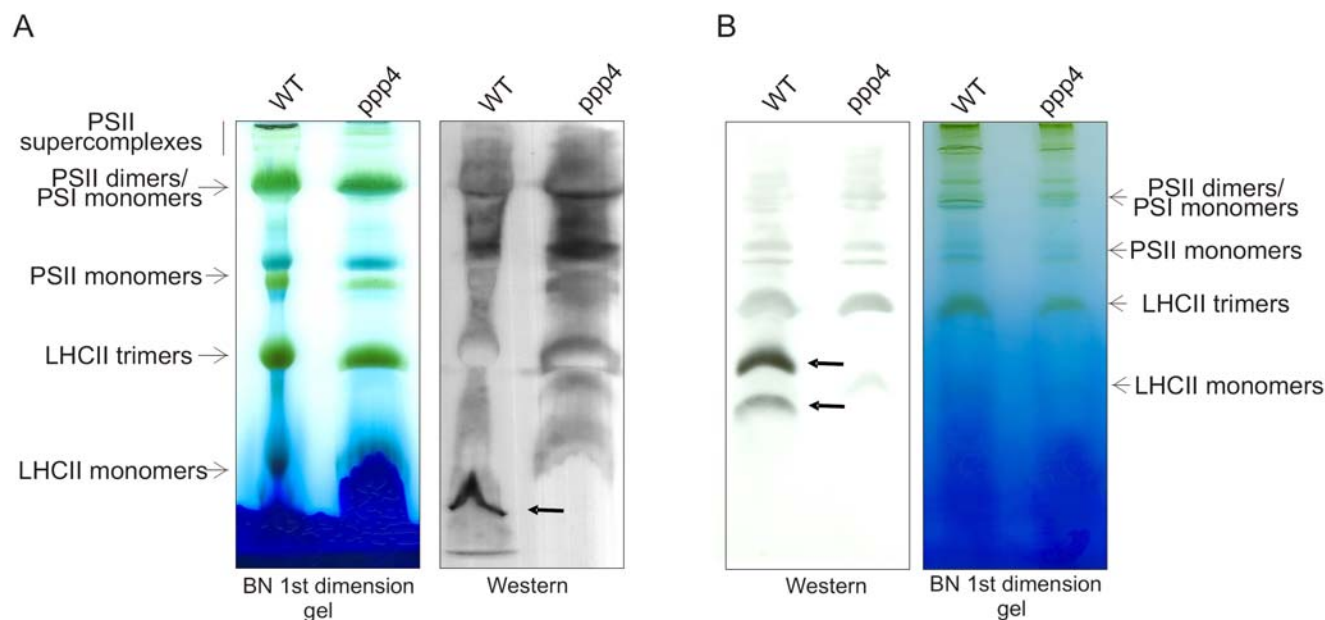
Fig 3.1.5 Gene models, T-DNA insertions and their effects on gene product accumulation

(A) Exons are depicted as open numbered boxes, introns as connecting black line. For each T-DNA mutant used in this study, the site and the orientation of the insertion is provided. Except for *tmp14-2* all mutant alleles stem from the insertion of Dissociation (DS) transposable elements. Both *ppp4* alleles are in the Landsberg *erecta* (*Ler*) background and were found in the IMA DS (*ppp4-1*; SGT_3_4785) and in the Exotic DS collection (*ppp4-2*; GT_5_18961). The *tmp14-1* allele was discovered in the RIKEN DS collection and has Noessen (No-0) background (RATM15-2546-1_H) and *tmp14-2* has originated from a T-DNA insertion of the pGKB5 T-DNA in the gene of the Wassilewskija (*WS*) ecotype (FLAG_218A11). (B) Western analysis was conducted on total leaf protein extract with PPP4, TMP14 specific antibodies and antibodies against Actin as loading control.

3.1.4 Localisation of PPP4 in BN-PAGE

Mass spectrometry (MS) -analysis of barley chloroplast complexes solubilised with β -dodecylmaltoside (β -DM) and separated by Blue Native PAGE (BN-PAGE; Schägger and von Jagow, 1991), demonstrated that the barley orthologue of PPP4 (also about 11 kDa) does not primarily migrate as a monomer. But as could be seen on the second dimension, where it was identified as a Coomassie stained spot, PPP4 migrates at a size slightly smaller than the LHCII monomers (about 60 kDa; Granvogl *et al.*, 2006). That PPP4 can be visualised by Coomassie staining indicates a high abundance of the protein in the thylakoid membrane, because the majority of other proteins stainable with Coomassie are components of the highly abundant photosynthetic complexes (Granvogl *et al.*, 2006).

To study, if these results obtained in barley, hold true also for *Arabidopsis* PPP4, BN-PAGE was carried out with solubilised *Arabidopsis* thylakoids. To investigate, if the PPP4 complex displays detergent-specific extraction properties, solubilisation was carried out independently with two detergents: (i) β -DM, which is routinely used for solubilising thylakoid complexes (Granvogl *et al.*, 2006) and (ii) digitonin, which had previously been shown to allow the solubilisation of a PSI:LHCII super-complex from the thylakoid membrane (Zhang and Scheller, 2004).



3.1.6 PPP4 is involved in complexes in the thylakoid membrane

(A) Left panel shows BN-PAGE with β -DM (1.25 %) solubilised thylakoids from WT and *ppp4* mutant plants and right panel depicts Western blot of the same gel, immuno-decorated with the specific antibody against PPP4. Arrows indicate the specific signal in the WT. (B) As in (A) except thylakoids were solubilised with 2.8% digitonin.

Complex separation by native first dimensions following solubilisation with β -DM, demonstrated that also *Arabidopsis* PPP4 migrates just below the LHCII monomers, which runs at about 60 kDa (Granvogl *et al.*, 2006). However, as can be seen in **Figure 3.1.6B** solubilisation with the detergent digitonin does result in the extraction of a larger PPP4-containing complex from the thylakoid membrane, as PPP4 co-migrates with two complexes on the BN-PAGE. The bigger of the two complexes migrates at a size between monomers and trimers (about 140 kDa) of LHCII, whereas the smaller one runs just below the LHCII monomers. In the subsequent steps of this thesis all solubilisation steps were performed by using digitonin in order to identify further components of the two PPP4-containing complexes.

Consequently, analysis of the second, denaturing SDS-PAGE was carried out and it could be shown that unlike in barley, *Arabidopsis* thylakoids do not contain sufficient PPP4 to be stained with colloidal Coomassie, as no spot became visible at the expected size and location. However, by comparing the protein spot patterns of silver stained BN second dimensions from WT and *ppp4* thylakoid complexes (**Figure 3.1.7**) it becomes evident that the protein can be visualised by silver staining. The identity of the respective spot in the WT second dimension as PPP4 was verified by excision and subsequent MS-analysis of the trypsin digested protein. Moreover, MS analysis identified TMP14 as a protein of slightly larger size (**Figure 3.1.7**, black arrow) than PPP4 (red arrow) co-migrating with the larger PPP4 containing complex. The spot co-migrating with the smaller complex of PPP4 was identified as TMP14-like (green arrow). For each respective spot the identified peptides yielded 46% of sequence coverage for the mature PPP4, 40% for TMP14 and 41% for TMP14-like (for fragmentation spectra of identified peptides see Chapter 6.1). Subsequent Western analyses of the WT second dimension with the available antibodies against PPP4 and TMP14 show that both can be found co-localised in four distinct positions. The two lower molecular weight complexes are according to the sizes of PPP4-containing complexes as also seen in the first dimension and contain the majority of both proteins. TMP14 is mostly co-localised with the higher molecular weight complex of the two. The two larger complexes, in which only small fractions of PPP4 and TMP14 co-migrate, are at the size of the Cyt *b₆f* monomer and at a size slightly smaller than PSII dimers and PSI monomers. Analyses of second dimensions of solubilised thylakoids from mutant plants indicate that PPP4 forms a complex of smaller size, if TMP14 is absent, whereas TMP14 complex assembly is impaired in the absence of PPP4. However, some TMP14 still forms a complex, as detectable by MS analysis of the excised spot at the same position as in the WT. Altogether, it can be concluded from analysing thylakoid complexes of WT, *ppp4* and *tmp14* plants that absence of neither PPP4 nor TMP14 affects the abundances and structures of the

major photosynthetic thylakoid complexes (neither does the double mutant; data not shown). However, the existence of a novel complex probably containing both PPP4 and TMP14 could be demonstrated by solubilising thylakoid membranes with digitonin.

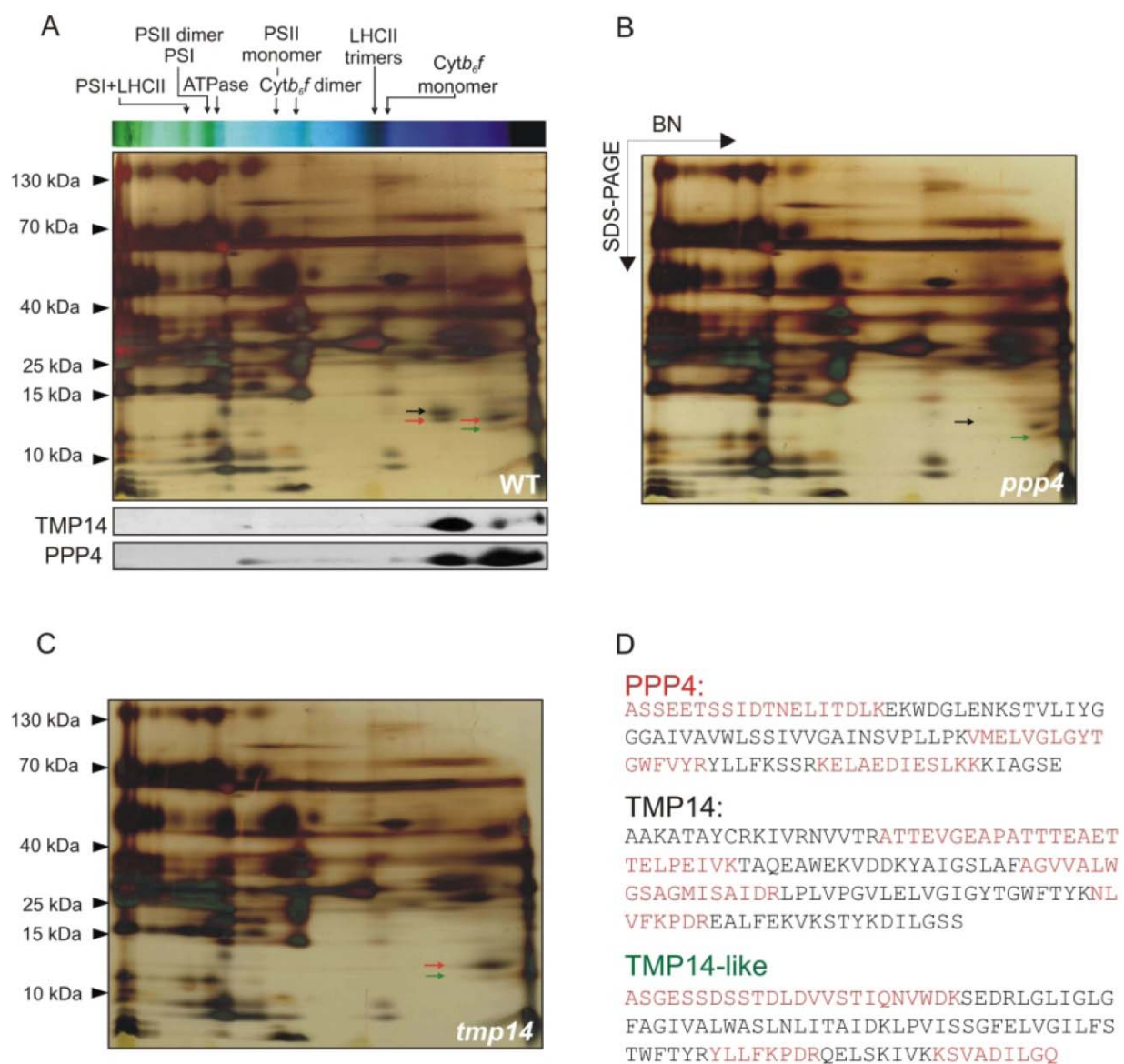


Fig 3.1.7 PPP4 co-migrates with TMP14 and TMP14-like

Two-dimensional separation of digitonin solubilised thylakoid protein complexes by BN/SDS-PAGE. After separation of the protein complexes of WT (**A**), *ppp4* (**B**) and *tmp14* (**C**) on a Blue-Native gel, the composition of their subunits was further analysed by subsequent denaturing Tris-Tricine SDS-PAGE. The gels were either stained with silver (A-C) or blotted onto PVDF membrane and immunodecorated with TMP14 and PPP4 specific antibodies (A). Silver-stained spots as indicated by arrows were excised and analysed by MS-analysis. Red, black and green arrows indicate spots of which the highest abundant protein is PPP4, TMP14 and TMP14-like, respectively. (**D**) Peptides identified by MS in each respective spot are indicated in red. Identification of the macromolecular protein complexes of thylakoid membranes is given on the top of gel (A).

3.1.5 TMP14 protein levels are decreased in *ppp4* mutants

Because in the previous experiments immuno-detection of TMP14 in the *ppp4* mutants (KO analysis and BN second dimension) indicated a severe reduction in protein amounts, quantification of relative TMP14 levels in total protein extract and in thylakoids was performed by Western analysis. Antibodies against Actin were used as loading controls for total protein extracts. The application of antibodies against Lhca3 to ensure equal loading of thylakoid proteins was employed, because this antibody was used by Khrouchtchova *et al.*, 2005 in their work on TMP14 for the same purpose. As can be seen in **Figure 3.1.8**, TMP14 protein accumulates up to about 75% of WT in *ppp4* total protein extract. However, the amount of TMP14 integrated in the thylakoid membrane is only about 50% in comparison to WT. This indicates that the reduction of TMP14 levels is probably due to stabilizing or integrating effects of PPP4 and does not result from changes in *TMP14* expression.

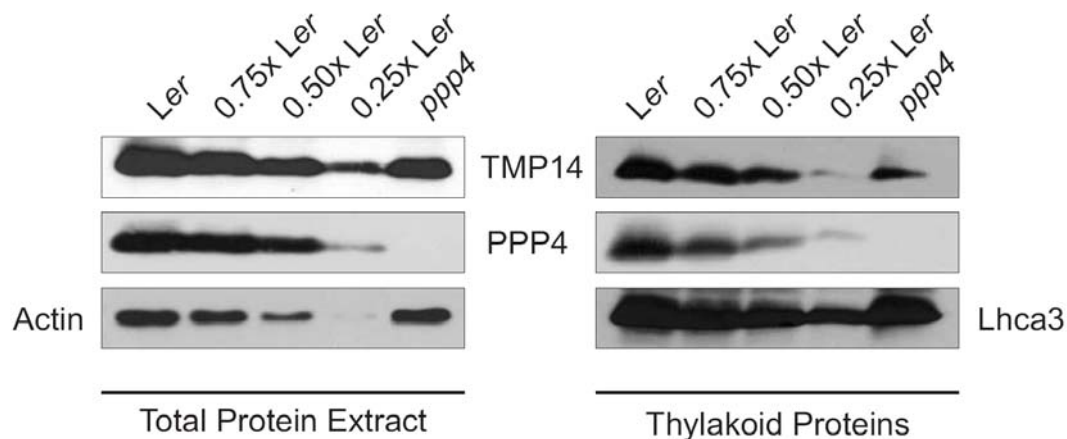


Fig 3.1.8 TMP14 protein abundance in the thylakoid membrane depends on presence of PPP4

Total protein extract (left panel) and thylakoid proteins (right panel) of *Ler* and *ppp4* plants corresponding to 5 μg of chlorophyll and decreasing amounts as indicated in the legend were separated by SDS-PAGE and immuno-detection was carried out with specific antibodies against TMP14, PPP4 and Actin, Lhca3 as loading control.

3.1.6 Investigating the interaction between PPP4 and TMP14

To verify the interaction of PPP4 and TMP14 two independent approaches were taken. Firstly, crosslinking with Bis (Sulfosuccinimidyl) suberate (BS^3), a membrane-impermeable crosslinking agent with an 11.4 \AA spacer arm was carried out and secondly, Co-IP was performed with digitonin solubilised thylakoids.

3.1.6.1 Epitope tagging of PPP4

Tagged versions of the PPP4 protein were created because of two reasons. Firstly, tagged proteins are routinely used for immuno-precipitation experiments, because of the specificity of the

commercially available tag antibodies. Secondly, indications for multimerisation of PPP4 necessitated the creation of a PPP4 of differing size. Therefore, the nucleotide sequences encoding the c-myc and the HA epitopes were fused to the 3' of the *PPP4* cDNA sequence. For this, full length *PPP4* cDNA was inserted into the binary vectors pPCV812 Δ *NotI*-Pily (*HA*) and pPCV812 Δ *NotI*-Lola (*c-myc*; Chapter 2.2.3.2), which both contain a double 35S promoter upstream of the insertion region. *Agrobacterium* mediated transformation of *ppp4-2* plants was carried out according to Chapter 2.2.3.3 and transformants were selected with hygromycin. Homozygous T3 lines were analysed for expression of the transgene by Western analysis of total protein extract, using specific antibodies against Actin as loading control, PPP4, HA and c-myc (**Figure 3.1.9**).

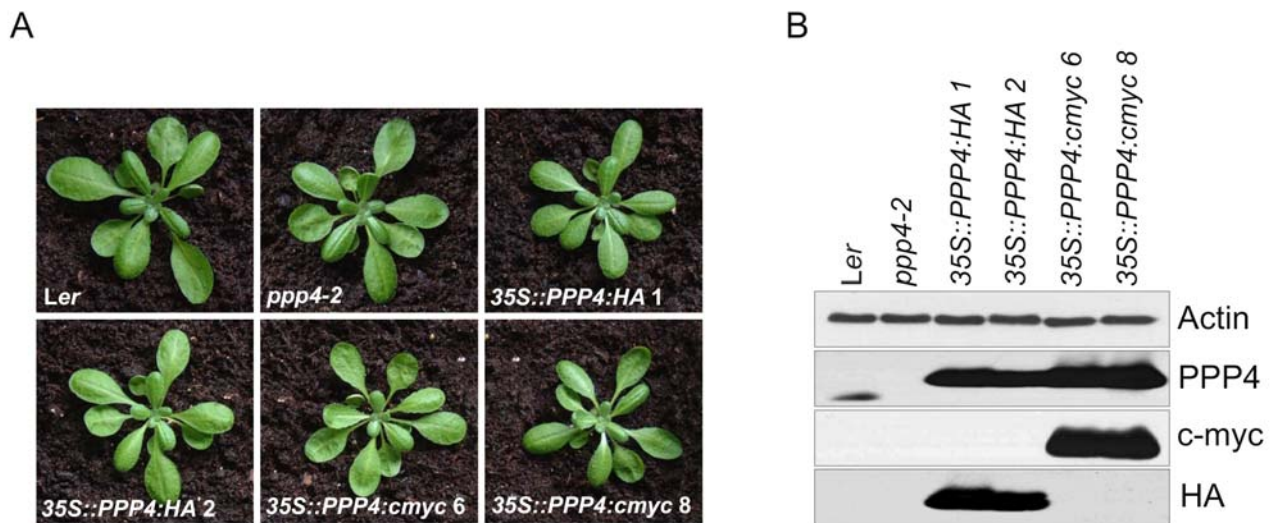


Fig 3.1.9 Transgenic plants expressing epitope tagged PPP4

The *PPP4* cDNA was inserted into the binary vectors pPCV812 Δ *NotI*-Pily (*Hemagglutinin*; *HA*) and pPCV812 Δ *NotI*-Lola (*c-myc*) flanked by a 35S promoter at the 5' and the respective tag coding sequence at the 3'. **(A)** Four week old WT, *ppp4-2* and *ppp4-2* plants transformed with both constructs. **(B)** Transgene expression analysis was carried out on total protein extract. *PPP4* is overexpressed in all four lines and tags are recognised by the respective antibodies as depicted on the right

As can be observed in **Figure 3.1.9B** the tagged proteins are expressed at higher levels in the transgenic plants than the native PPP4 in WT. The resulting tagged PPP4 has an apparent molecular weight of about 16 kDa. Because detection with the HA antibody yields some slight unspecific bands upon long exposure, work was continued with the 35S::*PPP4*:*c-myc* lines # 6 and # 8. To obtain plants expressing both native and tagged protein the line #6 was crossed with the *Ler* WT.

3.1.6.2 Crosslinking

Crosslinking is a powerful tool to dissect protein interactions. If putative interaction partners are known, the existence of a complex comprising these components can easily be demonstrated by crosslinking of proteins in a mutant lacking a specific protein, followed by Western detection using antibodies against the expected interaction partner protein and vice versa. Depending on the

structure and sequence of the interacting proteins, different crosslinkers are required to detect the interaction by covalently linking the interaction partners. Here, Bis (Sulfosuccinimidyl) suberate (BS³), a membrane-impermeable, non-cleavable crosslinking agent with an 11.4 Å spacer arm and its cleavable analog 3,3'-Dithiobis[sulfosuccinimidylpropionate] (DTSSP), which has a 12 Å spacer arm, were successfully employed to yield immuno-detectable PPP4 crosslinking products.

To investigate the existence of a complex containing TMP14 and PPP4, thylakoid membranes were crosslinked with BS³ according to the method described in Chapter 2.2.4.11. The Coomassie-stained gel shows that protein content and patterns are equal between the different samples (**Figure 3.1.10A**). Furthermore, it demonstrates that no unspecific crosslinking events have occurred as the protein patterns still resemble those of the untreated thylakoid proteome. In Western analyses the monomeric PPP4 can be detected in WT and *tmp14* as a strong band of about 11 kDa, in accordance with its deduced molecular mass of 11.4 kDa. A further strong band is visible in both samples at about 23 kDa and two weaker bands at about 34 kDa and 45 kDa, the sizes indicating that these PPP4 containing bands might be originating from crosslinking of components of a PPP4 tetramer. Additionally, to these four crosslinking products, four more immuno-reactive bands are present in the WT but not in the *tmp14* sample. The lack of these extra WT bands in *tmp14* demonstrates that they stem from a PPP4 TMP14 interaction. Immunodecoration of the same membrane with TMP14 antibodies shows that monomeric TMP14 can be detected in WT and *ppp4* as a weak double band of the expected molecular weight of 14 kDa (Hansson and Vener, 2003). A further, strong band is visible in both samples at about 28 kDa, suggesting the detection of a crosslinked TMP14 dimer. According to the results obtained with the PPP4 antibody, the TMP14 antibody recognises additional bands in WT crosslinked thylakoids, which are absent in the *ppp4* mutant sample. Merging the signals derived from immunodetection with the PPP4 and the TMP14 antibody, the bands missing in the mutants overlap in the WT, further indicating that they originate from a crosslinked interaction of both PPP4 and TMP14 (**Figure 3.1.10A**; right panel). That two immuno-detectable bands appear in WT at about 25 kDa might result from a post-translational modification of one of the two interaction partners leading to a slight increase of the size of the crosslinked product. In the *ppp4* sample two further clear bands are detected by the TMP14 antibody, one at about 40 kDa and one at about 45 kDa. Both of the two could be due to the detection of a TMP14 trimer of a predicted 42 kDa, which might preferentially form in the absence of PPP4. The other of the two bands might originate from the interaction of TMP14 with a further unknown protein. As this band shows exclusively in the *ppp4* mutant, the presence of the interaction might only occur in the absence of PPP4.

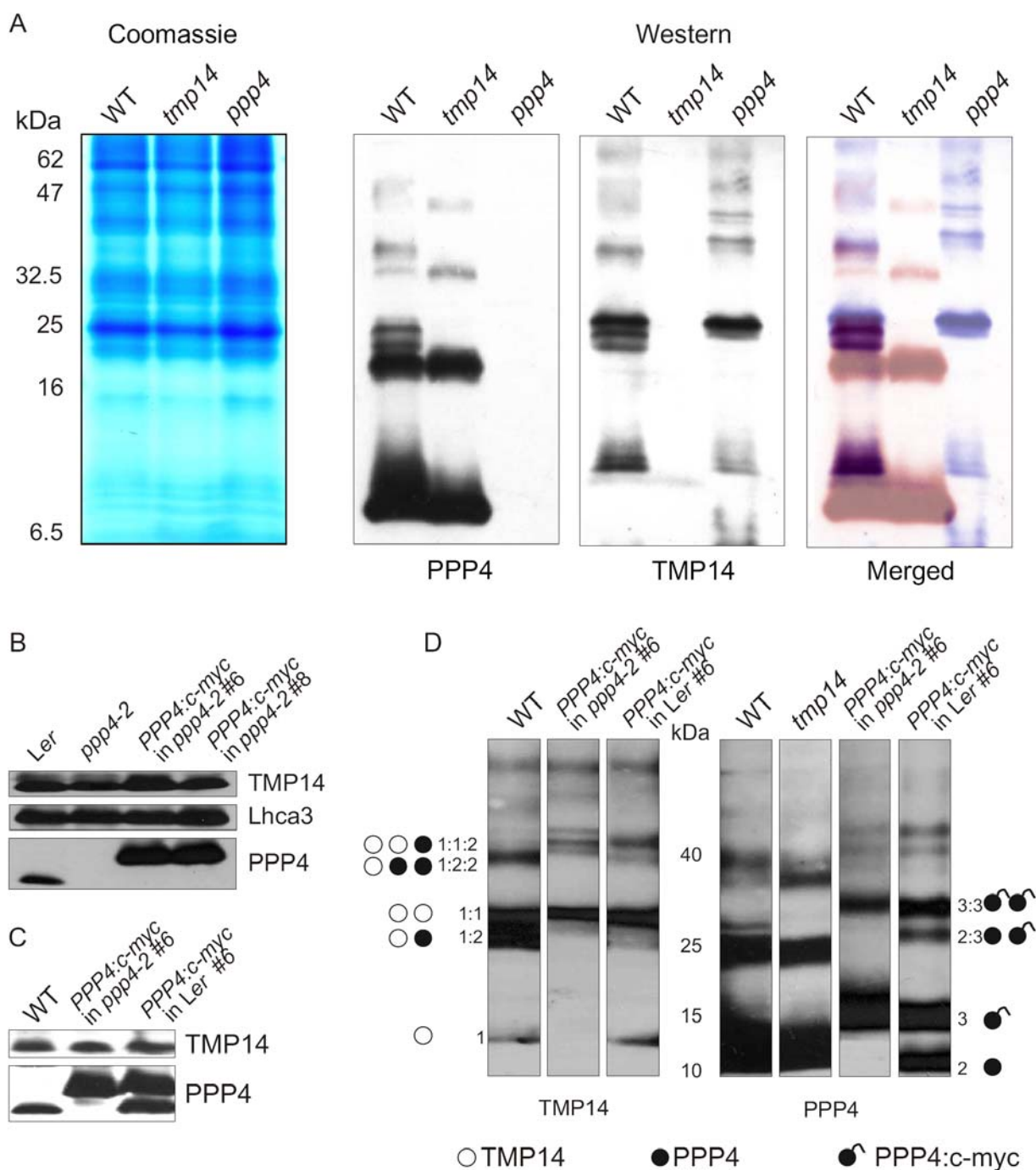


Fig 3.1.10 PPP4:TMP14 and PPP4:PPP4c-myc interactions can be crosslinked with BS³

(A) Thylakoid proteins of WT, *tmp14* and *ppp4* mutant plants were crosslinked with BS³, separated by SDS PAGE, subsequently either stained with colloidal Coomassie or transferred to PVDF and then immuno-decorated using specific PPP4 and TMP 14 antibodies. The signals resulting from detection with the TMP14 and PPP4 antibodies were converted into coloured bands (PPP4: red; TMP14: blue) and merged using Adobe Photoshop. (B,C) Western analysis of thylakoid extract from WT, *ppp4-2*, *35S::PPP4:c-myc* in *ppp4-2* #6, #8, *35S::PPP4:c-myc*#6 in *Ler* in order to quantify the relation of TMP14 and PPP4 levels (D) Thylakoid proteins from *Ler* and *ppp4-2* plants expressing *PPP4:c-myc* from a 35S promoter, *tmp14* and WT were crosslinked with BS³, separated by SDS-PAGE and immuno-decorated with the TMP14 and PPP4 antibodies. Numbers on left of TMP14 and on right of PPP4 hybridised blots indicate nature of crosslinking products (1: TMP14; 2:PPP4; 3:PPP4:c-myc).

When comparing the strength of the monomeric signals with the strength of signals of crosslinked products, it becomes obvious that crosslinking of TMP14 has progressed further than that of PPP4. Firstly, this could be due to the differences in amino acid sequence between PPP4 and TMP14 and the chemical properties of the crosslinker, which reacts with two amino groups on both sides of a 11.4 Å spacer, and covalently links them. TMP14 contains 12 and therefore five more basic amino acid residues than PPP4 in non-membrane spanning regions, which can be employed in the crosslinking reaction. Secondly, the higher rate of TMP14 crosslinking could be due to a better accessibility of the protein to the crosslinker. TMP14 might be part of the periphery of a bigger complex and thus be more exposed to the reactive agent.

To verify the existence of PPP4 multimers, the crosslinking reaction was carried out with *Ler* and *ppp4* plants expressing PPP4:c-myc (**Figure 3.1.10D**). Here, crosslinking of the overexpressed tagged PPP4 occurred at an increased rate as compared to the native PPP4. Accordingly, to allow visual separation of crosslinking products, incubation of thylakoids from PPP4:c-myc expressing plants with BS³ was reduced from 1 h to 30 min. Detection of PPP4 from **PPP4:c-myc** expressing *Ler* plants shows that besides the monomers of both PPP4 (**Figure 3.1.10D**: 2) and PPP4:c-myc (3) and the dimer of PPP4:c-myc (3:3) a specific crosslinking product is present at a size smaller than the PPP4:c-myc dimer. This probably presents a crosslinked PPP4, PPP4:c-myc interaction (3:2). The dimer of the untagged PPP4 cannot be detected here, probably because of the the lower rate of crosslinking reactions within the 30 min of incubation time. Crosslinked interactions between TMP14 and PPP4 are severely decreased in both PPP4:c-myc expressing backgrounds, as shown by immuno-decoration using the TMP14 antibody.

3.1.6.3 Co-immunoprecipitation (Co-IP)

To identify interaction partners of membrane proteins by co-immunoprecipitation (Co-IP) it is prerequisite to solubilise the membranes in such a way that the protein complexes stay intact. Because treatment with digitonin resulted in the detection of two complexes containing PPP4 and TMP14 in BN-gels (Figure 3.1.7), solubilisation was carried out with this detergent in order to verify the interaction of both proteins and to identify further interactors. As a preliminary experiment, Co-IP was carried out with the specific antibodies against PPP4 and TMP14 according to the method described in Chapter 2.2.4.12. However, only the TMP14 antibody was successfully employed for precipitation of the respective protein. Therefore, co-immunoprecipitation was performed with thylakoids of WT and *tmp14* mutant plants with this antibody in order to investigate, if also PPP4 can be precipitated and to ensure that precipitation of PPP4 depends on the presence of TMP14 and not on an unspecific interaction of the TMP14 antibody with the similar

PPP4 protein. Although Western analyses of *tmp14* total protein extracts (3.1.1.3 and 3.1.1.5) had not indicated any cross reactions of the specific antibodies, the absence of a cross reaction of the TMP14 antibody with the native PPP4 protein had to be established. According to **Figure 3.1.11A** immunodecoration with the TMP14 antibody yields a signal in the WT input and Co-IP lane, demonstrating that the TMP14 antibody was successfully employed for precipitation of the native protein. Indeed, using the PPP4 antibody a signal is visible in the all lanes except for the *tmp14* Co-IP lane, demonstrating that precipitation of PPP4 with the TMP14 antibody occurs only in the presence of TMP14. A control immuno-decoration with the PSI-F antibody results solely in detectable signals in the input and not in the Co-IP lanes, showing that the detection of PPP4 in the WT immunoprecipitate is not due to contamination with other thylakoid proteins.

To identify interaction partners besides PPP4, the co-immunoprecipitate was analysed by MS. As MS analysis is very sensitive and thus prone to measure the slightest contaminations, the precipitate from *tmp14* thylakoids was used as a negative control. Additionally, the co-immunoprecipitate of TMP14 from the *ppp4* thylakoids was analysed, because additional TMP14 crosslinking signals had appeared in this mutant, which were not present in the WT (Figure 3.1.10A). However, MS analysis only detected TMP14 in this precipitate, which might be due to the disbandment of the interaction of TMP14 with the unknown protein by the solubilisation with digitonin. As expected from Western analysis the WT sample contained TMP14 and the co-precipitated PPP4.

In order to test if also the reciprocal precipitation of TMP14 with PPP4 is possible, thylakoid membranes of WT, *Ler* and *ppp4* expressing *PPP4:c-myc* were isolated and Co-IP was performed with either antibodies against TMP14 or c-myc (**Figure 3.1.11B**). Using the TMP14 antibody both PPP4 forms can be co-precipitated, however with a bias to the native protein, when both forms are present. This underlines the results obtained from crosslinking of thylakoid proteins in the *PPP4:c-myc* overexpressing backgrounds, where interaction of TMP14 with PPP4 seemed to be suppressed (Figure 3.1.10D). With the c-myc antibody the native PPP4 can be precipitated in the presence of *PPP4:c-myc*. However, precipitation of detectable amounts of TMP14 with the c-myc antibody was not possible. This could be due to a displacement of the interacting TMP14 protein by this antibody.

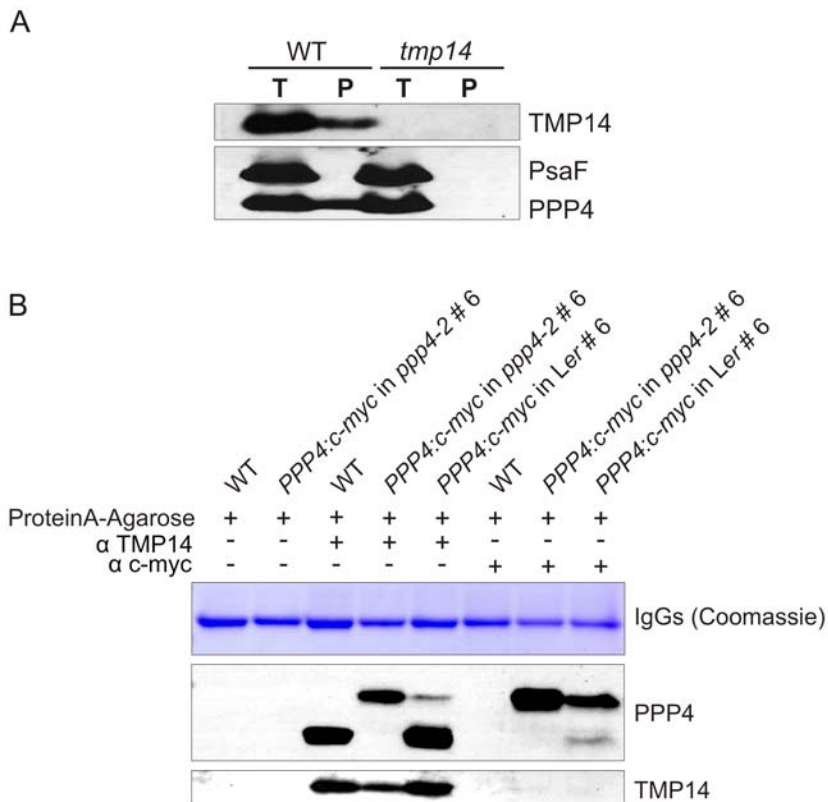


Fig 3.1.11 PPP4 co-precipitates with TMP14 and PPP4:c-myc

(A) Thylakoid membranes from WT (No-0) and *tmp14* mutants at a concentration of 1.5 mg chlorophyll ml⁻¹ were incubated with 1/6th volume of specific antibodies against TMP14 for 2h at 4°C and then treated with 2.5% digitonin for 1h at 4°C. Solubilised complexes were precipitated with ProteinA-Agarose by o/n end over end mixing at 4°C and following centrifugation. The pellet was washed five times and bound proteins were eluted by adding boiling SDS-PAGE loading dye. Thylakoid membrane (T) and immunoprecipitated (P) proteins were separated by SDS-PAGE, transferred to PDVF membrane and immuno-decorated with specific antibodies against TMP14, PPP4 and PSI-F. (B) Co-IP was carried out with thylakoid proteins from WT, *Ler* and *ppp4-2* plants expressing *PPP4:c-myc* as described in (A) with antibodies against TMP14 and c-myc.

3.1.7 TMP14 and PPP4 are not stably associated with any of the main photosynthetic complexes

In earlier work, TMP14 was reported to be a novel subunit of PSI based on the results that it co-migrated solely with PSI in both BN gels and sucrose gradient fractionations (Khrouchtchova *et al.*, 2005). It was therefore named PSI-P. This work also showed that TMP14/ PSI-P protein was absent in plants lacking the L and G subunits of PSI and that its levels were increased in a *psao* RNAi line. Because the results from BN gels, crosslinking and Co-IP experiments demonstrate that TMP14 is forming a complex with PPP4 and is not associated with any of the four major thylakoid complexes, two further experiments from the work of Khrouchtchova *et al.* were repeated to confirm that TMP14 is not associated with PSI and to investigate, if its levels as stated in the previous work depend on the presence of L and O subunits of PSI. Therefore, PSI was isolated by sucrose gradient

fractionation and Western analysis was carried out with antibodies against TMP14, PPP4 and PsaF. **Figure 3.1.12A** demonstrates that TMP14 and PPP4 can be detected in the thylakoids, but not in the PSI isolation, thereby confirming the results gained from BN gel analysis in this thesis (Chapter 3.1.4). For the second experiment, thylakoid proteins were isolated from *psal* (SALK_000637), *psao* (SALK_021621), *tmp14*, *ppp4* mutant plants and the corresponding WT ecotypes, separated by SDS-PAGE and Western analysis was carried out with specific antibodies against TMP14, PPP4, PsaL and PsaO (**Figure 3.1.12B**). Lhca3 hybridisation was used as loading control as in Khrouchtchova *et al.* (2005). However, contrary to their results, TMP14 levels are neither changed in the *psal* nor the *psao*, but are altered in the *ppp4* mutant background.

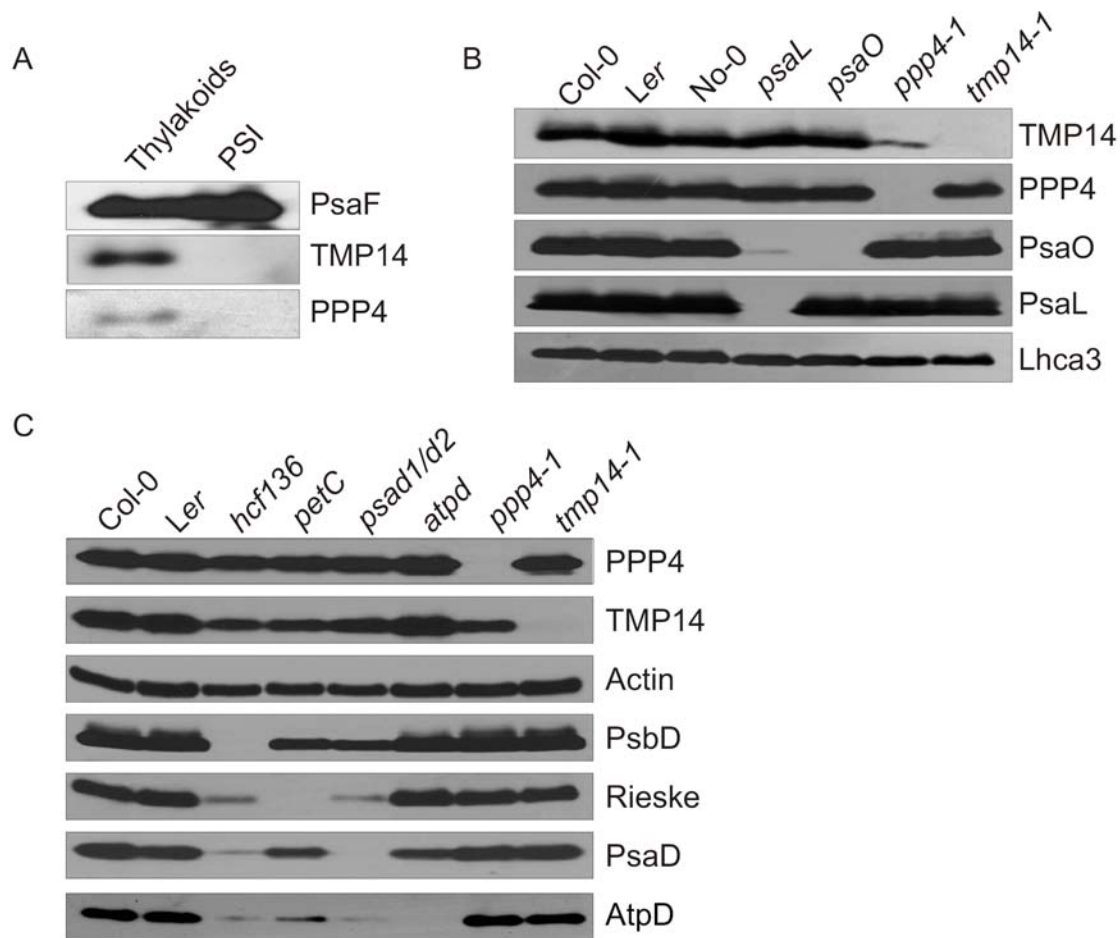


Fig 3.1.12 TMP14 and PPP4 are not constitutive components of one of the thylakoid photosynthesis complexes

(A) PSI was isolated from WT thylakoids via sucrose gradient centrifugation. Thylakoid and PSI proteins according to 5 μ g of chlorophyll were separated by SDS-PAGE and Western analysis was carried out using specific antibodies against PsaF, TMP14 and PPP4. (B) Thylakoid proteins according to 5 μ g of chlorophyll of the three ecotypes Col-0, Ler, No-0 and the four mutant lines *psal*, *psao*, *ppp4* and *tmp14* were separated by SDS-PAGE and Western analysis was performed with antibodies depicted on the right. (C) Immuno-detection of TMP14 and PPP4 in Col-0, Ler, *hcf136*, *petC*, *psad1/d2*, *atpd*, *ppp4* and *tmp14*. The applied antibodies are depicted on the right. Total protein extract corresponding to 40 μ g of protein was loaded each.

Additionally, it was tested, whether PPP4 and TMP14 belong to one of the other three main photosynthetic complexes. Therefore, total protein extracts were isolated from the PSII deficient *hcf136* mutant (Plücker *et al.*, 2002), the Cyt *b₆f* deficient *petc* mutant (Maiwald *et al.*, 2003), the PSI deficient *psad1 psad2* double mutant (Ihnatowicz *et al.*, 2003) and the ATP-synthase deficient *atpd* mutant (Maiwald *et al.*, 2003), all four grown heterotrophically on sucrose containing medium. Additionally, total protein was extracted from *tmp14*, *ppp4* and the two ecotypes Col-0 and *Ler*, which are the respective ecotypic backgrounds of *hcf136*, *psad1 psad2*, *atpd* and *petc*, *ppp4*. These plants were grown under the same conditions as the complex knock-out mutants.

If TMP14 and PPP4 were constitutively associated with one of the complexes, their lack would cause a destabilisation of these proteins, then leading to a severe decrease in TMP14 and PPP4 protein levels. However, Western analysis with the respective antibodies reveals that PPP4 is only slightly reduced in the mutants lacking PSII, the Cyt *b₆f* complex and PSI and that the apparent reduction can be due to less protein loaded, as also the Actin control gives a slightly weaker signal (**Figure 3.1.12C**). TMP14 levels show also a decrease in the same three mutant backgrounds, but more significantly than PPP4, which could indicate a differential regulation of both proteins

3.1.8 Photosynthetic parameter of WT, *ppp4*, *tmp14*, *ppp4 tmp14* and PPP4:c-myc overexpressors

Both mutant alleles *ppp4-1* and *ppp4-2* exhibit a decrease in the effective quantum yield of PSII (Φ_{II} , $(F_m' - F_0)/F_m'$) and an increase in PQ pool reduction as indicated by the parameter 1-qP ($1 - [(F_m' - F_s)/(F_m' - F_0)]$) (**Table 3.1.1A**). The measurement was carried out with the PAM 101/103 chlorophyll fluorometer and plants were illuminated with 80 $\mu\text{mol photons m}^{-2} \text{s}^{-1}$ for 15 min before determining photosynthetic parameters by giving an 800 ms saturating light pulse of 4000 $\mu\text{mol photons m}^{-2} \text{s}^{-1}$. Under these conditions the *tmp14* mutant showed no differences in parameters compared to WT.

To investigate the effect of the *tmp14* mutant background on photosynthetic parameters in the *ppp4* mutant and additionally to test complementation of the PPP4:c-myc construct, Chl *a* measurements and determination of P700 oxidation rate were carried out with *tmp14-1*, *ppp4-1*, a cross of both lines and the PPP4:c-myc overexpressing plants using the Dual-PAM-100 fluorometer. To exclude the influence of ecotypical differences in photosynthetic parameters between *Ler* (background of *ppp4-1*) and No-0 (background of *tmp14-1*) on the results obtained with the double mutant, WT plants of both genetic backgrounds and two double mutants as well as one WT segregating from one heterozygous double mutant were measured. Ecotypical differences between *Ler* and No-0 have already been described for the phytochrome-mediated response (Magliano *et al.*, 2005).

However, all three WT showed identical values and no differences were detected between the two double mutants. Therefore, ecotypical differences between *Ler* and No-0 regarding the photosynthetic parameters as measured in this thesis, could be excluded. Photosynthetic parameters were determined after light adaption of the plants to two different actinic light intensities. To investigate photosynthetic activity of mutants and overexpressors under low light, plants were illuminated with actinic light of $77 \mu\text{mol photons m}^{-2} \text{ s}^{-1}$ (**Table 3.1.1B**) before determining Chl *a* fluorescence and P700 absorption parameters. For high light $1052 \mu\text{mol photons m}^{-2} \text{ s}^{-1}$ was applied (**Table 3.1.1C**). In order to determine Chl *a* fluorescence parameters, plant were light adapted for 15 min. P700 oxidation rate was measured after 5 min of light adaption.

The results indicate that changes in photosynthetic parameters of *ppp4* are exacerbated in the *ppp4 tmp14* double mutant. In detail, after low actinic light illumination the values for 1-qP and $\Delta A/\Delta A_{\text{max}}$ are slightly increased whereas NPQ $((F_m - F_m')/F_m')$ and Φ_{II} are slightly decreased in both *ppp4* and the double mutant. In comparison to WT parameters measured in the *tmp14* mutant show the same trend as for *ppp4* and the double mutant, but for this mutant values are not significantly changed. When illuminated with high actinic light, only the $\Delta A/\Delta A_{\text{max}}$ parameter remains significantly changed in *ppp4* and the double mutant as compared to the WT, but contrary to the increase observed in low light this parameter is decreased. Also the NPQ appears to be lower, but differences from WT are not significant. The *35S::PPP4:c-myc* complements all significant changes, but values remain below WT at lower actinic light intensities for Φ_{II} and 1-qP. That values are different from WT in these plants might be due to two possibilities. (i) The higher abundance of PPP4 in the *35S::PPP4:c-myc* lines could have a direct effect on photosynthetic parameters. (ii) The tagged protein is not fully functional, because of differing properties caused by the tag. That PPP4:c-myc at least shows a different binding affinity to TMP14 in comparison to the native PPP4 has been shown by crosslinking and Co-IP.

To exclude that differences in pigment levels are responsible for the NPQ phenotype of *ppp4* plants, a quantitative analysis of leaf pigments was conducted, but only slight, significant increases could be observed in violaxanthin (WT: $33 \pm 2 \mu\text{mol per mmol chl}$; *ppp4*: 36 ± 1), lutein (WT: 123 ± 2 ; *ppp4*: 131 ± 2) and β -carotene levels (WT: 79 ± 1 ; *ppp4*: 84 ± 3). The lumenal localised violaxanthin de-epoxidase is activated by low pH (Hager, 1969) and therefore the increase in violaxanthin suggests that the decrease in NPQ might be due to a defect in lumen acidification.

| A | | | | | | |
|---|-----------------|-----------------|-----------------|-------------------|-----------------|-----------------|
| Photosynthetic Parameters 80 $\mu\text{mol photons m}^{-2}\text{s}^{-1}$ | | | | | | |
| | WT | <i>ppp4-1</i> | <i>ppp4-2</i> | | | |
| F_v/F_m | 0.84 \pm 0.00 | 0.85 \pm 0.00 | 0.85 \pm 0.00 | | | |
| Φ_{II} | 0.75 \pm 0.01 | 0.70 \pm 0.02 | 0.70 \pm 0.03 | | | |
| 1-qP | 0.09 \pm 0.00 | 0.15 \pm 0.03 | 0.13 \pm 0.03 | | | |
| B | | | | | | |
| Photosynthetic Parameters 77 $\mu\text{mol photons m}^{-2}\text{s}^{-1}$ | | | | | | |
| | WT | <i>tmp14-1</i> | <i>ppp4-1</i> | <i>ppp4 tmp14</i> | PPP4:c-myc #6 | PPP4:c-myc #8 |
| F_v/F_m | 0.84 \pm 0.00 | 0.84 \pm 0.00 | 0.84 \pm 0.01 | 0.84 \pm 0.01 | 0.83 \pm 0.01 | 0.83 \pm 0.01 |
| Φ_{II} | 0.75 \pm 0.01 | 0.75 \pm 0.00 | 0.73 \pm 0.02 | 0.69 \pm 0.03 | 0.72 \pm 0.02 | 0.72 \pm 0.02 |
| NPQ | 0.25 \pm 0.03 | 0.20 \pm 0.03 | 0.17 \pm 0.01 | 0.16 \pm 0.02 | 0.29 \pm 0.05 | 0.27 \pm 0.04 |
| 1-qP | 0.08 \pm 0.01 | 0.09 \pm 0.01 | 0.11 \pm 0.01 | 0.16 \pm 0.04 | 0.09 \pm 0.01 | 0.10 \pm 0.02 |
| $\Delta A/\Delta A_{\text{max}}$ | 0.04 \pm 0.01 | 0.05 \pm 0.02 | 0.08 \pm 0.02 | 0.12 \pm 0.02 | 0.06 \pm 0.01 | nd |
| C | | | | | | |
| Photosynthetic Parameters 1052 $\mu\text{mol photons m}^{-2}\text{s}^{-1}$ | | | | | | |
| | WT | <i>tmp14-1</i> | <i>ppp4-1</i> | <i>ppp4 tmp14</i> | PPP4:c-myc #6 | PPP4:c-myc #8 |
| F_v/F_m | 0.84 \pm 0.01 | 0.85 \pm 0.00 | 0.85 \pm 0.01 | 0.84 \pm 0.01 | 0.83 \pm 0.01 | 0.83 \pm 0.01 |
| Φ_{II} | 0.08 \pm 0.01 | 0.08 \pm 0.01 | 0.08 \pm 0.01 | 0.08 \pm 0.01 | 0.08 \pm 0.01 | 0.07 \pm 0.01 |
| NPQ | 2.15 \pm 0.05 | 2.19 \pm 0.03 | 2.05 \pm 0.06 | 2.03 \pm 0.09 | 2.16 \pm 0.18 | 2.25 \pm 0.12 |
| 1-qP | 0.87 \pm 0.01 | 0.88 \pm 0.01 | 0.87 \pm 0.01 | 0.87 \pm 0.02 | 0.87 \pm 0.03 | 0.88 \pm 0.02 |
| $\Delta A/\Delta A_{\text{max}}$ | 0.90 \pm 0.03 | 0.87 \pm 0.02 | 0.78 \pm 0.04 | 0.72 \pm 0.03 | 0.92 \pm 0.02 | nd |

Table 3.1.1 Photosynthetic parameters of *tmp14*, *ppp4*, *ppp4 tmp14* and *35S::PPP4:c-myc* plants

(A) Chl *a* fluorescence parameters of *Ler*, *ppp4-1* and *ppp4-2* as determined by measurement with the PAM 101/103 chlorophyll fluorometer after 15 min of 80 $\mu\text{mol photons m}^{-2}\text{s}^{-1}$ actinic light. (B) Chl *a* fluorescence and P700 absorption parameters of WT, *tmp14-1*, *ppp4-1*, *ppp4 tmp14* plants and in two lines overexpressing *PPP4:c-myc* as measured with Dual-PAM 100 after 5 min (P700) or 15 min (Chl *a*) of 77 $\mu\text{mol photons m}^{-2}\text{s}^{-1}$ actinic light (settings: actinic light, 5; measuring light, 5; saturation pulse: 5) (C) Chl *a* fluorescence and P700 absorption parameters in WT, *tmp14-1*, *ppp4-1*, *ppp4 tmp14* plants and in two lines overexpressing *PPP4:c-myc* as measured with Dual-PAM 100 after 5/ 15 min of 1052 $\mu\text{mol photons m}^{-2}\text{s}^{-1}$ actinic light (settings: actinic light, 17; measuring light, 5). Values are means (\pm SD) of 15 independent measurements for WT (*Ler*: 5, No-0: 5, *Ler* x No-0: 5), 10 for *ppp4 tmp14* and 5 for the other genotypes.

A decrease in the $\Delta A/\Delta A_{\max}$ and NPQ parameters are indicative for a defect in cyclic electron flow (CEF; Munekage *et al.*; 2002, DalCorso *et al.*, 2008) and as at least $\Delta A/\Delta A_{\max}$ is significantly reduced in *ppp4* and the double mutant, two assays were performed in order to elucidate a function of PPP4 and TMP14 in the cyclic electron transport. Firstly, an intact leaf assay for determining CEF was carried out by measuring the transient increase in NPQ after onset of low light. This measurement relates to the hypothesis that NPQ induction during the activation period of photosynthesis is caused by the transient acidification of the thylakoid lumen when CEF activity is higher than the activity of the ATP-synthase (DalCorso *et al.*, 2008). Secondly, to assess electron transfer from ferredoxin (Fd) to PQ during CEF around PSI, Fd-dependent reduction of PQ was monitored *in situ* as an increase in chlorophyll fluorescence under low measuring light. In WT, the addition of NADPH and Fd to ruptured chloroplasts induces a marked and rapid increase in chlorophyll fluorescence (Munekage *et al.*, 2002; DalCorso *et al.*, 2008). In this *in situ* assay NADPH is thought to transfer electrons to Fd via the reverse reaction of the Fd:NADPH oxidoreductase (FNR). In the intact leaf assay however, ecotypic differences could be observed, as No-0 has significantly lower transient NPQ than *Ler*. Therefore, a phenotype of the double mutant could at least partly be due to the genetic ecotypic background. As the *ppp4* mutant alone already shows a phenotype in the described changes of photosynthetic parameters, the transient increase in NPQ was measured with *ppp4-2* and *Ler*. When grown in the climate chamber at a 12h/12h light dark cycle, *ppp4* plants only show a slight decrease in NPQ in the steady state phase (**Figure 3.1.13A**). However, if measurements are performed with plants grown in continuous light, the transient increase in NPQ is significantly lower in *ppp4* as compared to WT (**Figure 3.1.13B**). This could indicate that acclimation of the plant to continuous light includes PPP4-dependent non-photochemical quenching.

In the *in situ* assay, all three WTs (*Ler*, No-0, *Ler* x No-0) show the same extent and kinetics of the increase in chlorophyll fluorescence. Therefore, only one WT curve is depicted in **Figure 3.1.13C**. The kinetic of the chlorophyll fluorescence increase is slower in *ppp4 tmp14* double mutant, yet no significant changes in the final level of chlorophyll fluorescence can be detected. However, Chl *a* fluorescence already increases in response to the addition of NADPH.

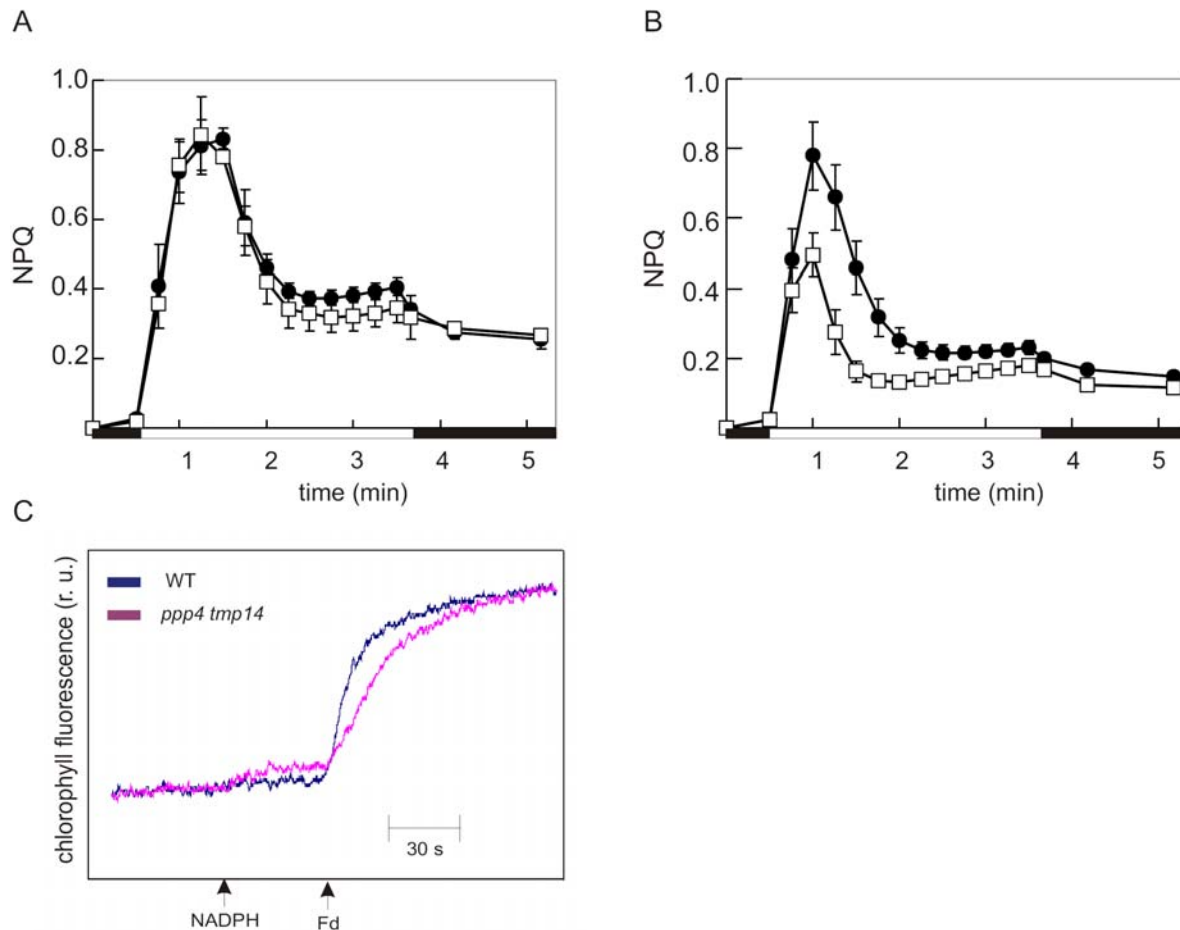


Fig 3.1.13 Cyclic electron flow measurements

(**A+B**) Time courses of induction and relaxation of NPQ monitored during dark-to-light ($80 \mu\text{mol photons m}^{-2} \text{s}^{-1}$, white bar) transition of *Ler* (filled circles) and *ppp4-2* (open squares) grown in a 12 h/12 h dark light cycle (**A**) or in continuous light (**B**). The 3 min light period (white bar) was followed by a 2 min dark period (black bar). Values are means (\pm SD) of five independent measurements each per time point (**C**) Quantification of CEF *in situ*. Increases in chlorophyll fluorescence were measured in ruptured chloroplasts under low measuring light ($1 \mu\text{mol photons m}^{-2} \text{s}^{-1}$), after the addition of NADPH and Fd. At this light intensity, the fluorescence level should predominately reflect the reduction of plastoquinone by cyclic electron transport from ferredoxin, not by PSII photochemistry (Munekage *et al.*, 2002).

3.1.9 Topology of PPP4 and TMP14

As mentioned afore, TMP14 was first described, because of its posttranslational modification by phosphorylation of the N-terminus (Hansson and Vener, 2003), which was found by trypsin digestion of all stromal side exposed proteins and subsequent enrichment of phosphopeptides. Because TMP14 has two predicted transmembrane domains, this indicates that both termini are stromal exposed. To determine PPP4 and to verify TMP14 topology, thylakoids were subjected to mild digestion with trypsin for 10 min with the aim to solely target tryptic sites on the stromal side of the thylakoid membrane. Both proteins contain multiple trypsin cleavage sites in their N-terminus, which also bears the sequence of the epitopes, against which specific antibodies were made. Therefore, stromal side treatment with trypsin of a topology in which the N- and C-termini of

the proteins were exposed to the stromal side (topology 1, **Figure 3.1.14B**), would result in destruction of the epitopes and absence of detectability. Because PPP4 has one tryptic site in the transmembrane regions connecting loop, treatment with trypsin on a stromal exposed loop topology (topology 2) would result in detectable product of 5 kDa for PPP4 with the specific antibody. The tryptic digest was additionally performed with thylakoids of *tmp14* and *ppp4* mutants in order to evaluate if the absence of one interaction partner would change accessibility of the other to the protease, and with *PPP4:c-myc* expressing plants as a confirmation for PPP4 topology. Because the TMP14 antibody reacts unspecifically with chlorophyll on the PVDF membrane, thylakoid proteins were precipitated with acetone after the trypsin treatment to avoid this unspecific interaction during Western detection. The reaction of the antibody with the low molecular chlorophyll could interfere with the detection of smaller TMP14 degradation products. As an indication that tryptic proteolysis took place only at the stromal side of the membrane and no unspecific cleavage of luminal proteins occurred, Western analysis of the treated thylakoid extracts was performed with an antibody against the luminal protein PsbO, a component of the PSII oxygen evolving complex (**Figure 3.1.14A**). This shows that after 10 min of digestion PsbO remains intact. Hybridisation with an antibody against the stromal side localised AtpB confirms activity of trypsin. Western detection with the specific antibodies against TMP14 and PPP4 clearly indicates that both proteins are protected from trypsin treatment, because their amount does not decrease, but even seems to increase after the protease treatment. This result could be due to a negative effect of associated proteins on the accessibility of PPP4 and TMP14 to the detergent SDS in the loading buffer after acetone precipitation. If the associated proteins, which together with PPP4 and TMP14 precipitate in acetone as a partly insoluble fraction, are partially removed by proteolytic cleavage before the precipitation, higher amounts of PPP4 and TMP14 would be soluble. A 10 min trypsin treatment of TMP14 results in a detectable fragment of smaller size, which indicates that the TMP14 N-terminus with its 8 tryptic sites is heavily protected and cleavage might have occurred at an arginine residue two amino acids upstream of the predicted transmembrane domain or at the only luminal exposed tryptic site. Digested PPP4 exhibits one degradation product after 10 min of slightly smaller size. Therefore topology 1 with stromal localised N- and C-terminus appears likely. Verification of this result arises from *PPP4:c-myc* digestion. The amount of detectable c-myc is decreasing and an increasing amount of normal sized PPP4 indicates that the c-myc tag is cleaved off.

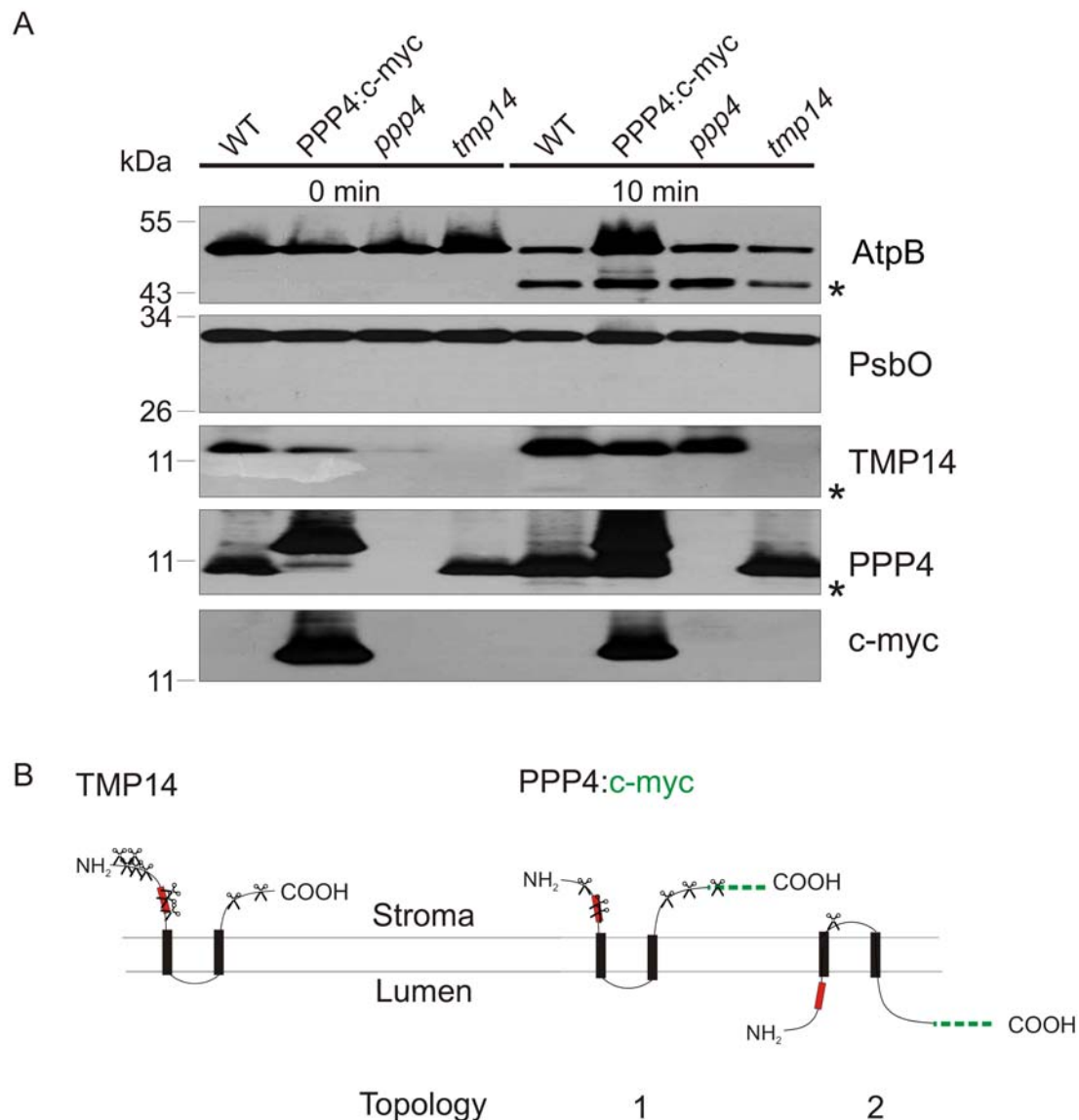


Fig 3.1.14 Determination of PPP4 topology by stromal side tryptic digest of thylakoid proteins

(A) Thylakoids were isolated from WT, *35S::PPP4:c-myc*, *ppp4* and *tmp14* and incubated with 10 $\mu\text{g/ml}$ trypsin. Samples were taken at 0, 10 and 20 min after the addition of trypsin and proteins were separated by SDS-PAGE. Immuno-detection was carried out with specific antibodies against AtpB, as a control for trypsin activity, PsbO as a control for absence of trypsin in the lumen, TMP14, PPP4 and c-myc. Asterisks indicate degradation products. (B) Schematic drawings of probable topologies. Scissors indicate possible luminal accessible tryptic sites. Red boxes indicate location of epitopes used for antibody production. Dashed green line stands for c-myc tag fused to PPP4. For PPP4 topology 1 could be supported.

Additionally, lack of PPP4 does not result in enhanced degradation of TMP14 or vice versa. Both proteins even seem to be more protected in the absence of the interaction partner, as no degradation product can be detected in the respective other mutant. Interestingly, the increase by trypsin treatment of Western detectable TMP14 is even higher in the *ppp4* mutant background as compared to WT, indicating that more TMP14 precipitates in SDS-loading dye in the absence of PPP4,

speculatively because of an increased association with other hydrophobic proteins. Two results obtained by this experiment suggest that TMP14 and PPP4 are associated with other proteins in the thylakoid membrane: (i) hardly any digestion of PPP4 and TMP14 takes place despite the high number of tryptic sites in the experimentally shown stromal localised N- and C- termini (TMP14: 8 N-terminal, 3 C-terminal; PPP4: 3 N-terminal, 3 C-terminal). (ii) PPP4 and TMP14 from untreated thylakoids seem to only be partly solubilised in Laemmli buffer, whereas solubilisation is markedly increased if samples are treated with trypsin.

3.1.10 Analysis of thylakoid protein composition

The analysis of thylakoid proteome composition of WT, *ppp4*, *tmp14* and *ppp4 tmp14* does not show any highly significant differences between WT and mutants as can be seen in **Figure 3.1.15A**. However, PGR5 content is lower in the No-0 background, which could account for the differences observed in the transient increase in NPQ after light onset between the different ecotypes, as described in Chapter 3.1.8. Additionally, a slight increase in PGRL1 levels can be observed in all mutant backgrounds, especially in the double mutants. To investigate, whether PPP4 and TMP14 protein levels are altered in the *pgr11ab* mutant, chloroplast proteins were isolated from WT and *pgr11ab* double mutants. Immunodetection with specific antibodies against PPP4 and TMP14 showed no differences in protein levels as compared to WT, which can be seen in **Figure 3.1.15B**.

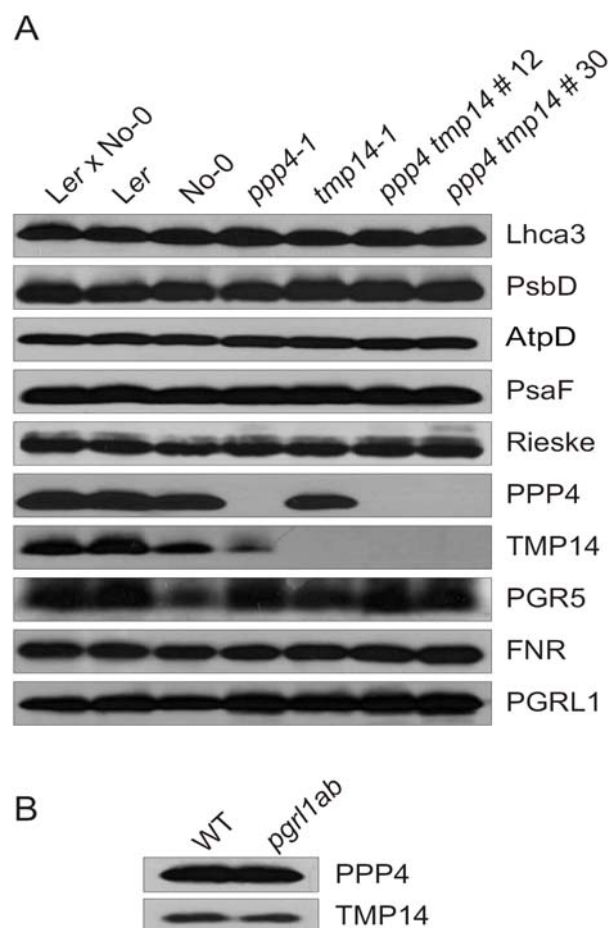
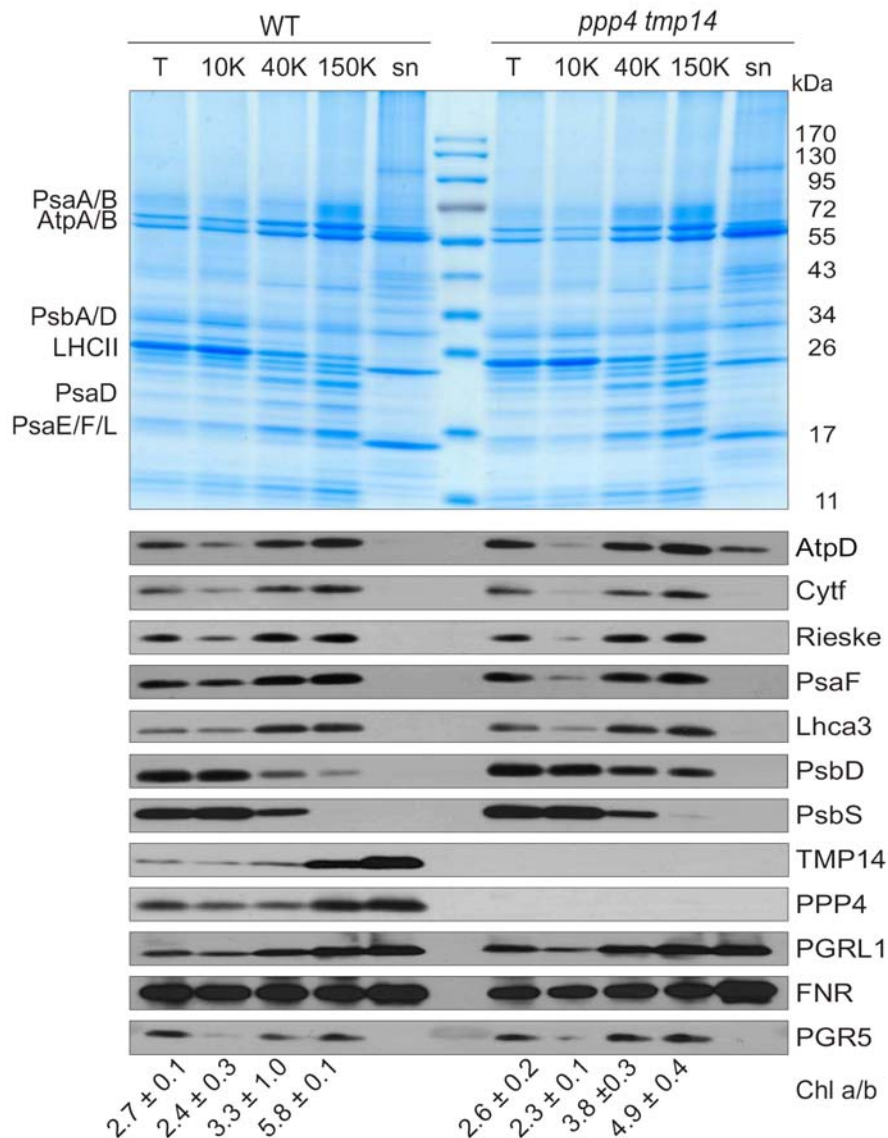


Fig 3.1.15 Thylakoid proteome analysis

(A) Thylakoid protein composition in *Ler*, No-0, *Ler x No-0*, *ppp4-1*, *tmp14-1* and two independent homozygous *ppp4 tmp14* lines. Thylakoids were extracted and protein according to 5 μ g of chlorophyll was separated by SDS-PAGE. Replicate filters were hybridised with specific antibodies as depicted on the right. **(B)** Chloroplasts were isolated from WT and *pgr11ab* mutant plants and proteins according to 5 μ g of Chl were separated by SDS-PAGE and replicate filters were hybridised with PPP4 and TMP14.

3.1.11 Location of thylakoid proteins in WT and *ppp4 tmp14*

To identify the specific localisation of PPP4 and TMP14 within the thylakoid membrane and to investigate, if a lack of PPP4 and TMP14 causes changes in the spatial arrangement of thylakoid complexes, thylakoids of WT and the *ppp4 tmp14* double mutant were fractionated into grana, intermediate membranes and stromal lamellae by a short treatment with the detergent digitonin and subsequent differential centrifugation (Chapter 2.2.4.8). The rationale of this experiment is that the low concentration of digitonin and the short solubilisation time, followed by dilution, leads to the detachment of vesicles from exposed regions of thylakoid membranes. With differential centrifugation different sized vesicles can be precipitated. The 10000g (10K) fraction mainly consists of the granal thylakoids, the 40000g (40K) of intermediate/ margin regions and the 150000g (150K) of stromal lamellae. In this work, additionally the proteins from the supernatant after centrifugation at 150000g for 90 min were isolated by acetone precipitation, to see if PPP4 and TMP14 were present. The membrane proteins contained within in this fraction are due to a preferential extraction by digitonin. The Coomassie stained gel and the Western results in **Figure 3.1.16** demonstrate that the analysed subunits of photosynthetic complexes are primarily found according to their known localisation in both WT and *ppp4 tmp14*. As such no significant difference in the spatial organisation can be assigned. However, the chlorophyll a/b ratio, which was measured from all precipitated fractions in three independent fractionation experiments, appears to be significantly lower in the stromal fraction of the *ppp4 tmp14* mutant, indicating that more PSII antenna is present. This is underlined by the coomassie staining of the gel, which demonstrates a higher amount of LHCII in the stromal lamellae fraction of the *ppp4 tmp14* mutant. Western analysis of the different thylakoid fractions with the specific antibodies against PPP4 and TMP14 demonstrate a localisation of both proteins in the stroma lamella regions of the thylakoid membrane, whereby the exclusion of TMP14 from the other regions is more evident than for PPP4. The supernatant, which contains lumenal, contaminating stromal and solubilised membrane proteins as well as thylakoid membrane threads, also includes a substantial amount of PPP4 and TMP14 as can be seen in the Coomassie stained gel, which shows two bands of the size of PPP4 and TMP14 in the WT, which are lacking in the double mutant (**Figure 3.1.16**, asterisks). Interestingly, two further proteins can be identified by immunodetection to be present in the supernatant, the ferredoxin:NADPH oxidoreductase (FNR) and PGRL1, a protein involved in the cyclic electron flow around PSI (Dal Corso *et al.*, 2008), which functions in the PGR5 dependent pathway.

**Fig 3.1.16****Fractionation of thylakoids**

Thylakoids were extracted from WT and *ppp4 tmp14* double mutants and treated with 0.1 % digitonin for 1 min, followed by dilution in 10 volumes and differential centrifugation at 10000g (10K; grana), 40000g (40K; intermediate membranes) and 150000g (150K; stroma lamellae). Soluble protein was precipitated with 5 volumes of 100% acetone. Proteins according to 5 μ g of chlorophyll from untreated thylakoids (T), grana (10 K), intermediate membranes (40 K), stroma lamellae (150 K) and precipitated supernatant protein originating from 40 μ g of treated thylakoids (sn) were separated by SDS-PAGE and replicate filter were hybridised with specific antibodies as depicted on the right. Numbers underneath state Chl a/b ratio of fractions of three independent experiments.

Coomassie stained bands from the supernatant were analysed by MS and the identity of the putative PPP4 and TMP14 bands was verified. Additionally, the Coomassie stained protein bands running just above the 34 kDa marker band, contained both forms of FNR, the thylakoid associated (At5g66190) and the soluble protein (At1g20020) as well as PGRL1. Results obtained from analysing the supernatant indicate that the complex of PPP4 and TMP14 is easily extracted by digitonin. This could be due to a localisation in exposed regions with high lipid to protein ratio. Moreover, also PGRL1 and thylakoid associated FNR are located in thylakoid regions with such properties.

3.1.12 Investigating phosphorylation of thylakoid proteins in WT and *ppp4 tmp14*

Because TMP14 has previously been described as a phospho-protein phosphorylated at a threonine residue (Hansson and Vener, 2003) and detection with a phospho-threonine antibody has been published (Khrouchtchova *et al.*, 2005), WT and *ppp4 tmp14* thylakoids were isolated from dark (D), low light (LL) and far-red (FR) adapted plants in the presence of the phosphatase inhibitor NaF to investigate phosphorylation. Western analysis was performed with phospho-threonine antibodies (Figure 3.1.17), but no immuno-detectable band of the size of TMP14 could be identified that was present in WT, but absent in the double mutant. However, the specificity of phospho-threonine antibodies highly varies between commercially available batches. Instead of detecting phosphorylated TMP14, this experiment led to the identification of a slightly higher phosphorylation state of LHCII and the PSII components CP43, D1 and D2. This is in line with the slightly higher reduction rate of the plastoquinone pool in the *ppp4 tmp14* double mutant, as determined by the PAM fluorometer (Chapter 3.1.8), because thylakoid kinase activity is known to be induced by reduction of the plastoquinone pool (Ihnatowicz *et al.*, 2008).

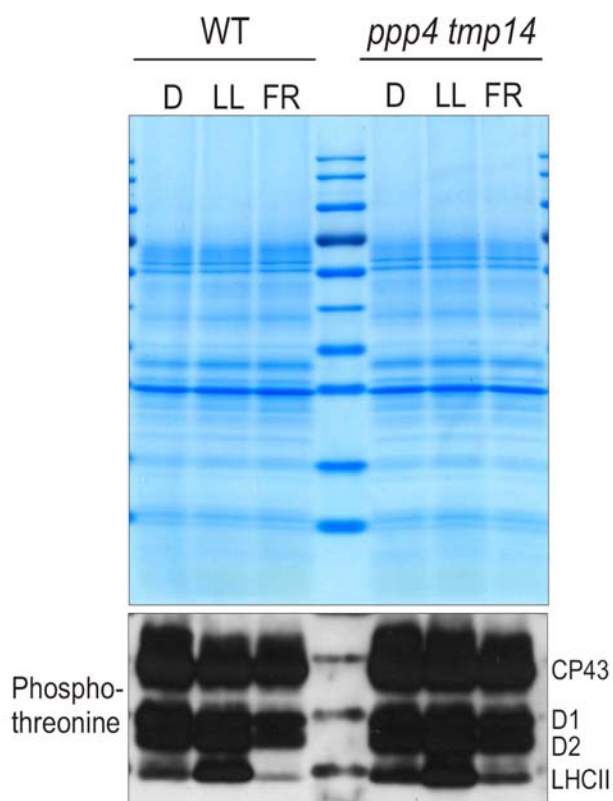


Fig 3.1.17 Phosphorylation pattern in WT and *ppp4 tmp14*

Thylakoids were isolated from WT and *tmp14 ppp4* plants adapted to dark (D), low light (LL) and far-red light (FR) in the presence of 10 mM NaF. Proteins were separated by SDS-PAGE and either stained with Coomassie or transferred to PVDF membrane followed by hybridisation with phospho-threonine antibodies from Cell Signaling (New England Biolabs; Frankfurt, Germany).

3.1.13 Characterisation of PPP4-like and TMP14-like

Both TMP14-like and PPP4-like are predicted by ChloroP to have an N-terminal chloroplast transit peptide, which contains for TMP14-like 55 amino acids and for PPP4-like 51 amino acids. Both proteins have been identified in the chloroplast by shot-gun proteomics (Kleffman *et al.*, 2004) and the presence of TMP14-like in the thylakoid membrane was shown by Friso *et al.*, 2004 by the

same method. Localisation of both proteins in the chloroplast was verified with transient expression of a C-terminal RFP fusion in *Arabidopsis* protoplasts (**Figure 3.1.18A**). Here, the auto-fluorescence of the chlorophyll (Auto) and the RFP-fluorescence of the fusion proteins overlap as can be seen in the merged pictures. Expression analysis using Genevestigator shows that the gene encoding TMP14-like has a similar expression pattern as *PPP4* and *TMP14* and also two other genes encoding photosynthetic proteins *PetC* and *Lhca1* (**Figure 3.1.18B**). It is also highest expressed in green tissue, whereas *PPP4*-like expression peaks in seeds and in root tips. The calculated molecular weight of the mature protein is 11 kDa for TMP14-like and 15.7 kDa for *PPP4*-like.

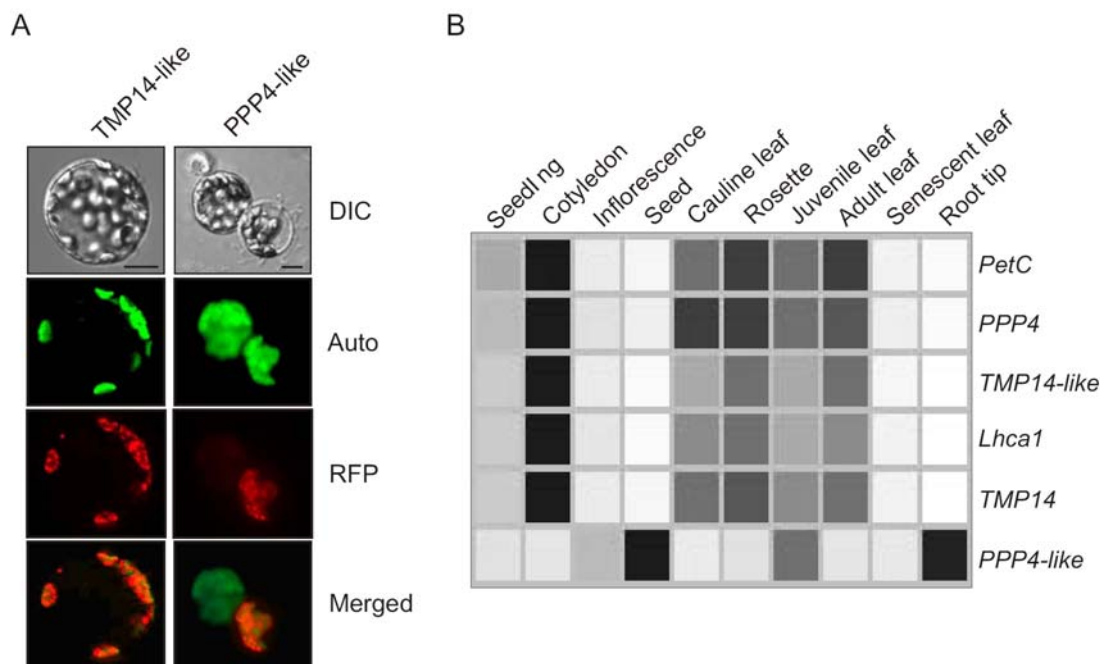


Fig 3.1.18 Gene expression and gene product localisation of *TMP14-like* and *PPP4-like*

(A) *Arabidopsis* protoplasts were transiently transfected by polyethylene glycol-mediated DNA uptake with the fusion constructs of the full coding sequence with dsRED and analyzed by using fluorescence microscopy. In the upper panels, the Differential Interference Contrast (DIC) view of the protoplasts is displayed. The second and third from the top show auto-fluorescence of the chlorophyll and RFP fluorescence, respectively and the lower panel shows a merged image of the latter. Scale bar, 20 μ m. Organ and growth stage specific gene expression of *PPP4*, *TMP14*, *TMP14-like* and *PPP4-like* was analysed with Genevestigator. *PetC* encoding the Rieske subunit of Cyt *b₆f* and *Lhca1* were used as control for photosynthetic gene expression. All gene-level profiles were normalized for colouring in such way that for each gene the highest signal intensity obtains value 100% (black) and absence of signal obtains value 0% (white).

The gene structures of *PPP4-like* and *TMP14-like* are depicted in **Figure 3.1.19A** and identification of intron-exon structure was performed as described in Chapter 3.1.3 for *PPP4* and *TMP14* insertion lines. One T-DNA insertion line each for *TMP14-like* and *PPP4-like* could be identified by screening T-DNA insertion flanking databases. The presence of the insertion and the exact insertion point were confirmed by PCR with gene and T-DNA border specific primers and

subsequent sequencing of the amplified product. The absence of transcript was verified by RT-PCR using primer combinations up- and downstream of the insertions (**Figure 3.1.19B**). Furthermore, photosynthetic parameters were determined in *tmp14-like* and *ppp4-like*, but no significant difference to WT could be detected (data not shown). Because the TMP14-like protein migrates with the smaller PPP4 containing complex as shown by MS analysis of second dimension silver stained protein spots (Figure 3.1.7), crosslinking with BS³ was carried out with thylakoids from WT, *tmp14*, *tmp14-like* and *ppp4-like* plants (**Figure 3.1.19C**), but changes in PPP4 crosslinking products are only visible in the *tmp14*, but not in the other two mutant backgrounds.

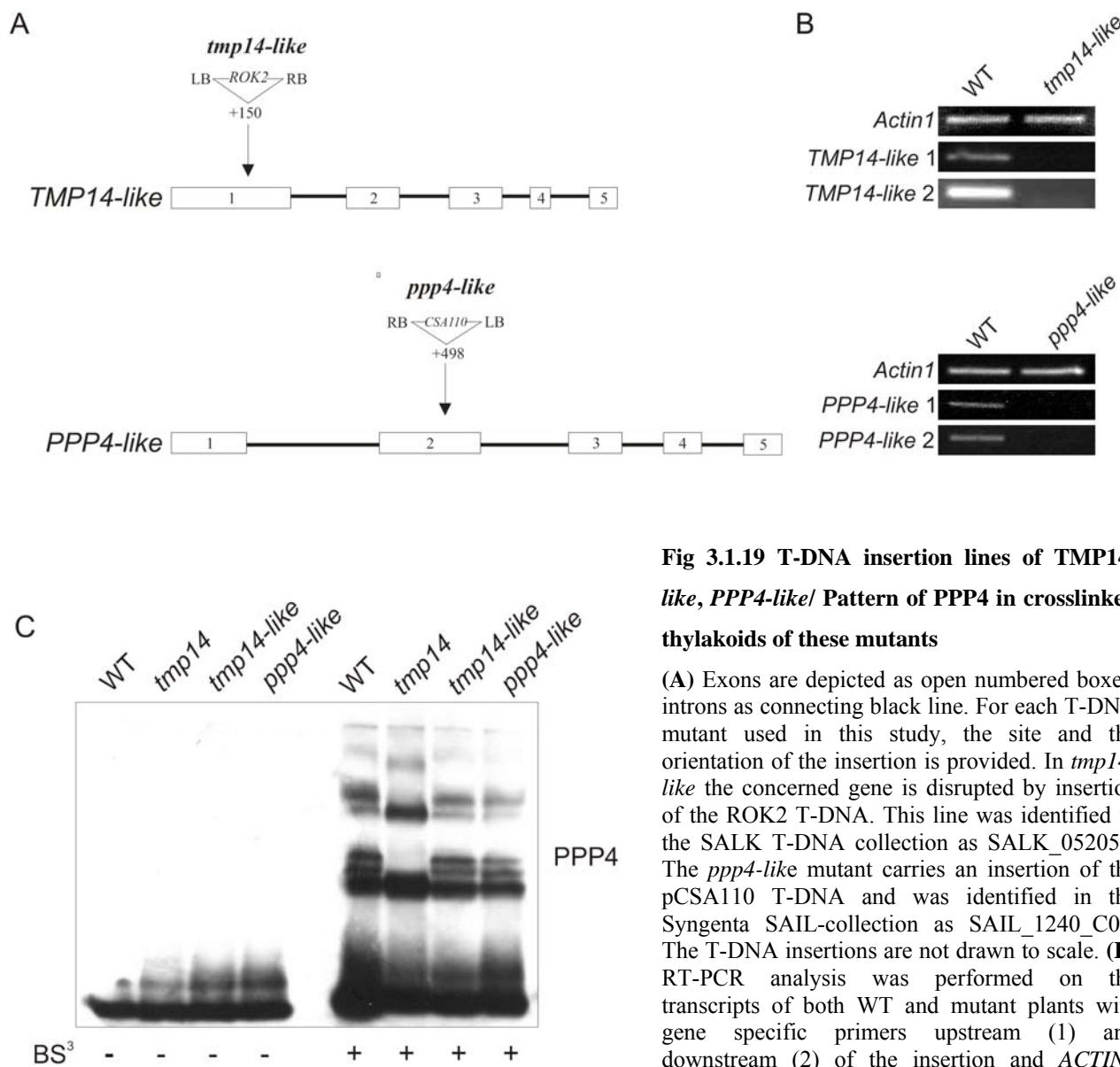


Fig 3.1.19 T-DNA insertion lines of TMP14-like, PPP4-like/ Pattern of PPP4 in crosslinked thylakoids of these mutants

(A) Exons are depicted as open numbered boxes, introns as connecting black line. For each T-DNA mutant used in this study, the site and the orientation of the insertion is provided. In *tmp14-like* the concerned gene is disrupted by insertion of the ROK2 T-DNA. This line was identified in the SALK T-DNA collection as SALK_052057. The *ppp4-like* mutant carries an insertion of the pCSA110 T-DNA and was identified in the Syngenta SAIL-collection as SAIL_1240_C05. The T-DNA insertions are not drawn to scale. (B) RT-PCR analysis was performed on the transcripts of both WT and mutant plants with gene specific primers upstream (1) and downstream (2) of the insertion and *ACTIN1* primers as positive control. (C) Thylakoid proteins from WT, *tmp14*, *tmp14-like* and *ppp4-like* were isolated and crosslinked with BS³, separated by SDS-PAGE and immunodetection was carried out with the PPP4 antibody.

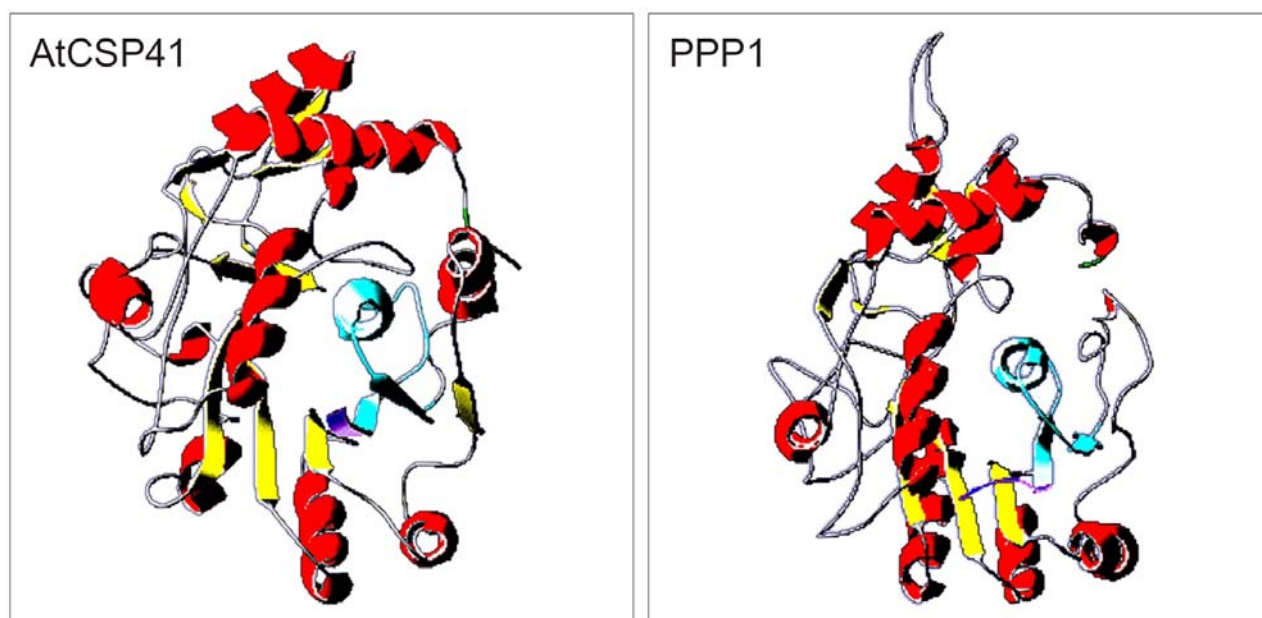
3.2 Characterisation of PPP1

The *Arabidopsis* protein Putative Photosynthetic Protein 1 (PPP1) is homologous to AtCSP41, of which the spinach orthologue was described to be a member of the complex that binds the 3' stem loop of the *petD* transcript and cleaves specifically within this structure (Yang *et al.*, 1996; Yang and Stern, 1997; Bollenbach and Stern, 2003). Orthologues of both PPP1 and CSP41 were co-purified with the plastid encoded RNA-polymerase (PEP) in *Sinapis alba* (Pfannschmidt *et al.*, 2000) and the plastid 70S ribosome in *Chlamydomonas reinhardtii* (Yamaguchi *et al.*, 2003). Additionally, in *Arabidopsis* both proteins have been found co-migrating with the ribosomal 50S proteins L31 and L5 in native gels (Peltier *et al.*, 2006). Taken together, these results strongly suggest a putative function of PPP1 in plastid gene expression.

3.2.1 Gene expression, protein structure and localisation

It was shown that the expression of *PPP1* (*At1g09340*), but not of the homologous *AtCSP41* (*At3g63140*) is co-regulated with those of nuclear photosynthetic genes (supplementary data, Biehl *et al.*, 2005). However, the Digital Northern analysis employing Genevestigator states that the expression of both genes is highest in green tissue (<https://www.genevestigator.ethz.ch>). *PPP1* and *AtCSP41* derive from a common ancestor of cyanobacterial origin and the encoded proteins have diverged to such extent that in *Arabidopsis* the homology of PPP1 to AtCSP41 is relatively moderate (35% identity and 53% similarity; Yamaguchi *et al.*, 2003). The three dimensional protein structures of PPP1 and AtCSP41 can be modelled, as the proteins belong to the short chain dehydrogenase/ reductase family of archaea, eubacteria, and eukarya (Baker *et al.*, 1998), for which the three dimensional structures of several members are known. Proteins of this family employ NAD(P)(H) as cofactors for their enzymatic activity and thus a binding domain can be defined (Jörnvall *et al.*, 1995; **Figure 3.2.1**). Prediction of the three-dimensional structures using the 3D-jigsaw server, which builds three-dimensional protein models based on homologues of known structure (<http://www.bmm.icnet.uk/~3djigsaw>) and subsequent visualisation by Swiss PDB Viewer (<http://expasy.org/spdbv/>) demonstrates that the structural scaffold is highly similar (**Figure 3.2.1.A**). However, PPP1 carries two extensive stretches lacking secondary structure, which are not present in AtCSP41. The first one is located downstream of the N-terminal nucleotide binding domain (blue) and the second one at the C-terminus preceding two α - helices. The predicted molecular weight of the mature PPP1 protein is 37 kDa and of AtCSP41 36 kDa (ProtParam, www.expasy.org).

A



B

| | | |
|----------------|-----|---|
| slr1540 | 1 | -----MRILIM---GGTRFIGTHLCRVLVAQGHVFLFNRGNRP-----DPVNGVAQ |
| PPP1 | 49 | ---ASSEKKILIM---GGTRFIGLFLSRILVKEGHQVTLFTRGKSPIAKQLPGESDQDFADFSSKILH |
| AtCSP41 | 73 | ASSVGEKKNVLIIVNTNSGGHAVICGFYFAKELLSAGHAVTILITVVGDESSEKMKKPPFNRFSEIVSGGGKT |
| | | |
| slr1540 | 37 | IHGDRRVAEQLREKLEKEEFDVIFDNNGRELSDTQPLVDLYNG-RVQQFVYMSSAGVYQASSQMPHRET |
| PPP1 | 104 | LKGDRKDYDFVKSSLSAEGFDVVDINGREAEEVEPILEALP--KLEQYIYCSSAGVYLKSDILPHCEE |
| AtCSP41 | 134 | VWGN---PANVANVVGGETFDVVIDNNGKDLDTVRPVVDWAKSSGVKQFLFISSAGIYKSTEQPPHVEG |
| slr1540 | 84 | DAVDPSRHKGKFETERYLAOSGIPWTAIRPTYIYGPHNYNALESWFFDRLVRGRAIPIPGNGQYITQL |
| PPP1 | 151 | DAVDPKSRHKGKLETESLLOSQKGNWTSIRPVYIYGPIINYNPVEEWWFFHRLKAGREIPVPSNGIQISQL |
| AtCSP41 | 178 | DAVKAD---ACHVVVEKYLAETFGNWAASFRCQYMIQSGNKNKDCEEWFFDRIIVRRAVPIPGSGLQLTNI |
| slr1540 | 143 | GHVEDLATAMAKTIVT-PAAIGQIYNISGDRYVTMNGLAQACATAAGLDPQGVKLVHYDPKDFDFGKRR |
| PPP1 | 209 | GHVKDLATAFLNVLGN-EKASREIFNISGEKYVTFDGLAKACAKACGFPEP--EIVHYNPKEFDGKRR |
| AtCSP41 | 235 | SHVRDLSMITSAVANPEAASGNIFNCVSDRAVTLDGMAKLCAAAAG---KTVEIVHYDPKAIGVDAKK |
| slr1540 | 202 | AFPLRQOHFFADIQKAQDHLDPNYGLVEGLKNSFOLDYIPSGKGEEKGDFDLDEQIILAFS----- |
| PPP1 | 268 | AFPPRDQOHFFASVEKAKHVLGKPEFDLVEGLTDSYNLDEG-RGTFRKEADFITDDMILSKKLVLQ-- |
| AtCSP41 | 295 | AFLFRNMHFYAEPRAAKDLLGWESKTNLPEDLKERF-EYVVKIGRDKKEIKFELDDKILEALKTPVAA |

Fig 3.2.1 Predicted three dimensional structure of mature PPP1 and AtCSP41

(A) Atom coordinates of PPP1 and AtCSP41 without cTP were predicted by the 3D-JIGSAW (version 2.0, www.bmm.icnet.uk/servers/3djigsaw) server, which builds three dimensional structures based on homologous proteins of known structure. The three dimensional protein models were visualised using Deepview Swiss-Pdb Viewer (<http://expasy.org/spdbv>). The N-terminus of the protein is depicted in purple, the C-terminus in green. The putative NAD(P) binding domain (NBD) is shown in light blue. (B) Alignment of PPP1, AtCSP41 protein sequences without cTP and sequence of the homologous *Synechocystis* sp. PCC 6803 protein slr1540 (<http://bacteria.kazusa.or.jp/cyano/>) using Clustal W (Thompson *et al.*, 1994) and Boxshade. Conserved amino acids are highlighted by black boxes, whereas grey ones indicate closely related amino acids.

PPP1 and CSP41 have both been experimentally localised in the chloroplast by proteomic studies (Kleffmann *et al.*, 2004). Stable expression of a PPP1:CFP fusion in *Arabidopsis* confirmed the chloroplast localisation and additionally demonstrated a localisation of PPP1 in the stromules, which are stroma filled tubules extending from and occasionally connecting plastids (Raab *et al.*, 2006). Fractionation of *Arabidopsis* chloroplasts and followed by immuno-detection of PPP1, RbcL and Lhcb3 as stromal and thylakoid control respectively, shows that PPP1 is indeed localised in the stroma and does not associate with the thylakoid membrane (**Figure 3.2.2**).

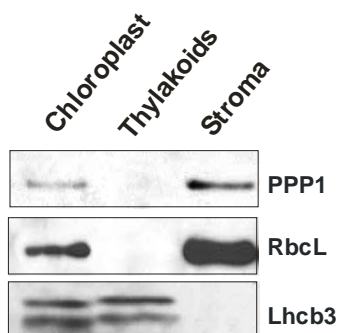


Fig 3.2.2 PPP1 is a stromal protein

Arabidopsis chloroplasts were isolated, followed by separation of stromal contents from thylakoid membranes. Chloroplast and thylakoid proteins corresponding to 5 µg of Chlorophyll and stromal proteins deriving from lysed chloroplast corresponding to 15 µg of chlorophyll were loaded. Immuno-detection was carried out using the PPP1 antibody (Chapter 2.2.4.1), RbcL and Lhcb3 antibodies.

3.2.2 Phenotypical analysis of knock-out mutants of *PPP1* and *CSP41*

Two mutant alleles were identified for *PPP1* by screening the T-DNA Express database. The *ppp1-1* mutant line has already been described previously (Hassidim *et al.*, 2007), showing that transcript is present upstream of the insertion, but not downstream. It was also demonstrated that transcript levels of the truncated transcript were higher. Analysis of transcript levels upstream of the insertion site yielded the same result, when repeated within the scope of this thesis (data not shown). However, the lack of PPP1 protein in both *ppp1-1* and *ppp1-2* was proven by using a specific PPP1 antibody against a peptide sequence of the N-terminus downstream of the predicted nucleotide binding domain (Chapter 2.2.4.1; **Figure 3.2.3B**). For *AtCSP41* no publicly available mutant allele exists. Thus, the Csaba Koncz (MPIZ Cologne) library of genomic DNA from insertion mutants was screened with gene specific and T-DNA specific primers (Rios *et al.*, 2002). The line 61.888 was identified to contain an insertion in the second exon of *AtCSP41*. In this line the T-DNA has inserted as a tandem with the left borders facing the genomic flanking regions on both sides. The absence of *AtCSP41* transcript was verified by RT-PCR using primers upstream of the insertion site (**Figure 3.2.3C**). As can be seen in **Figure 3.2.3D** both mutant alleles for *PPP1* display a reduction in leaf size and show pale-green pigmentation, when grown in the greenhouse with long-day illumination (16h light, 8h dark). When grown in the climate chamber with a 12h light 12h dark regime (**Figure 3.2.3E**), the mutants are only slightly smaller and have WT pigmentation. The growth and appearance of *atcsp41* is WT-like under all conditions tested, whereas a *ppp1 atcsp41* double mutant displays the *ppp1* mutant phenotype (**Figure 5.2.3D**).

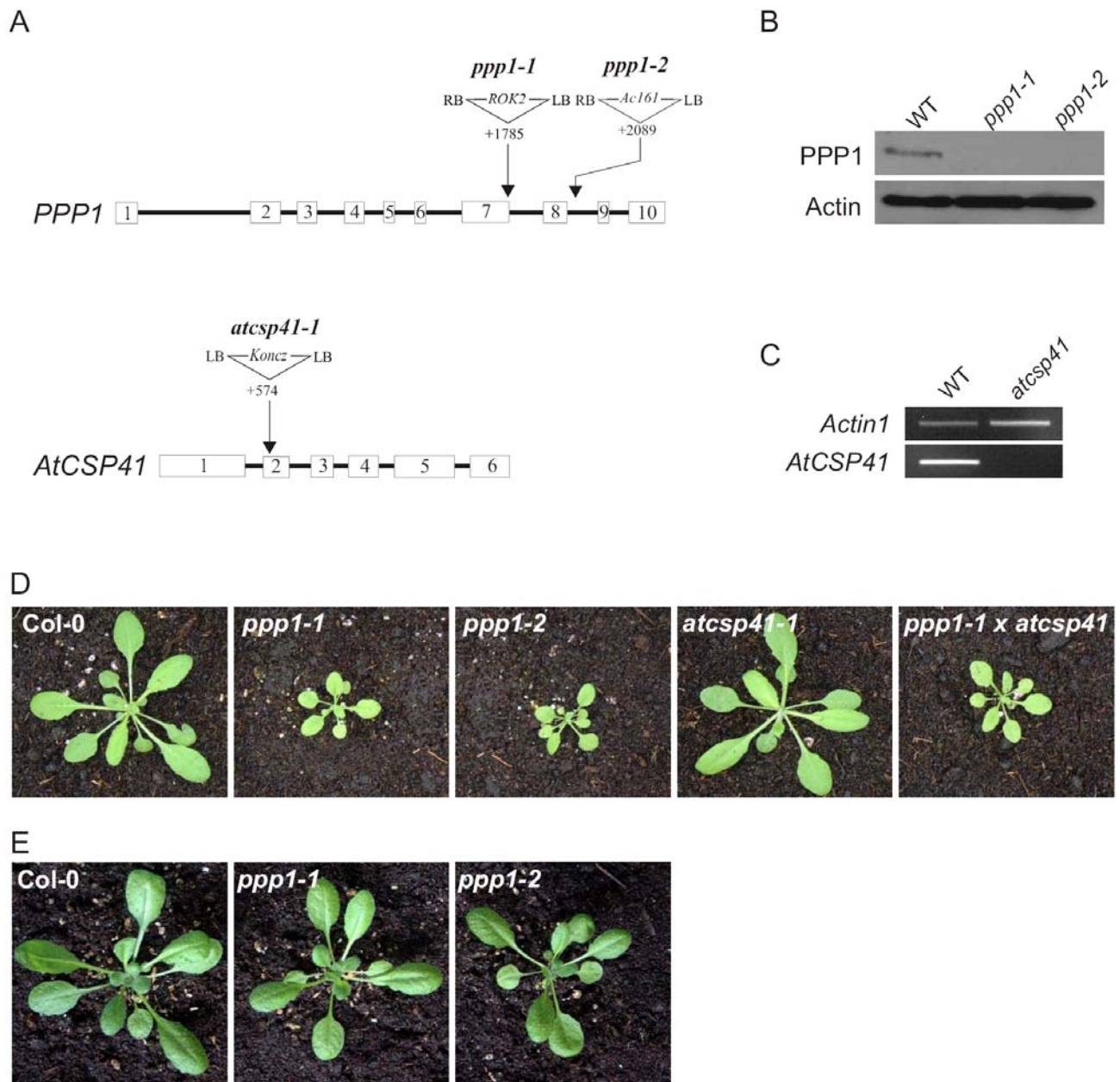


Fig 3.2.3 Location of insertion in the mutant alleles and mutant phenotype

(A) The translated exons are shown as white numbered boxes and the introns as black lines. Both, orientation and site of insertions are depicted. All three mutant alleles originate from T-DNA insertions: *ppp1-1* from the SALK T-DNA collection as SALK_021748, *ppp1-2* from the GABI-KAT collection as GABI_452H11 and the *atcsp41* allele from screening the T-DNA collection of C Koncz (Max-Planck-Institute for Plant Breeding Research, Cologne, Germany) as 61.888. (B) Protein analysis of PPP1 in WT and both mutant alleles. Total leaf protein was extracted and 40 μ g of protein each lane was loaded on an SDS-gel. The filter was immuno-decorated with a PPP1 specific antibody (Chapter 2.2.4.1) and an antibody against Actin as loading control. (C) Expression analysis of *AtCSP41* in WT and mutant. RT-PCR analysis was performed on the transcripts of both WT and mutant plants with gene specific primers upstream of the insertion and actin primers as positive control. (D) Growth of WT, *ppp1-1*, *ppp1-2*, *atcsp41* and *ppp1 atcsp41* plants in the greenhouse (16 h/ 8 h light dark cycle of natural sun-light supplemented with HQI light; Osram). (E) Growth of WT, *ppp1-1* and *ppp1-2* in the climate chamber (12 h/ 12h light dark cycle of 120 μ mol photons $m^{-2}s^{-1}$).

3.2.3 Leaf pigments and photosynthetic parameters

Because leaf pigmentation was altered in the *ppp1* mutants when grown in the greenhouse, a quantitative analysis of leaf pigments of these plants and WT was carried out by HPLC (Chapter 2.2.6). In the greenhousegrown plants the chlorophyll a/b ratio remains unchanged in the mutant, but total chlorophyll content is slightly decreased as compared to WT (**Table 3.2.1**). The major difference of the *ppp1* mutant lies in an increased level of the xanthophyll-cycle pigments Violaxanthin, Antheraxanthin and Zeaxanthin (VAZ), which indicates that mutant chloroplasts suffer enhanced photo-oxidative stress (Demmig-Adams and Adams, 1992).

| Leaf Pigments | LL (100 $\mu\text{mol photons m}^{-2}\text{s}^{-1}$) | | |
|---------------|---|-----------------|-----------------|
| | Col-0 | <i>ppp1-1</i> | <i>ppp1-2</i> |
| Chl a/b | 3.14 \pm 0.02 | 3.14 \pm 0.03 | 3.13 \pm 0.06 |
| Chl a + b | 2 638 \pm 49 | 2415 \pm 202 | 2422 \pm 216 |
| Lutein | 134 \pm 3 | 137 \pm 4 | 145 \pm 6 |
| Nx | 35 \pm 0 | 38 \pm 1 | 37 \pm 1 |
| VAZ | 31 \pm 1 | 39 \pm 2 | 39 \pm 2 |
| β -Car | 73 \pm 6 | 75 \pm 5 | 74 \pm 6 |

Table 3.2.1 Pigment analysis of *ppp1-1* and *ppp1-2* grown at 100 $\mu\text{mol photons m}^{-2}\text{s}^{-1}$

Leaf pigments analysis was performed with WT and the two mutant alleles grown under low-light conditions (LL) in the greenhouse. Pigment content was determined by HPLC of five plants for each genotype. The carotenoid content is given in mmol per mol Chl (*a + b*), and the Chl content is expressed as nmol Chl (*a + b*) per g fresh weight. Mean values \pm SD are shown. Nx, neoxanthin; VAZ, xanthophyll cycle pigments (violaxanthin + antheraxanthin + zeaxanthin); β -Car, β -carotene.

To investigate, if a more pronounced phenotype can be obtained by elevated stress conditions, WT, *ppp1-1*, *atcsp41* and the respective double mutant plants were grown for four weeks under higher light intensities (400 $\mu\text{mol photons m}^{-2}\text{s}^{-1}$) and pigment analysis was carried out. Only *ppp1* and *ppp1 atcsp41* plants show differences to WT (**Table 3.2.2**). As expected, plants lacking PPP1 exhibit even more enhanced VAZ pigment levels when grown at higher light intensities. Additionally, the decrease in the levels of chlorophylls per fresh weight is more evident, but also a decrease in the Chl *a/b* ratio can be observed. This is indicative for an increase either in the PSII/PSI, or in the antenna/ reaction centre ratio. The decrease in β -carotene levels in the mutant supports an increase in the PSII/PSI ratio, because 22 molecules of this pigment are associated with PSI, while PSII only binds seven (Nelson and Yocum, 2006). The *atcsp41* mutant shows WT pigment levels, whereas the double mutant behaves exactly like the *ppp1* mutant.

| | Col-0 | HL (400 $\mu\text{mol photons m}^{-2}\text{s}^{-1}$) | | |
|-------------------------------|----------------|---|-----------------|---------------------|
| | | <i>ppp1-1</i> | <i>atcsp41</i> | <i>ppp1 atcsp41</i> |
| Chl a/b | 3.54 \pm 0.2 | 3.02 \pm 0.14 | 3.63 \pm 0.06 | 3.01 \pm 0.09 |
| Chl a + b | 1518 \pm 104 | 1008 \pm 180 | 1702 \pm 378 | 1003 \pm 88 |
| Lutein | 139 \pm 6 | 160 \pm 8 | 135 \pm 6 | 151 \pm 4 |
| Nx | 35 \pm 1 | 42 \pm 2 | 35 \pm 0 | 43 \pm 2 |
| VAZ | 51 \pm 6 | 126 \pm 8 | 52 \pm 2 | 119 \pm 6 |
| β-Car | 96 \pm 3 | 78 \pm 5 | 96 \pm 2 | 78 \pm 6 |

Table 3.2.2 Pigment analysis of *ppp1-1*, *atcsp41* and *ppp1 atcsp41* grown at 400 $\mu\text{mol photons m}^{-2}\text{s}^{-1}$

Leaf pigments analysis was performed with WT, *ppp1-1*, *atcsp41* and the *ppp1 atcsp41* double mutant grown under higher light conditions (HL) of 400 $\mu\text{mol photons m}^{-2}\text{s}^{-1}$ in the climate chamber. Pigment content was determined by HPLC of five plants for each genotype. The carotenoid content is given in mmol per mol Chl (*a* + *b*), and the Chl content is expressed as nmol Chl (*a* + *b*) per g fresh weight. Mean values \pm SD are shown. Nx, neoxanthin; VAZ, xanthophyll cycle pigments (violaxanthin + antheraxanthin + zeaxanthin); β -Car, β -carotene.

To analyse if *ppp1*, *atcsp41* and the respective double mutant display a change in their capability of photosynthetic electron transport, Chl *a* fluorescence and P700 absorption were measured employing the PAM fluorometer. The maximum (F_v/F_m) and the effective quantum yields (Φ_{II}) of greenhouse grown WT, *ppp1*, *atcsp41* and the double mutant were determined and *ppp1* and the double mutant exhibit a slight decrease in both parameters as compared to WT (**Table 3.2.3**).

| Photosynthetic Parameters | Col-0 | LL (100 $\mu\text{mol photons m}^{-2}\text{s}^{-1}$) | | |
|-------------------------------|-----------------|---|-----------------|---------------------|
| | | <i>ppp1</i> | <i>atcsp41</i> | <i>ppp1 atcsp41</i> |
| F_v/F_m | 0.81 \pm 0.01 | 0.79 \pm 0.01 | 0.81 \pm 0.00 | 0.78 \pm 0.02 |
| Φ_{II} | 0.75 \pm 0.00 | 0.73 \pm 0.00 | 0.75 \pm 0.01 | 0.72 \pm 0.01 |

Table 3.2.3 Chlorophyll a fluorescence measurements of WT, *ppp1-1*, *atcsp41* and *ppp1 atcsp41* plants

The photosynthetic parameters F_v/F_m and Φ_{II} were determined from 4 week old plants grown in the greenhouse at 100 $\mu\text{mol photons m}^{-2}\text{s}^{-1}$. Actinic light was 80 $\mu\text{mol photons m}^{-2}\text{s}^{-1}$. The values represent the average of 10 independent measurements each.

For a detailed analysis of *ppp1* photosynthetic performance, the light dependance of photosynthetic parameters was determined with plants grown in the greenhouse in a 16h/ 8h light/ dark cycle as well as with plants grown in the climate chamber in a 12h/ 12h light/ dark cycle (**Figure 3.2.4, 3.2.5**). The *ppp1* mutants from both growth conditions show a decrease in the Electron Transport Rate (ETR), an increase in NPQ and in the P700 oxidation rate. However, the decrease in ETR is more prominent in *ppp1* mutants grown in the greenhouse, whereas the capacity of NPQ is even higher in plants grown in the climate chamber. Only *ppp1* mutants grown in the climate chamber show a WT like F_v/F_m -value, indicating normal PSII abundance and activity.

Altogether, *ppp1* plants grown in the climate chamber (**Figure 3.2.4.B/D**; **Figure 3.2.5.B/D**) show a phenotype indicative for a constraint in carbon fixation at higher actinic light intensities (Golding and Johnson, 2003). In detail, if carbon fixation is limited, PSI acceptors are over-reduced and alternative pathways such as cyclic electron flow around PSI (Shikanai, 2006) or the water-water cycle (Rizhsky *et al.*, 2003) are favoured. These alternative pathways reduce plastoquinone, leading to an enhanced acidification of the lumen, which is exacerbated by the reduction in ATP net consumption through carbon fixation. Besides causing an increase in non-photochemical quenching, the low luminal pH is thought to lead to an increase in P700 oxidation and a decrease in ETR by slowing down the electron proton symport of the plastoquinone pool.

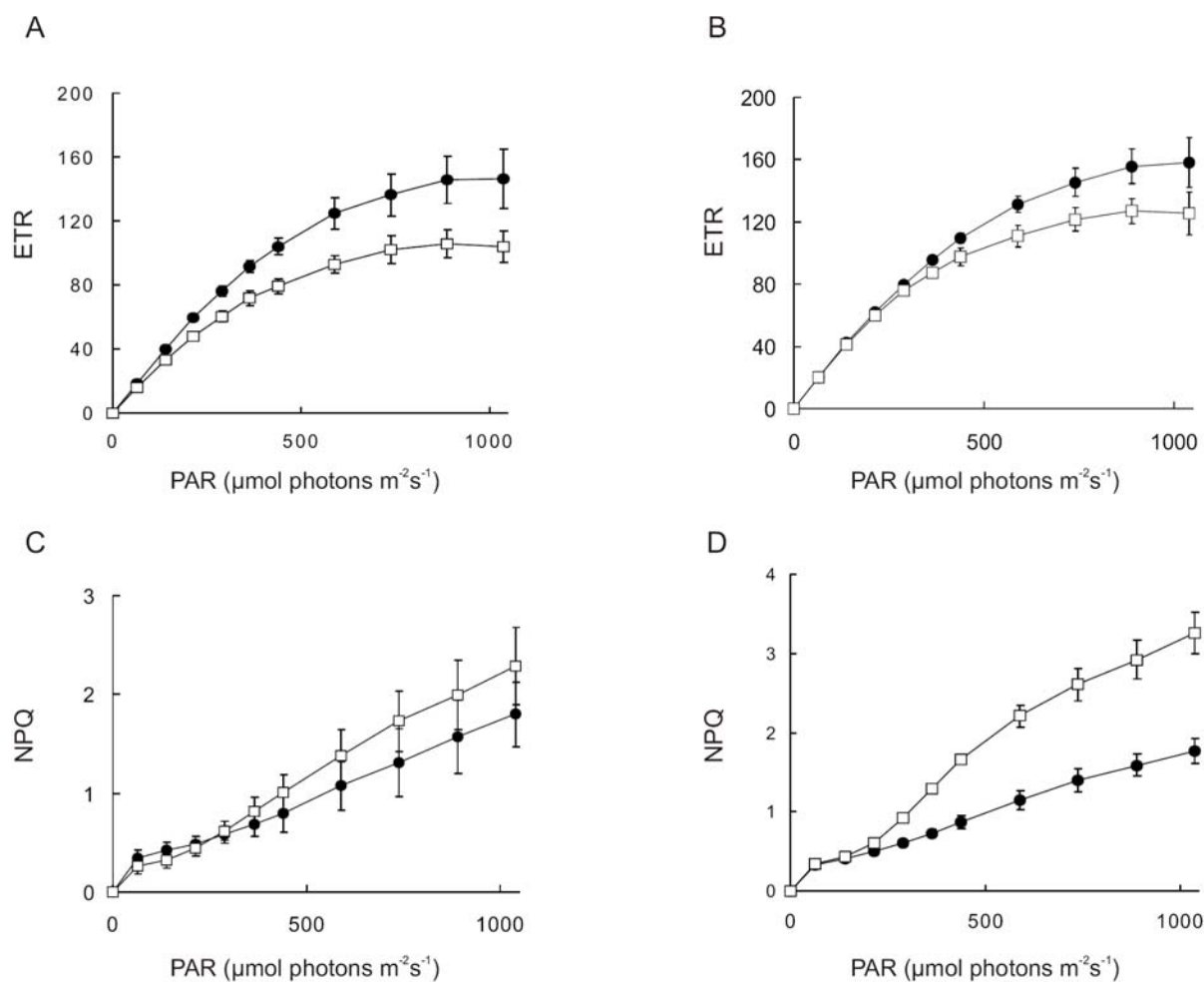


Fig 3.2.4 Chlorophyll a fluorescence measurements

WT (filled circles) and *ppp1* (white squares) plants grown in the greenhouse (**A**, **C**) or in the climate chamber (**B**, **D**) were analysed with the PAM-fluorometer. In (**A**) and (**B**) the Electron Transport Rate (ETR) and in (**C**) and (**D**) the non-photochemical quenching of PSII were determined by measuring Chl *a* fluorescence. Leaves were illuminated for 15 Min with actinic light of different light intensities, steady state fluorescence was determined as F_s and a saturating light pulse of 800 ms and 5000 $\mu\text{mol photons m}^{-2}\text{s}^{-1}$ was given yielding F_m . ETR was calculated as $\text{PAR} \times \Phi_{\text{II}} \times 0.5 \times 0.84$, Φ_{II} as $(F_m - F_s)/F_m$ and NPQ as $(F_m - F_m')/F_m'$.

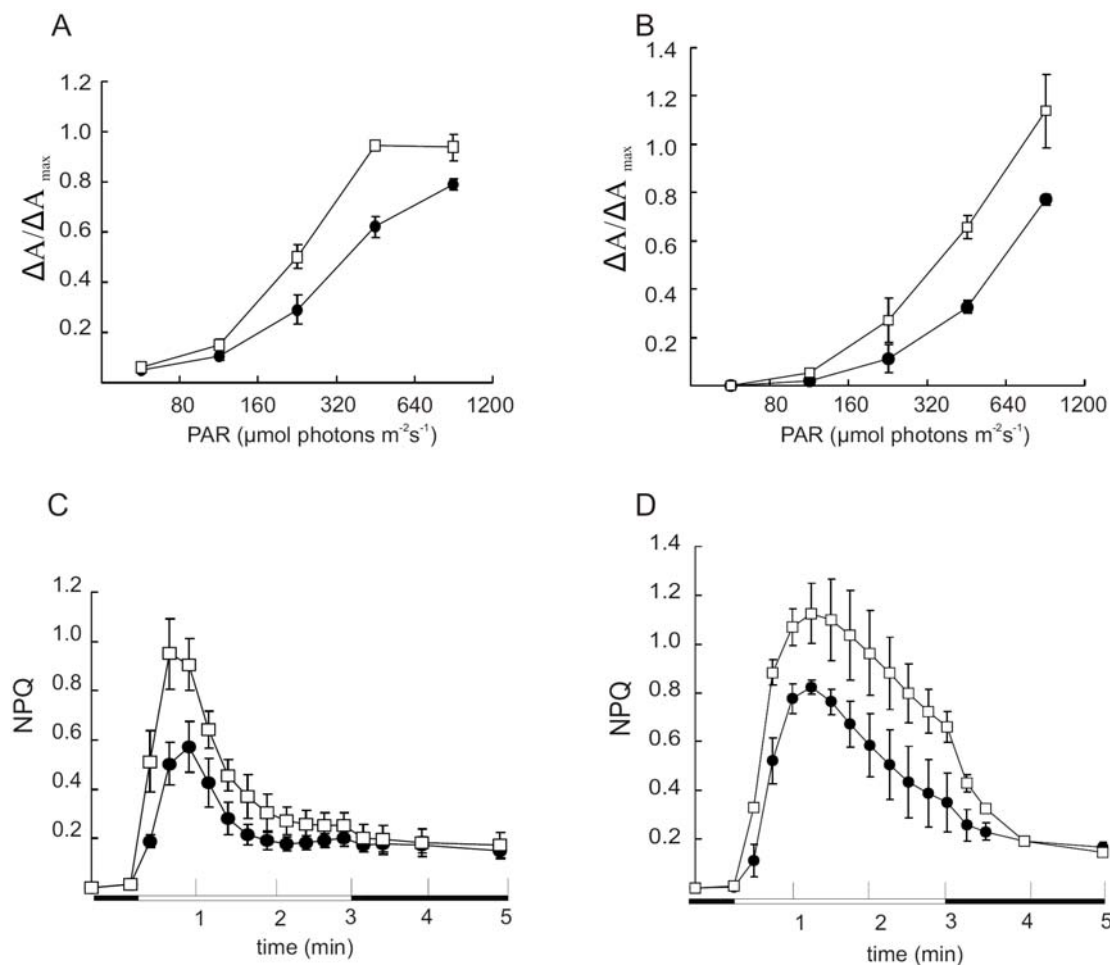


Fig 3.2.5 P700 oxidation rate and transient NPQ measurements

(A+B) The P700 oxidation rate was determined of WT (filled circles) and *ppp1* (white squares) plants grown in the greenhouse (A) or in the climate chamber (B). Absorbance changes at 830 nm were recorded, while illuminating the leaves for 5 min with actinic light of different light intensities giving ΔA and far-red light to yield ΔA_{\max} . P700 oxidation ratio was calculated as $\Delta A/\Delta A_{\max}$. Each value represents the average of 5 independent measurements (\pm SD). (C+D) Time courses of induction and relaxation of NPQ monitored during dark-to-light ($80 \mu\text{mol photons m}^{-2} \text{s}^{-1}$, white bar) transition of WT and *ppp1* plants grown in the greenhouse. NPQ was calculated as $(F_m - F_m')/F_m'$ (C) or the climate chamber (D). The 3 min light period (white bar) was followed by a 2 min dark period (black bar). Note that NPQ induction during the activation period of photosynthesis is thought to be caused by the transient acidification of the thylakoid lumen when CEF activity is higher than the activity of the ATP synthase.

3.2.4 Analysis of the abundance of photosynthetic proteins

Abundances of chloroplast proteins were investigated by Western analysis of total protein extract of WT and *ppp1-1* mutant plants grown in the greenhouse or the climate chamber using antibodies against one subunit of each multi-protein complex. Protein levels were normalised with Actin (Figure 3.2.6). The Western analysis demonstrates that in mutant plants grown in the greenhouse levels of most examined proteins are decreased to 50% of WT. Exceptions are the nucleus encoded Lhcb1 protein of the light harvesting complex of PSII (LHCII), which shows slightly increased levels and the large subunit of the Ribulose-biphosphate carboxylase/ oxygenase (Rubisco, RbcL), of which levels are $\sim 35\%$ of WT. The chloroplast protein levels of the *ppp1* plants grown in the

climate chamber equals WT, except for a decrease in the large and the small subunit of Rubisco (80% of WT).

Additionally, thylakoid complexes of WT and *ppp1-1* mutant plants grown in the greenhouse were analysed by Blue native (BN)-PAGE (**Figure 3.2.6C**). Here, protein samples according to same amounts of chlorophyll were loaded. In the *ppp1-1* mutant inter-complex stoichiometry remains largely unchanged, except for an increase in free LHCII monomers and a decrease in PSII supercomplexes.

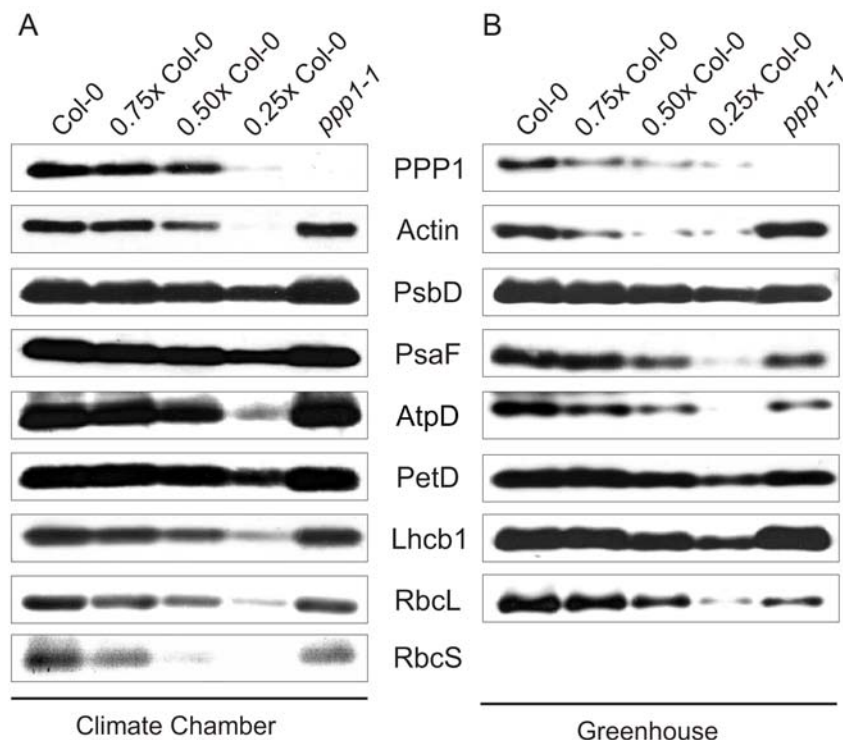


Fig 3.2.6 Chloroplast protein composition

Levels of thylakoid membrane polypeptides in mutant and WT plants. 40 μ g of total protein of *ppp1-1* plants and 40 μ g and decreasing amounts of WT plants grown in the climate chamber (A) or in the greenhouse (B) were separated by SDS-PAGE and subsequently transferred to PVDF membranes. Replicate filters were immunolabelled with antibodies. Three independent experiments were performed, and representative results are shown. (C) Thylakoids from WT and *ppp1-1* plants grown in the greenhouse were solubilised with 1.25 % β -DM and separated by Blue native (BN)-PAGE. Identity of complexes is depicted on the right.

3.2.5 Chloroplast expression analysis

To investigate if the decrease in protein levels from plants grown in the greenhouse was due to changes in transcript levels, total leaf RNA was analysed by Northern hybridisation with probes specific for *petD*, *psaB*, *psbA* and *ACTIN1* as loading control (Chapter 2.2.2.2; **Figure 3.2.7B**). Whereas *psaA* transcript is increased more than two fold in the *ppp1-1* mutant, *rbcL* is slightly decreased and *psbA* transcripts show WT levels. These results are supported by an expression analysis of all chloroplast genes by qRT-PCR (supplementary data, Chapter 6.2), which shows a significant up-regulation of *psaA* in *ppp1-1* and no significant changes for *rbcL* and *psbA*.

Additionally, the chloroplast and cytoplasmic translational rates were examined by a ³⁵S methionine *in vivo* translation assay (Chapter 2.2.4.15; **Figure 3.2.7A**). The results of this experiment show that radioactive labelling of both subunits of the Rubisco, RbcL and RbcS is decreased in the *ppp1-1* mutant background. That disruption of expression of one of the Rubisco subunits effects expression of the other has been repetitively observed and therefore the co-regulation of Rubisco subunit expression is in accordance with previous publications (Schmidt and Mishkind, 1983; Rodermel *et al.*, 1996; Pesaresi *et al.*, 2001). A further difference can be observed in the translation of the D1 protein of PSII (PSII-D1), which seem to be increased marginally.

To investigate if the changes seen in the *in vivo* translation assay can be correlated with an alteration of the polysome association of *rbcL* and *psbA* transcript, polysome formation on both transcripts was assessed by sucrose density-gradient fractionation. Transcripts associated with polysomes have higher sedimentation rates than those associated with singular ribosomes or ribosome free mRNA. The proportion of transcripts, which are polysome-associated compared to unassociated allows to estimate the efficiency of translation initiation and elongation (Barkan, 1993). Significant differences can neither be detected in the association of *rbcL* transcript, nor of *psaA* and *psbA* (**Figure 3.2.7C**). Altogether, these results indicate that in the *ppp1-1* mutant background less RbcL protein is stably expressed. However, defects leading to this phenotype are neither related to differential transcription, because transcript levels remain relatively unchanged, nor to defects in the translational apparatus, because initiation, elongation and termination of translation seem to be functional in *ppp1*.

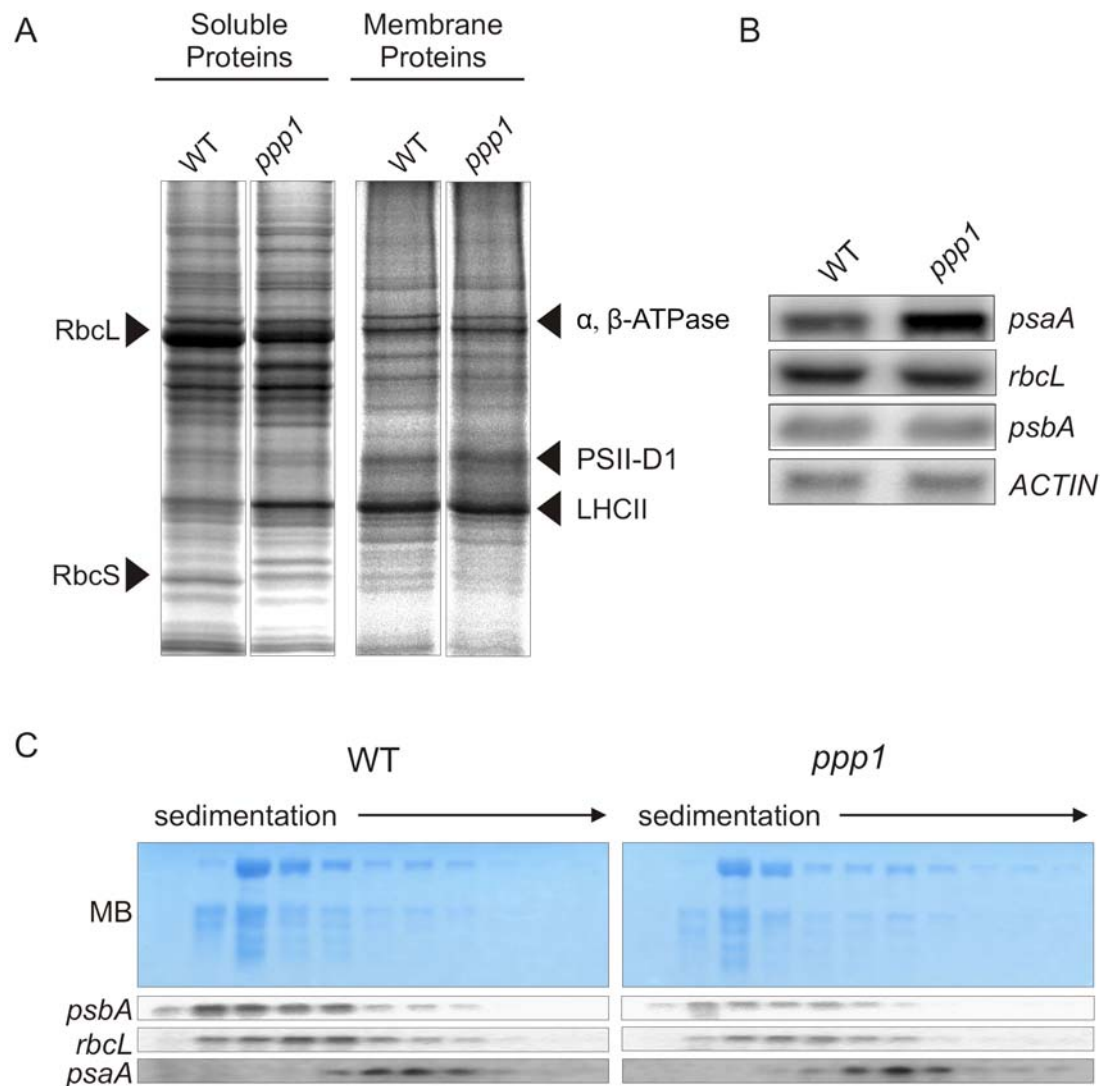


Fig 3.2.7 Effect of the *ppp1* mutation on chloroplast gene expression

(A) *In vivo* translation assay. ^{35}S Methionine was applied to leaves of WT and *ppp1* plants grown in the greenhouse (16 h/8 h light / dark cycles) for 1h, illuminated with $50 \mu\text{mol photons m}^{-2}\text{s}^{-1}$. Soluble and membrane proteins were isolated from WT and mutant leaves, separated by SDS-PAGE and analysed by fluorography. The most intensely labelled band corresponds to the large subunit of Rubisco. (B) Northern analysis of plastid transcripts. Total leaf RNA (20 μg) of WT and *ppp1* mutant plants were hybridised with gene specific probes against ACTIN1 as loading control, *psbA*, *rbcL* and *psaA*. (C) Association of chloroplast mRNA with polysomes. Total extracts from 4-week-old WT and *ppp1* mutant plants were fractionated on sucrose gradients. Eleven fractions of equal volume were collected from the top to the bottom of the sucrose gradients. An equal proportion of the RNA purified from each fraction was analysed by gel-blot hybridisation. The membrane was stained with methylene-blue as loading control and transcripts of *psbA*, *rbcL* and *psaA* were detected with gene-specific probes.

3.2.6 Analysis of transcript processing

CSP41 was reported to be involved in cleavage of the 3' stem loop of chloroplast transcripts (Bollenbach *et al.*, 2003). Because similarities in primary amino acid sequence, as well as in the predicted three dimensional structures of CSP41 and PPP1, are present, it was investigated, whether the phenotype of the decrease in RbcL protein abundance could be correlated with a defect in *rbcL* transcript processing in the *ppp1* mutant. Additionally, because all results indicating a 3' stem-loop

PCR products probably stem from degradation products, because they either start at base 1, the start-codon or terminate at base 1440, the stop-codon, with at least the respective 5' end found in the mutants impeding with binding of the ribosome and thus translation. These results suggest that transcript degradation is enhanced in all mutant backgrounds.

3.2.7 Effect of the absence of photosynthetic complexes on PPP1 abundance

The effect of the absence of each of the four photosynthetic complexes on PPP1 and RbcL protein levels was examined. PPP1 and RbcL abundance is greatly reduced in PSII, Cyt *b₆f* and PSI knock-outs (**Figure 3.2.9**; for further information see Chapter 3.1.7). Whereas RbcL levels are also slightly reduced in the *atpd* mutants, PPP1 protein accumulates to levels even higher than in WT. Besides increased degradation of the RbcL protein because of oxidative stress, the highly reduced amounts of PPP1 might represent one of the mechanisms leading to the down-regulation of RbcL protein. However, other mechanisms in the regulation of RbcL abundance must exist to explain its altered levels for instance in plants lacking the ATP-synthase complex. One of these mechanisms is the autoregulation of Rubisco large-subunit translation according to its assembly state, which has recently been described for tobacco (Wostrikoff and Stern, 2007) and *Chlamydomonas* chloroplasts, where this process is known to be modulated by oxidative stress (Irihimovitch *et al.*, 2000; Cohen *et al.*, 2005)

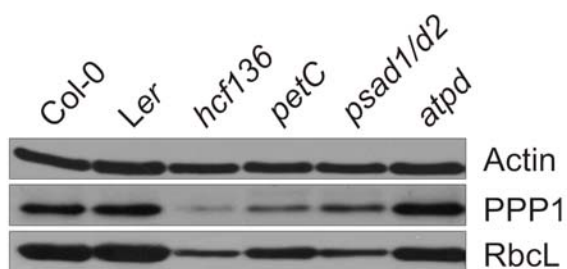


Fig 3.2.9 The abundance of PPP1 and RbcL in the absence of photosynthetic complexes

Immunodetection of PPP1 and RbcL in Col-0, *Ler*, *hcf136*, *petC*, *psad1/d2*, *atpd*. The applied antibodies are depicted on the right. Total protein extract corresponding to 40 μ g of protein was loaded each.

3.2.8 A PPP1:CFP fusion complements the *ppp1* mutant phenotype

To investigate the putative RNA-binding function of PPP1, RNA Co-Immunoprecipitation Chips (RIP-Chip) analysis has been initiated (Schmitz-Linneweber *et al.*, 2005). In this method, immunoprecipitated RNA and supernatant RNA are coupled to two different fluorescent dyes and are then hybridised to an oligonucleotide Chip with probes covering all plastid transcripts. However, the peptide antibody against PPP1 did not recognise the protein in its native state and thus was not suitable for co-immunoprecipitation. An alternative for RIP-Chip analysis were plants expressing the PPP1:CFP fusion under the control of a *35S* promoter (Raab *et al.*, 2006). To confirm complete functionality of this fusion protein, *ppp1-1* mutant plants were transformed with the construct to test

for complementation. Homozygous T3 were grown in the greenhouse to investigate the complementation of the growth phenotype by the introduced fusion protein. In 80% of analysed lines the growth phenotype was reverted (two lines shown: **Figure 3.2.10A**). Total protein was extracted from complemented mutant plants and it was shown by hybridisation with PPP1 and CFP (Invitrogen) specific antibodies that they contained the bigger 64 kDa fusion protein (PPP1: 37 kDa, CFP: 27 kDa), but not the native PPP1 protein (**Figure 3.2.10B**). Both antibodies yielded a further signal at approximately 70 kDa, which probably represents the immature form of the PPP1:CFP fusion protein before import into the chloroplast. Additionally, the Coomassie staining demonstrates that RbcL protein levels are WT-like in the CFP:PPP1 overexpressors, further verifying the complete physiological functionality of the fusion protein.

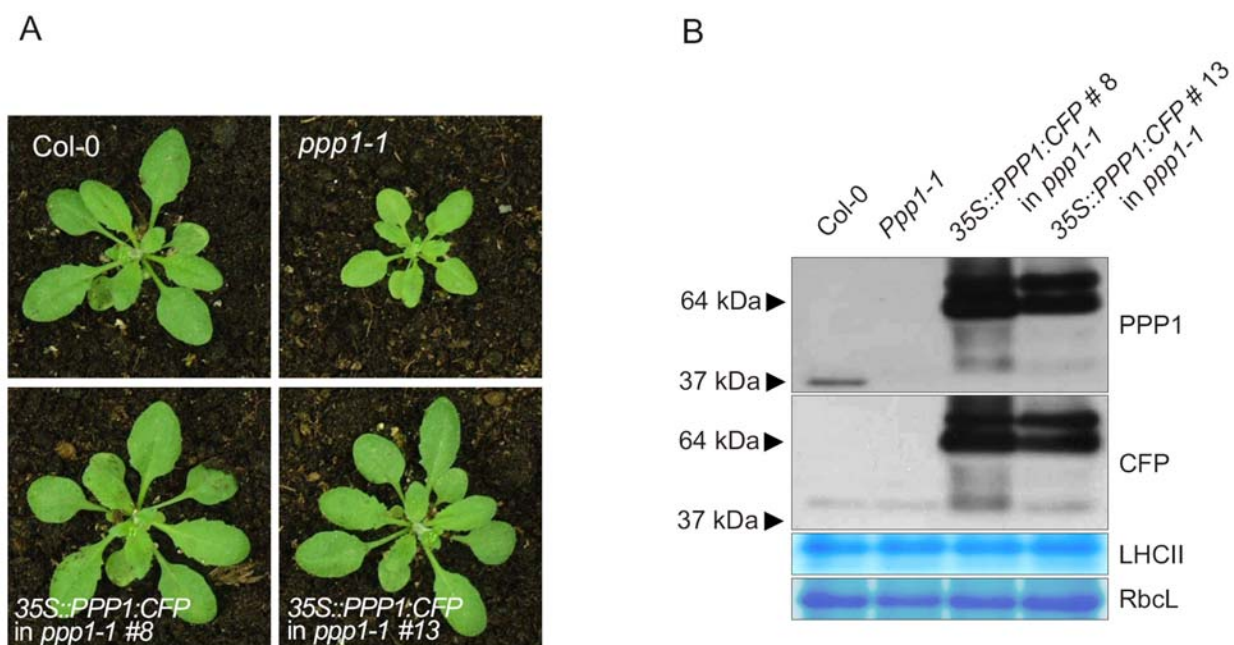


Fig 3.2.10 Transgenic plants expressing CFP tagged PPP1 in a *ppp1-1* mutant background

(A) Four week old WT, *ppp1-1* and *ppp1-1* plants grown in the greenhouse (16 h light/ 8 h dark cycles) transformed with the *PPP1:CFP* construct. (B) Transgene expression analysis was carried out on total protein extract. *PPP1:CFP* is over-expressed in the two lines and CFP is recognised by the specific antibody against CFP and PPP1. The growth phenotype and the reduction in RbcL protein levels are complemented in both lines.

3.2.9 Germination assay

The expression rates of some photosynthetic genes are regulated by the phytohormone abscisic acid (ABA) (Seki *et al.*, 2002). Also the transcription of *PPP1* responds negatively to ABA (Hoth *et al.*, 2002). Because *PPP1* is a putative RNA-binding protein, it was assumed that it might carry out regulatory functions in the chloroplast in response to this phytohormone (Raab *et al.*, 2006). As ABA levels within the plant directly correlate with the degree of seed germination, an assay was performed to elucidate a possible function of *PPP1* in the complex ABA signalling network. The

germination was carried out with both *ppp1* mutant alleles. Homozygous mutants and WT plants were identified as progeny from one heterozygous plant and the germination assay was performed on their progeny, which had been harvested simultaneously in order to avoid genetic and environmental background specific differences in germination rates. This experiment was carried out in collaboration with S. Raab (University of Nürnberg-Erlangen, Germany). Both alleles show a significant reduction in germination rate in comparison to WT, when exogenous ABA is applied (**Figure 3.2.11**). For *ppp1-1*, a concentration of 1 μ M ABA yielded the highest difference in germination rate, whereas for *ppp1-2* 0.5 μ M was sufficient to inhibit germination.

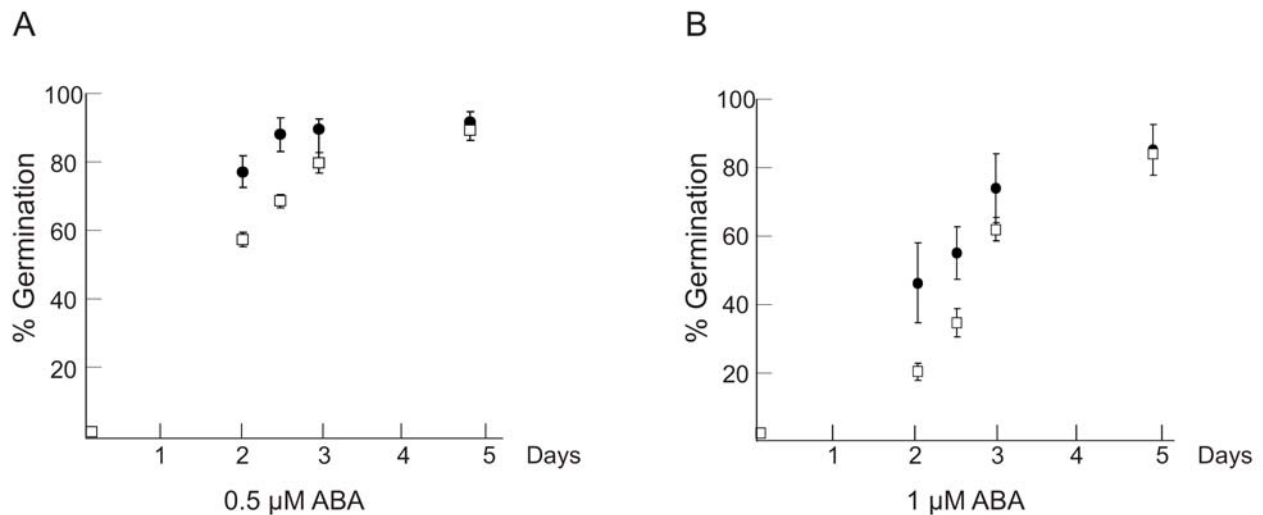


Fig 3.2.11 The *ppp1* mutants display a delayed germination rates in response to ABA

Seed dormancy of wild-type, *ppp1-1* (B) and *ppp1-2* (A) seeds. In both independent experiments freshly harvested Seeds were plated on ABA-containing medium (A: 0.5 μ M ABA; B: 1 μ M ABA) and maintained at 22°C. The degree of germination of WT (closed circles) and *ppp1* (open squares) seeds was monitored after 2, 2.5, 3 and 5 days.

4 Discussion

4.1 PPP4/TMP14

4.1.1 Novel family of chloroplast localised proteins

Within this thesis a novel protein family consisting of four *Arabidopsis* proteins with unknown functions has been characterised. All four members have sequence similarities, especially in the two predicted transmembrane helices. The location of these four proteins in the chloroplast as suggested before by proteomic analyses (Kleffmann *et al.*, 2004), was verified by transient expression of RFP-fusions in *Arabidopsis* protoplasts for TMP14-like and PPP4-like, by MS analysis of thylakoid proteins from BN second dimensions for PPP4, TMP14 and TMP14-like and by Western analysis for PPP4 and TMP14. The latter demonstrated that both PPP4 and TMP14 are primarily localised in the stroma lamellae. Here, PPP4 and TMP14 interact as shown by crosslinking and Co-IP, in a previously un-described complex.

4.1.2 A novel thylakoid complex predominantly localised in the stromal lamellae

This work demonstrates the existence of a novel thylakoid complex, which as minimal constituents contains PPP4 and TMP14. Each of both proteins seems to be able to form homomeric complexes in the absence of the other interaction partner as shown by BN page analysis and crosslinking for both and for PPP4 additionally by Co-IP. Whereas PPP4 accumulates to the same levels in *tmp14* as in WT, TMP14 levels are decreased in the *ppp4* background. Photosynthetic measurements demonstrated that this novel complex is indeed involved in photosynthesis, as parameters are changed in *ppp4* and *ppp4 tmp14* mutants. Differences to WT present in the *ppp4* single mutants are exacerbated in the double mutant background. Considering the lack of phenotype in the *tmp14* mutant, where PPP4 protein accumulates to WT levels, it can be concluded that presence of PPP4 is sufficient to carry out the physiological function. Conversely, in *ppp4* mutants an effect on photosynthetic parameters is evident, indicating that TMP14 can only partly carry out the function of PPP4, which could be due to its reduced amounts present in the thylakoid membrane. In the double mutant, where both proteins are absent, the phenotype is enhanced, which supports the idea that TMP14 can to some extent carry out the physiological function of PPP4. As such, it can be speculated that heteromeric and homomeric complexes of both proteins at least partially act redundant and that the physiological function carried out by PPP4 and TMP14 requires a certain amount of complexes, which are not present in the *ppp4* mutant. However, despite the evidence for these complexes, it remains unclear, if complex formation is necessary for the proteins' functions.

As will be described in the following section, some other properties of both proteins do differ and therefore it appears likely that both proteins carry out further protein specific functions.

Both crosslinking experiments and protease protection assays indicate that TMP14 interacts with other proteins especially in the absence of PPP4. Electrostatic interactions with additional proteins seem to be important for the anchorage of TMP14 in the thylakoid membrane. In the case of PPP4 only the protease protection assay is indicative for the existence of associated proteins. The MS analysis of the co-immunoprecipitate derived from digitonin-solubilised thylakoids did not identify any other interaction partners of this complex. Therefore, it can be assumed that digitonin destroys the association of other proteins. Accordingly, the complex containing PPP4 and TMP14, migrating at the size of the Cyt *b₆f* monomer in BN gels most probably also represents a multimeric form of both components. The lack of co-migration of PPP4 and TMP14 with the Cyt *b₆f* dimer represents one further indication against the interaction of PPP4 and TMP14 with this essential photosynthetic complex. Moreover, it was shown, that presence of the Cyt *b₆f* complex is not mandatory for accumulation of PPP4 and TMP14, because both proteins can be found in plants lacking this complex. Concomitantly, in mutants devoid of the other major thylakoid complexes, PSII, PSI and ATP-synthase, PPP4 and TMP14 protein levels are relatively stable. Therefore it can be concluded that the complex comprising PPP4 and TMP14 is not stably associated with any of the four major thylakoid complexes. Interestingly, TMP14 accumulates to lower levels than PPP4 in the plants lacking one of the respective complexes (exception is *atpd*, where both proteins are present at WT levels), suggesting that differential regulatory mechanisms are involved.

The obtained data allow speculation about the functional composition of the heteromeric complex. Because no further components of this complex could be precipitated by Co-IP, it can be assumed that the heteromeric complex solubilised with digitonin solely consists of PPP4 and TMP14 subunits. If one now postulates that complex formation is indispensable for the function of PPP4 and TMP14 and as a consequence according to the photosynthetic parameters measured in the mutants that homomeric and heteromeric complexes act redundant, it can be estimated that all three complexes capable of performing the so-far unknown photosynthetic activity should contain the same amount of subunits. To speculate about a putative size and composition of the heteromeric complex containing PPP4 and TMP14 the following experimental results have to be taken into consideration: (i) the molecular size of the complex solubilised with digitonin, (ii) the ratio of PPP4 and TMP14 in this complex and (iii) the crosslinking pattern observed in the respective other mutants to estimate number of subunits composing the functional complex.

The digitonin solubilised, heteromeric complex has a slightly higher molecular weight than the LHCII monomer, which runs at about 60 kDa (Granvogl *et al.*, 2006) and contains as visualised by silver staining of the second dimension slightly more TMP14 than PPP4 (reaction was quenched before saturation of signal strength). In crosslinked thylakoids of *ppp4* mutant plants, the TMP14 pattern can be interpreted as the result of five proteins interacting, whereas for PPP4 the biggest crosslinking product seems to represent a tetramer. However, TMP14 crosslinking is always further progressed and therefore it cannot be excluded that amounts of crosslinked PPP4 pentamers deriving from the applied experimental conditions, are below the detection level. Conclusively, the heteromeric complex is bigger than 60 kDa, the highest molecular crosslinking product seems to be a pentamer and it contains more TMP14 than PPP4. Therefore, the existence of a heteromeric complex consisting of three TMP14 and two PPP4, with a molecular weight of 65 kDa appears possible. Further experiments need to be conducted to clarify the composition of this new complex

4.1.3 Phenotype of *ppp4* and *ppp4 tmp14* mutants in relation to specific processes of photosynthesis

Measurements of photosynthetic parameters employing the PAM fluorometer showed a slight, but significant phenotype in the *ppp4* mutant, which was exacerbated in the *ppp4 tmp14* double mutant. Parameters changed in these mutants are a decrease in NPQ under both light and high light, an increase in 1-qP under low light and an increase in $\Delta A / \Delta A_{\max}$ in low and a decrease in high light. The WT-like F_v / F_m indicates that PSII abundance and function is unchanged in these mutant plants. Additionally, the lower NPQ excludes that PPP4 and TMP14 are components of carbon fixation, because an impairment in this process should cause higher NPQ (Johnson and Golding, 2003). However, defects in the linear electron flow, in regulatory processes of photosynthesis or in the cyclic electron flow around PSI could at least partially account for the changes in photosynthetic parameters observed in the *ppp4* and *ppp4 tmp14* mutants. To investigate the physiological function of both proteins, the photosynthetic phenotypes of *ppp4* and *ppp4 tmp14* will be compared with phenotypes of mutants impaired in the respective processes of photosynthesis. Then further results obtained in this work will be put into context in the attempt to survey possible functions of PPP4 and TMP14 in this process.

4.1.3.1 Linear electron flow

The increase of 1-qP, $\Delta A / \Delta A_{\max}$ and the decrease of NPQ in *ppp4* and *ppp4 tmp14* plants under low light illumination could point to a defect in linear electron flow downstream of PSII. Firstly, because of the co-migration of PPP4 and TMP14 with the Cyt *b₆f* complex, a possible involvement

at the level of Cyt *b₆f* will be discussed. Concurrently, similar changes in photosynthetic parameters as stated above are present in the partially Cyt *b₆f* defective mutants *petL* and *pgr1*, when measured with low actinic light. However, PAM measurements of these mutants at higher light intensities result in increasing differences of NPQ in comparison to WT, whereas the *ppp4* and the *ppp4 tmp14* double mutations lead only to a marginal reduction in NPQ and the $\Delta A/\Delta A_{\max}$ value, of which the latter is even slightly increased in *petL* and *pgr1* under high light. Furthermore, these partially Cyt *b₆f* defective mutants do not exhibit the changes in the kinetics of *in situ* cyclic electron flow (CEF) measurement, which occur in the *ppp4 tmp14* mutant (Schwenkert *et al.*, 2007; Munekage *et al.*, 2001; Okegawa *et al.*, 2005). Therefore, a defect in the linear electron transport chain at the Cyt *b₆f* complex appears unlikely.

Mutants with impairments in PSI function, such as *psad1* (Ihnatowicz *et al.*, 2004), *psae1* (Ihnatowicz *et al.*, 2007) and *psag* (Zygadlo *et al.*, 2005) show a marked increase in 1-qP, because electron flow is partially blocked at PSI. They also show deficiencies in PSI function, a feature that can not be found in *ppp4* and *ppp4 tmp14* mutant plants. Further evidence against a role of PPP4 and TMP14 in PSI stems from the biochemical analyses, which exclude an interaction of PPP4 and TMP14 with this thylakoid complex.

4.1.3.2 Regulatory processes in photosynthesis

Conversely, regulatory processes of photosynthesis might be affected in the *ppp4*, *ppp4 tmp14* mutants. Under low light state transition balances the excitation energy between the two photosystems by the formation of a PSI-LHCII complex (for a review, see Allen and Forsberg 2001). Plants lacking the kinase STN7 cannot perform this process (Bellafiore *et al.*, 2005; Bonardi *et al.*, 2005). Therefore, they show an increased 1-qP and a slightly decreased NPQ, when measured under low light illumination. However, the $\Delta A/\Delta A_{\max}$ value remains unchanged in *stn7* plants (E. Aseeva, Botany, LMU, Munich; pers. com.), whereas in the *ppp4* and *ppp4 tmp14* mutants the P700 oxidation rate is higher than in WT. This, together with the increased phosphorylation rate of LHCII and the decreased Chl *a/b* ratio in the stromal lamellae fraction of the *ppp4 tmp14* double mutant, suggests that the mutant plants show increased LHCII phosphorylation and that the changes in 1-qP and NPQ cannot be due to a defect in this process.

One further regulatory mechanism is the conversion of excess light energy into heat (qE), involving the PSII protein PsbS, low lumenal pH and xanthophyll cycle pigments (Li *et al.*, 2000; Li *et al.*, 2004). Defects in qE only slightly affect photosynthetic parameters when measured with low actinic light, as can be seen in the *psbs* mutant, which is impaired in qE. Here, the photosynthetic parameters NPQ and 1-qP also resemble those of *ppp4* and the *ppp4 tmp14* double mutant (Li *et al.*,

2002). However, as the NPQ value measured with high actinic light consists substantially of qE , *psbs* mutants display a largely decreased NPQ under these conditions. The $\Delta A/\Delta A_{\max}$ value of *psbs* mutants has not been published. However, another mutant defective in qE (*que1*), of which the specific location of the mutation has not been mapped yet, shows an increase in the $\Delta A/\Delta A_{\max}$ value, when measured with low light and a slight decrease when measured with high light (Kalituhno *et al.*, 2006). Conclusively, photosynthetic parameters of mutants with defects in qE resemble those of *ppp4* and *ppp4 tmp14* mutants, except for their immense decrease in NPQ under high light. Further experimental evidence against a direct involvement of PPP4 and TMP14 in the process of qE is the the predominant localisation of both proteins in the stromal lamellae, whereas qE is executed by LHCII (Ruban *et al.*, 2007), of which the majority is localised in the thylakoid grana. Additionally, neither levels nor thylakoid localisation of the PsbS protein is altered in the *ppp4 tmp14* mutants. That *ppp4* is not defective in the xanthophyll cycle can be concluded from the only slight increase in violaxanthin pigments as compared to WT, which rather supports that the decrease in NPQ might be due to lower acidification of the lumen (Hieber *et al.*, 2000). As such it can be excluded that the phenotype of mutants lacking PPP4 and TMP14 is due to a defect in the execution of the qE process, which therefore indicates a defect in modulating the ΔpH across the thylakoid membrane. Two mechanisms are thought to be part of this modulation (Kramer *et al.*, 2004): (i) The cyclic electron flow around PSI, which will be further discussed in the next chapter and (ii) changes in conductivity of the ATP-synthase to protons. The latter mechanism is not likely to be affected in the *ppp4* and *ppp4 tmp14* mutant backgrounds, because only some of their photosynthetic parameters could be explained by changes in the ATP-synthase conductivity. In detail, the measured differences at low light could be due to a higher conductivity of the ATP-synthase, resulting in decreased low luminal pH, but the high light mutant parameter $\Delta A/\Delta A_{\max}$ cannot be explained by this. Additionally, little is known about the mechanism of changes in ATP-synthase conductivity (Kanazawa and Kramer, 2002; Takizawa *et al.*, 2008) and the presented work does not support an interaction of PPP4 and TMP14 with the ATP-synthase, which would be expected, if proteins had influence on its conductivity.

4.1.3.3 Cyclic electron flow around PSI (CEF)

Cyclic electron flow around PSI (CEF) is a mechanism that can modulate acidification of the lumen (Munekage *et al.*, 2002). The *pgr1lab* mutant is impaired in the antimycin A sensitive cyclic electron flow or the switch between LEF and this pathway (DalCorso *et al.*, 2008). When photosynthetic parameters are measured with low actinic light, these mutants display a reduction in NPQ and an increase in $1-qP$ in about as much as the *ppp4 tmp14* double mutant (G. DalCorso,

Department of Botany, LMU, Munich; pers. com). This phenotype can be explained considering that with impairments in cyclic electron flow, fewer protons are translocated into the lumen, this leading to a decrease in heat dissipation of light energy, which is proportional to the acidification of the lumen. The NPQ is therefore lower. If light energy conversion into heat is reduced, more of this energy will be used for charge separation at PSII leading to a higher reduction of the plastoquinone pool by PSII (higher 1-qP). However, the $\Delta A/\Delta A_{\max}$ ratio is also increased in *ppp4* and *ppp4 tmp14* plants, a phenotype not observed in the *pgr1lab* mutant. Yet, this phenotype in the *ppp4* and *ppp4 tmp14* plants can be explained by the higher reduction of the plastoquinone pool under low light growth conditions, which leads to an increased amount of phosphorylated LHCII at PSI, possibly resulting in higher oxidation rates of P700 due to an increase in antenna size. That *pgr1lab* does not show this phenotype might be due to a direct function in PSI, with which the PGRL1 protein has been shown to be associated (DalCorso *et al.*, 2008).

Differences between the phenotypes of *ppp4* and *ppp4 tmp14* compared to *pgr1lab* become evident, when photosynthetic parameters obtained from high light illumination are compared. Here the $\Delta A/\Delta A_{\max}$ value approaches zero and NPQ is reduced to half of WT in the *pgr1lab* mutant. In *ppp4* and *ppp4 tmp14* NPQ is only slightly reduced and $\Delta A/\Delta A_{\max}$ is significantly lower, but still about 80% of WT. Mutants of *ppp4* and *ppp4 tmp14* lack the strong NPQ phenotype indicating that proton translocation by CEF is only marginally impaired. But together with the decrease in P700 oxidation rate, it can be proposed that CEF indeed is slightly affected and therefore leads to the over-reduction of the stroma and consequently to an indirect decrease of the $\Delta A/\Delta A_{\max}$ value by charge recombination (DalCorso *et al.*, 2008; Endo *et al.*, 2005; Munekage *et al.*, 2002).

Besides the antimycin A-sensitive CEF pathway there is also the NdH dependent CEF pathway (Munekage *et al.*, 2004), which is thought to be minor in comparison to the antimycin A-sensitive CEF. Mutants in this pathway do not exhibit the changes in the photosynthetic parameters as measured in this thesis for *ppp4* and *ppp4 tmp14* mutant plants (Muraoka *et al.*, 2006; Munshi *et al.*, 2006; Kamruzzaman *et al.*, 2005), however it cannot be excluded that growth conditions of reported mutants differed. Electrons from the PQ pool can also be transferred to oxygen, a process referred to as chloro-respiration (Cournac *et al.*, 2000). It has been proposed that plants lacking the capability to reduce oxygen should have a higher 1-qP and a lower $\Delta A/\Delta A_{\max}$ value. This process is thought to be of special importance under high light (Rosso *et al.*, 2006) and therefore no changes in photosynthetic parameters would be expected under low light. As *ppp4* and *ppp4 tmp14* mutant plants exhibit changes especially under low light, an involvement of PPP4 and TMP14 in this process appears unlikely.

4.1.3.3.1 In-depth analysis of CEF in *ppp4* and *ppp4 tmp14* mutants

From this comparison of photosynthetic phenotypes observed in the *ppp4* mutant and in the *ppp4 tmp14* double mutant with those of plants lacking or being impaired in physiological processes of photosynthesis, it can be concluded that PPP4 and TMP14 are not essential constituents of one of these processes. However, PPP4 and TMP14 might be involved in their regulation or partially in their functionality. The preceding discussion of possible pathways involving PPP4 and TMP14 suggests that they function in the modulation of the pH gradient and thereby in qE.

Accordingly, the most likely candidate for a process that involves the PPP4 TMP14 complex is the cyclic electron flow around PSI, as the Chl *a* fluorescence and P700 absorption phenotypes of *ppp4* and *ppp4 tmp14* can be explained by a mostly low light and not high light dependent impairment in CEF downstream of PSI. To further investigate the hypothesis of an involvement of PPP4 and TMP14 in CEF, attention has to be paid to the phenotypes in CEF observed with either the *ppp4* mutant in the *in vivo* measurement or the *ppp4 tmp14* double mutants in the *in situ* measurement.

The *in vivo* experiment was performed by measuring the transient increase of NPQ after light onset. This measurement relates to the hypothesis that NPQ induction during the activation period of photosynthesis is caused by the transient acidification of the thylakoid lumen when CEF activity is higher than the activity of the ATP-synthase (DalCorso *et al.*, 2008). In this experiment the *ppp4* mutants behave like WT and only in the steady state show a slight reduction in NPQ. However, when plants are grown in continuous light, they exhibit a significant decrease in the transient NPQ. Accordingly, it can be concluded that normally PPP4 is not involved in the enhanced CEF during light onset, but that the process of acclimation of the plant to continuous light involves PPP4-regulated transient NPQ.

In the *in situ* measurements the *ppp4 tmp14* double mutants display an increase in Chl *a* fluorescence already after addition of NADPH, indicating that more Fd is stably bound to thylakoid complexes, as has been shown for *psad1* and *psae1*. These mutants exhibit increased cyclic electron flow (DalCorso *et al.*, 2008). A further phenotype that *psad1*, *psae1* and *ppp4 tmp14* have in common is the increased abundance of the PGRL1 protein in the thylakoid membrane. This suggests that when PPP4 and TMP14 are missing, the plant senses a disturbance and accordingly increases PGRL1 protein levels and the amount of thylakoid membrane bound Fd. But contrary to *psad1* and *psae1*, the *ppp4 tmp14* mutant plants do not exhibit enhanced cyclic electron flow in the *in situ* measurement, as fluorescence reaches WT steady state levels. This demonstrates that an increase of cyclic electron flow as measured in the *psae* or *psad* mutants does not occur in this double mutant, despite the increase in PGRL1 levels and membrane bound Fd, which is thought to

cause enhanced CEF (DalCorso *et al.*, 2008). A further phenotype of *ppp4 tmp14* mutants in the *in situ* experiment, are the decreased kinetics of the increase in Chl *a* fluorescence following the addition of Fd. This indicates changes in the electron transport from NADPH via Fd to plastoquinone in the double mutant. One possible explanation is the impairment in FNR function. However, levels and localisation of this protein are not changed in the *ppp4 tmp14* double mutants. The second possible explanation is a decreased capability of the proteins involved in PQ reduction to carry out this process in the *ppp4 tmp14* double mutant, which would implicate a direct function of PPP4 and TMP14 in CEF.

A further indication for a possible functional interaction of PPP4 and TMP14 with components of cyclic electron flow, is the susceptibility of PPP4 and TMP14 to extraction by digitonin, which was also shown for PGRL1 and thylakoid associated FNR, but not for other thylakoid proteins. From this experimental result a localisation of all four proteins in the same region of stromal thylakoid membranes can be hypothesised. To investigate if PPP4 and TMP4 transiently interact with these essential components of CEF, split-ubiquitin analysis in yeast will be carried out in future experiments.

4.1.3.3.2 Speculation about an involvement of PPP4 and TMP14 in CEF processes

If one assumes that PPP4 and TMP14 carry out a function in CEF, the lack of which is especially measurable in low light, one firstly has to speculate about low light CEF, the occurrence of which is disputed (Laisk *et al.*, 2005). However, the hypothesis has been put forth that, as has been shown in *Chlamydomonas* (Finazzi and Forti, 2004), association of LHCII with PSI (in state 2), which occurs in vascular plants in PSII favouring low light, might result in an increase in CEF. One indication for this hypothesis is the co-ordinated upregulation of both state 2 transition and CEF in the *psad1* mutant (Pesaresi *et al.*, 2002; DalCorso *et al.*, 2008). If indeed state 2 transition results in increased cyclic electron flow in plants, there should be substantial amounts of CEF under PSII favouring low light. That low light CEF plays a physiological role, is supported by the visible phenotypes of *pgr1lab* and *pgr5* plants grown at such light intensities (Munekage *et al.*, 2002, DalCorso *et al.*, 2008). A lack of antimycin A-sensitive CEF should account for the changes of photosynthetic parameters in the *pgr1lab* mutant, when measured with low light. As *ppp4* and *ppp4 tmp14* exhibit similar changes and as also parameters measured at high light have the same trend as in *pgr1lab*, there is the possibility that the complex comprised of PPP4 and TMP14 might have a function in the same process. The nature of the changes in photosynthetic parameters in *ppp4* and *ppp4 tmp14* as compared to WT and *pgr1lab* suggests that the physiological function of PPP4 and TMP14 occurs throughout light conditions and is not enhanced by environmental stimuli, which increase CEF,

such as high light. Concomitantly, CEF at transition of dark to light is not influenced by a lack of PPP4. Therefore, if PPP4 and TMP14 are involved in antimycin A-sensitive CEF, the co-existence of an additional process, which is upregulated in response to high light or dark to light transition, represents a crucial requirement.

But, if one now postulates an involvement of PPP4 and TMP14 in CEF, what could be the functions of PPP4 and TMP14 in this process? There are two possibilities. Firstly, both proteins might be components of the postulated enzyme Fd-PQ oxidoreductase (FQR). Secondly, they might regulate CEF. Some results obtained in this thesis support a structural function. Firstly, PPP4 and TMP14 form a heteromeric complex comprised of several subunits, which cannot be found stably associated with any other complex and thus seems to represent a structural entity. Secondly, this complex is highly abundant in the thylakoid membrane, as shown by silver-staining of BN second dimensions.

4.1.4 Conclusions

Many questions about the function of this novel complex remain open. Prerequisite for further speculations are an in-depth analysis of other interaction partners, of which the presence but not the identity has been shown by several biochemical approaches. Furthermore, application of inhibitors of CEF should be able to strengthen or weaken the involvement of PPP4 and TMP14 in this pathway. Antimycin A is known to impair the pathway also involving PGR5 (Munekage *et al.*, 2002, Munekage *et al.*, 2004). Additionally, the possibility has to be taken into account that the other two members of this novel protein family PPP4-like and TMP14-like carry out the same function. Single mutants of *ppp4-like* and *tmp14-like* do not exhibit changes in photosynthetic parameters. Therefore, the analysis of further double, triple and ultimately the quadruple mutant should yield additional information about the function of the complex. Furthermore, the silencing of the gene encoding the only member of this novel protein family in the single cell alga *Chlamydomonas reinhardtii*, in which CEF is a crucial mechanism under oxygen depleted conditions (Finazzi and Forti, 2004) might clarify if this protein is essential for optimal photosynthesis and CEF.

4.2 The putative RNA-binding protein PPP1

4.2.1 Physiological role: Chloroplast gene expression

The nuclear co-regulation of genes encoding photosynthetic proteins and those encoding the chloroplast expressional apparatus (Biehl *et al.*, 2005) led to the postulation of a mechanism coordinating the expression of plastome and nuclear encoded components of the photosynthetic machinery (Leister, 2005). Because of the stromal localisation of PPP1 and its published co-localisation with components of the plastid expressional apparatus (Yamaguchi *et al.*, 2003; Pfannschmidt *et al.*, 2001; Peltier *et al.*, 2006), a function in the expression of chloroplast genes appears likely. Furthermore, as *PPP1* expression is co-regulated with photosynthetic genes, the encoded protein might represent one of the components executing nuclear control on the expression of chloroplast photosynthetic genes in order to achieve co-ordination of plastome and nuclear encoded protein levels in the chloroplast. This work was performed with the aim to elucidate the effect of PPP1 on chloroplast gene expression and grasp its mode of function.

Under optimum growth conditions as prevailing in the climate chamber, *ppp1* plant appearance resembles WT, except for a slight retardation in growth. However, regarding photosynthetic parameters recorded by illumination with higher actinic light intensities, *ppp1* plants show a clear phenotype. They exhibit increased non-photochemical quenching, a higher P700 oxidation state and a decrease in the electron transport rate, all three combined being indicative for a defect in carbon fixation (Golding and Johnson, 2003; Golding *et al.*, 2004). In line with the results obtained by PAM measurement, the analysis of the chloroplast proteome shows that protein levels of both subunit of the carbon fixing enzyme Rubisco, RbcL and RbcS are slightly reduced, whereas the levels of components of the electron transport chain remain unchanged. Therefore, it can be assumed that in climate chamber conditions, lack of PPP1 solely causes a reduction in Rubisco levels. Because of its plastid stromal localisation and its predicted function in gene expression, a role of PPP1 in *rbcL* expression can be assumed. However, two results obtained from the chloroplast proteome analysis of *ppp1* plants grown in the greenhouse suggests that PPP1 might influence levels of more chloroplast proteins: (i) although light intensity in average is about the same as in the climate chamber, levels of Rubisco are half in comparison to plants grown in the climate chamber, indicating that downregulation of Rubisco levels might be partially of secondary nature; (ii) no increase can be observed in the PSII/PSI ratio of plants grown in the greenhouse, as would be expected from a limitation in terminal electron acceptors of PSI (Allahverdiyeva *et al.*, 2005). The unchanged PSII/PSI ratio in *ppp1* plants grown in the greenhouse is caused by an equal

downregulation of both complexes to 50% of WT. If the reduction of *rbcL* expression was the primary effect in the *ppp1* plants, their phenotype should be comparable to the tobacco *rbcS* antisense lines published by Jiang and Rodermel (1995), which contain about 30-40% of Rubisco. Here, Cyt f levels are slightly reduced and LHCII levels are slightly increased, these results being in line with the *ppp1* phenotype. However, the Chl *a/b* ratio is decreased, a change in line with an enhanced PSII/PSI ratio as expected from Allahverdiyeva *et al.* (2005), which cannot be observed in *ppp1* plants grown in the greenhouse. Yet, comparing these two results, one has to consider that plant-specific differences might exist. The question if PPP1 could be involved more globally in regulating the abundance of chloroplast proteins and thereby execute a general nuclear control can easily be speculated on, when the extensive demand for the expression of the high abundant protein, Rubisco is considered. Results obtained in this thesis by radioactive labelling of chloroplast proteins, shows that after one hour RbcL represents the most labelled protein, followed by LHCII and PSII-D1 (Chapter 3.2.5). Therefore, it can be postulated that in optimal environmental conditions as present in the climate chamber, a normal expressional set without PPP1 is sufficient for the expression of all plastid genes except for *rbcL*, because of its high demand. Sub-optimal conditions in the more variable light and temperature regimes of the greenhouse should result in increased oxidative stress for chloroplast proteins, and therefore probably require an enhanced expression of photosynthetic proteins encoded in the nucleus, as well as in the chloroplast. Assuming that PPP1 is a crucial component of regulating chloroplast gene expression, the higher demand of protein turn-over would be impaired in plants lacking this protein and thus lead to a decrease in functional complexes. However, for the preceding speculations, we have to exclude a regulation of the *psbA* expression by PPP1, because the turn-over of the encoded protein PSII-D1 is higher than of any other thylakoid peptides (Matteo *et al.*, 1981) and therefore would be a second component highly influenced by sub-optimal expressional activity in the chloroplast. The experimental results show that translation of PSII-D1 is even slightly increased in the *ppp1* mutant. Therefore, *psbA* expression cannot be controlled by PPP1.

Despite all collected experimental evidences, the mode of action of the control of gene expression by PPP1 remains elusive. Indications that PPP1 acts post-transcriptionally, derive from chloroplast transcriptome (supplementary data) and gel blot analyses, which demonstrate that *rbcL* transcript levels are not significantly changed in the mutant, although a decrease in RbcL protein levels can be observed by Western analysis. The *in vivo* translation-assay shows that translation of *rbcL* is lowered, but polysome assembly of the transcript is unchanged in the mutant, indicating that neither initiation of translation, elongation nor termination are significantly affected (Barkan, 1993). These

results suggest that PPP1 might be involved in posttranslational processes such as stabilising and folding of the nascent polypeptide chain. However, PPP1 was shown to bind *petD* mRNA *in vitro* by Raab *et al.*, which together with the co-migration with the ribosomal subunits (Peltier *et al.*, 2006) suggests regulation at an earlier step of gene expression. To further dissect the function of PPP1, interactions with either mRNAs or other proteins need to be experimentally tested. RNA immuno-precipitation Chips (RIP-Chips) are carried out in co-operation with Christian Schmitz-Linneberger (Berlin). Preliminary results indicate that PPP1 binds the majority of chloroplast mRNAs, which further supports firstly a more global function of PPP1 in chloroplast gene expression and secondly regulation of chloroplast gene expression by PPP1 at transcript level.

4.2.2 The homologue AtCSP41

Because of protein sequence homologies, similarities in the three dimensional structures and reported co-localisations with the 70S ribosome or some of its components (Yamaguchi *et al.*, 2003; Peltier *et al.*, 2006), it was of interest to investigate, if PPP1 and AtCSP41 have redundant functions. The phenotypic analyses of the respective knock-out mutants show that AtCSP41 does not seem to carry out the same physiological function as PPP1, because the *atcsp41 ppp1* double mutant lacks a synthetic phenotype. However, if PPP1 and AtCSP41 interact *in vivo*, AtCSP41 stability could be dependent on the presence of PPP1 and therefore the *ppp1* mutant could already resemble the double mutant, lacking both PPP1 and AtCSP41 protein. Therefore it cannot be excluded that PPP1 and AtCSP41 carry out the same enzymatic activity. Since it has been reported that CSP41 (Yang and Stern, 1997, Bollenbach *et al.*, 2003) is involved in 3' stem-loop processing, transcript end mapping was performed in *ppp1*, *atcsp41* and *ppp1 atcsp41* double mutant background on *rbcL*, *psbA* and *petD* (data of latter two not shown). This analysis demonstrated differences in transcript ends in all three mutant backgrounds with bias to shorter mRNAs as compared to WT, but never in the 3' stem loop of these transcripts. However, cleavage of the stem loop is thought to result in degradation of the transcript (Rott *et al.*, 1998) and therefore these ends should be short-lived. These results do not exclude that PPP1 and AtCSP41 are involved in transcript processing, but they rather indicate that PPP1 and AtCSP41 impede degradation.

4.2.3 Involvement of PPP1 in ABA signalling

Because it was reported that the expression of *PPP1* is highly downregulated by ABA (Hoth *et al.*, 2002), it was investigated, if a lack of PPP1 causes a differential response of the plant to this phytohormone. Raab *et al.* (2006) speculated that the signal of the phytohormone ABA might be transferred into the chloroplast via RNA binding proteins to change gene expression. If PPP1

enhances chloroplast gene expression, downregulation of its expression by ABA in the nucleus should result in downregulation of its function in chloroplast gene expression. Because lack of PPP1 seems to primarily target *rbcL* expression, a decrease in Rubisco would be expected. This is in line with the negative regulation of a minimal light-responsive unit found in several RBCS promoters by ABA (Acevedo-Hernandez *et al.*, 2005), posing the prospect that ABA downregulates carbon-fixation by repressing expression of Rubisco. However, a recent publication indicates that at least in tobacco, lower amounts of RbcS in the chloroplast lead to an auto-downregulation of *rbcL* expression by unassembled RbcL protein (Wostrikoff and Stern, 2007), making PPP1 dispensable for a coordination of the expression of both Rubisco subunits.

The germination assays carried out with WT and both *ppp1* mutant alleles allowed the investigation, if lack of PPP1 changes germination behaviour. This experiment was solely carried out with plants grown in the climate chamber, where the *ppp1* mutant shows a reduction in Rubisco levels. Interestingly, the mutant seeds showed an enhanced sensitivity in their germination rate to ABA, indicating higher endogenous levels of this phytohormone or perturbations in ABA signalling. To answer the question of how a lack of PPP1 can influence ABA signalling, the biosynthesis pathway of ABA has to be taken into consideration. ABA originates from the same biosynthetic pathway as the carotenoids, the 2-C-methyl-D-erythritol-4-phosphate (MEP) pathway, of which the last enzymatic steps occur in the cytosol (Nambara and Marion-Poll, 2005). Direct plastidic precursors of ABA are the Xanthophyll-cycle pigments (violaxanthin, antheroxanthin and zeaxanthin) and neoxanthin (Schwartz *et al.*, 2003). Overexpression of the zeaxanthin epoxidase (ZEP) causes an enhanced accumulation of ABA in seeds (Lindgren *et al.*, 2003). Therefore, it can be concluded that modulation of the VAZ-pool can influence ABA levels. One phenotype of *ppp1* plants grown in the climate chamber is the capacity for enhanced non-photochemical quenching, as demonstrated by analysing the transient increase in NPQ. For non-photochemical quenching, violaxanthin needs to be converted into zeaxanthin, which occurs by activation of the violaxanthin de-epoxidase (VDE) by low lumenal pH (Niyogi *et al.*, 1998; Bugos and Yamamoto, 1996). In line with the phenotype of the ZEP-overexpressing plants, the increased enzymatic reversion of zeaxanthin by ZEP after the NPQ-spike could be a signal activating ABA-biosynthesis at least in the differentiated chloroplasts of green seeds. Because the *ppp1* mutant grown in the climate chamber mimics a limitation in carbon fixation- which in nature occurs under environmental conditions of low CO₂, as caused by drought (Golding and Johnson, 2003)- the increase in ABA levels might have physiological relevance. As amounts of ABA in the seed directly correlate with the dormancy length (Karszen *et al.*, 1983), an increase in ABA levels as response to limitations in

carbon fixation would postpone germination, which might be advantageous for the survival of the plant. To allow further characterisation of the influence of VAZ pool modulations on ABA production, additional mutants with changes in NPQ and VAZ pigments will be analysed regarding ABA dependent germination behaviour. Additionally, to dissect ABA biosynthesis in response to modulation of its plastidic carotenoid precursors, *ppp1* has been crossed into an ABA luciferase reporter line (Christmann *et al.*, 2005). This will facilitate to analyse if modulation of the VAZ pool results in differential production of ABA and when, if this mechanism is restricted to seeds or can be observed also in leaves.

5 References

A

- Acevedo-Hernandez, G.J., Leon, P., and Herrera-Estrella, L.R.** (2005). Sugar and ABA responsiveness of a minimal *RBCS* light-responsive unit is mediated by direct binding of ABI4. *Plant J* **43**, 506-519.
- Albertsson, P.A., Andreasson, E., and Svensson, P.** (1990). The domain organization of the plant thylakoid membrane. *FEBS Lett* **273**, 36-40.
- Allahverdiyeva, Y., Mamedov, F., Maenpaa, P., Vass, I., and Aro, E.M.** (2005). Modulation of photosynthetic electron transport in the absence of terminal electron acceptors: characterization of the *rbcL* deletion mutant of tobacco. *Biochim Biophys Acta* **1709**, 69-83.
- Allen, J.F., and Forsberg, J.** (2001). Molecular recognition in thylakoid structure and function. *Trends Plant Sci* **6**, 317-326.
- Allen, J.F., Alexciiev, K., and Hakansson, G.** (1995). Photosynthesis. Regulation by redox signalling. *Curr Biol* **5**, 869-872.
- Allen, K.D., Duysen, M.E., and Staehelin, L.A.** (1988). Biogenesis of thylakoid membranes is controlled by light intensity in the conditional chlorophyll *b*-deficient *CD3* mutant of wheat. *J Cell Biol* **107**, 907-919.
- Alonso, J.M., Stepanova, A.N., Leisse, T.J., Kim, C.J., Chen, H., Shinn, P., Stevenson, D.K., Zimmerman, J., Barajas, P., Cheuk, R., Gadrinab, C., Heller, C., Jeske, A., Koesema, E., Meyers, C.C., Parker, H., Prednis, L., Ansari, Y., Choy, N., Deen, H., Geralt, M., Hazari, N., Hom, E., Karnes, M., Mulholland, C., Ndubaku, R., Schmidt, I., Guzman, P., Aguilar-Henonin, L., Schmid, M., Weigel, D., Carter, D.E., Marchand, T., Risseuw, E., Brogden, D., Zeko, A., Crosby, W.L., Berry, C.C., and Ecker, J.R.** (2003). Genome-wide insertional mutagenesis of *Arabidopsis thaliana*. *Science* **301**, 653-657.
- Anderson, J.M.** (1982). The role of chlorophyll-protein complexes in the function and structure of chloroplast thylakoids. *Mol Cell Biochem* **46**, 161-172.
- Aro, E.M., Suorsa, M., Rokka, A., Allahverdiyeva, Y., Paakkarinen, V., Saleem, A., Battchikova, N., and Rintamaki, E.** (2005). Dynamics of photosystem II: a proteomic approach to thylakoid protein complexes. *J Exp Bot* **56**, 347-356.
- Aronsson, H., and Jarvis, P.** (2002). A simple method for isolating import-competent *Arabidopsis* chloroplasts. *FEBS Lett* **529**, 215-220.

B

- Baker, M.E., Grundy, W.N., and Elkan, C.P.** (1998). Spinach CSP41, an mRNA-binding protein and ribonuclease, is homologous to nucleotide-sugar epimerases and hydroxysteroid dehydrogenases. *Biochem Biophys Res Commun* **248**, 250-254.
- Barber, J.** (1982). The control of membrane organization by electrostatic forces. *Biosci Rep* **2**, 1-13.

- Barber, J.** (2006). Photosystem II: an enzyme of global significance. *Biochem Soc Trans* **34**, 619-631.
- Barkan, A.** (1988). Proteins encoded by a complex chloroplast transcription unit are each translated from both monocistronic and polycistronic mRNAs. *Embo J* **7**, 2637-2644.
- Barkan, A., and Goldschmidt-Clermont, M.** (2000). Participation of nuclear genes in chloroplast gene expression. *Biochimie* **82**, 559-572.
- Bassi, R., dal Belin Peruffo, A., Barbato, R., and Ghisi, R.** (1985). Differences in chlorophyll-protein complexes and composition of polypeptides between thylakoids from bundle sheaths and mesophyll cells in maize. *Eur J Biochem* **146**, 589-595.
- Bellaïf, S., Barneche, F., Peltier, G., and Rochaix, J.D.** (2005). State transitions and light adaptation require chloroplast thylakoid protein kinase STN7. *Nature* **433**, 892-895.
- Biehl, A., Richly, E., Noutsos, C., Salamini, F., and Leister, D.** (2005). Analysis of 101 nuclear transcriptomes reveals 23 distinct regulons and their relationship to metabolism, chromosomal gene distribution and co-ordination of nuclear and plastid gene expression. *Gene* **344**, 33-41.
- Bollenbach, T.J., and Stern, D.B.** (2003). Secondary structures common to chloroplast mRNA 3'-untranslated regions direct cleavage by CSP41, an endoribonuclease belonging to the short chain dehydrogenase/reductase superfamily. *J Biol Chem* **278**, 25832-25838.
- Bollenbach, T.J., Tatman, D.A., and Stern, D.B.** (2003). CSP41a, a multifunctional RNA-binding protein, initiates mRNA turnover in tobacco chloroplasts. *Plant J* **36**, 842-852.
- Bonardi, V., Pesaresi, P., Becker, T., Schleiff, E., Wagner, R., Pfannschmidt, T., Jahns, P., and Leister, D.** (2005). Photosystem II core phosphorylation and photosynthetic acclimation require two different protein kinases. *Nature* **437**, 1179-1182.
- Breyton, C., Nandha, B., Johnson, G.N., Joliot, P., and Finazzi, G.** (2006). Redox modulation of cyclic electron flow around photosystem I in C3 plants. *Biochemistry* **45**, 13465-13475.
- Bugos, R.C., and Yamamoto, H.Y.** (1996). Molecular cloning of violaxanthin de-epoxidase from romaine lettuce and expression in *Escherichia coli*. *Proc Natl Acad Sci* **93**, 6320-6325.

C

- Chenna, R., Sugawara, H., Koike, T., Lopez, R., Gibson, T.J., Higgins, D.G., and Thompson, J.D.** (2003). Multiple sequence alignment with the Clustal series of programs. *Nucleic Acids Res* **31**, 3497-3500.
- Chow, W.S., Ford, R.C., and Barber, J.** (1981). Possible effects of the detachment of stromal lamellae from granal stacks on salt-induced changes in spillover. A study by sonication of chloroplasts. *Biochim Biophys Acta* **635**, 317-326.
- Christmann, A., Moes, D., Himmelbach, A., Yang, Y., Tang, Y., and Grill, E.** (2006). Integration of abscisic acid signalling into plant responses. *Plant Biol (Stuttg)* **8**, 314-325.
- Clayton, R.K.** (1980). Photosynthesis: Physical mechanisms and chemical patterns. (Cambridge, England: Cambridge University Press).
- Clough, S.J., and Bent, A.F.** (1998). Floral dip: a simplified method for *Agrobacterium*-mediated transformation of *Arabidopsis thaliana*. *Plant J* **16**, 735-743.

- Cohen, I., Knopf, J.A., Irihimovitch, V., and Shapira, M.** (2005). A proposed mechanism for the inhibitory effects of oxidative stress on Rubisco assembly and its subunit expression. *Plant Physiol* **137**, 738-746.
- Cournac, L., Redding, K., Ravenel, J., Rumeau, D., Josse, E.M., Kuntz, M., and Peltier, G.** (2000). Electron flow between photosystem II and oxygen in chloroplasts of photosystem I-deficient algae is mediated by a quinol oxidase involved in chlororespiration. *J Biol Chem* **275**, 17256-17262.
- Cruz, J.A., Avenson, T.J., Kanazawa, A., Takizawa, K., Edwards, G.E., and Kramer, D.M.** (2005). Plasticity in light reactions of photosynthesis for energy production and photoprotection. *J Exp Bot* **56**, 395-406.

D

- DalCorso, G., Pesaresi, P., Masiero, S., Aseeva, E., Schunemann, D., Finazzi, G., Joliot, P., Barbato, R., and Leister, D.** (2008). A Complex Containing PGRL1 and PGR5 Is Involved in the Switch between Linear and Cyclic Electron Flow in *Arabidopsis*. *Cell* **132**, 273-285.
- Dekker, J.P., and Boekema, E.J.** (2005). Supramolecular organization of thylakoid membrane proteins in green plants. *Biochim Biophys Acta* **1706**, 12-39.
- Demmig-Adams, B., and Adams, W.W., 3rd.** (1993). The Xanthophyll Cycle, Protein Turnover, and the High Light Tolerance of Sun-Acclimated Leaves. *Plant Physiol* **103**, 1413-1420.
- Deng, X.W., Tonkyn, J.C., Peter, G.F., Thornber, J.P., and Gruissem, W.** (1989). Post-transcriptional control of plastid mRNA accumulation during adaptation of chloroplasts to different light quality environments. *Plant Cell* **1**, 645-654.
- Drager, R.G., Zeidler, M., Simpson, C.L., and Stern, D.B.** (1996). A chloroplast transcript lacking the 3' inverted repeat is degraded by 3'→5' exoribonuclease activity. *RNA* **2**, 652-663.

E

- Emanuelsson, O., Nielsen, H., and von Heijne, G.** (1999). ChloroP, a neural network-based method for predicting chloroplast transit peptides and their cleavage sites. *Protein Sci* **8**, 978-984.
- Emanuelsson, O., Nielsen, H., Brunak, S., and von Heijne, G.** (2000). Predicting subcellular localization of proteins based on their N-terminal amino acid sequence. *J Mol Biol* **300**, 1005-1016.
- Endo, T., Kawase, D., and Sato, F.** (2005). Stromal over-reduction by high-light stress as measured by decreases in P700 oxidation by far-red light and its physiological relevance. *Plant Cell Physiol* **46**, 775-781.
- Estevez, J.M., Cantero, A., Reindl, A., Reichler, S., and Leon, P.** (2001). 1-Deoxy-D-xylulose-5-phosphate synthase, a limiting enzyme for plastidic isoprenoid biosynthesis in plants. *J Biol Chem* **276**, 22901-22909.

F

- Farber, A., Young, A.J., Ruban, A.V., Horton, P., and Jahns, P.** (1997). Dynamics of Xanthophyll-Cycle Activity in Different Antenna Subcomplexes in the Photosynthetic Membranes of Higher Plants (The Relationship between Zeaxanthin Conversion and Nonphotochemical Fluorescence Quenching). *Plant Physiol* **115**, 1609-1618.
- Finazzi, G., and Forti, G.** (2004). Metabolic Flexibility of the Green Alga *Chlamydomonas reinhardtii* as Revealed by the Link between State Transitions and Cyclic Electron Flow. *Photosynth Res* **82**, 327-338.
- Frey, A., Audran, C., Marin, E., Sotta, B., and Marion-Poll, A.** (1999). Engineering seed dormancy by the modification of zeaxanthin epoxidase gene expression. *Plant Mol Biol* **39**, 1267-1274.
- Friso, G., Giacomelli, L., Ytterberg, A.J., Peltier, J.B., Rudella, A., Sun, Q., and Wijk, K.J.** (2004). In-depth analysis of the thylakoid membrane proteome of *Arabidopsis thaliana* chloroplasts: new proteins, new functions, and a plastid proteome database. *Plant Cell* **16**, 478-499.
- Froehlich, J.E., Wilkerson, C.G., Ray, W.K., McAndrew, R.S., Osteryoung, K.W., Gage, D.A., and Phinney, B.S.** (2003). Proteomic study of the *Arabidopsis thaliana* chloroplastic envelope membrane utilizing alternatives to traditional two-dimensional electrophoresis. *J Proteome Res* **2**, 413-425.

G

- Golding, A.J., and Johnson, G.N.** (2003). Down-regulation of linear and activation of cyclic electron transport during drought. *Planta* **218**, 107-114.
- Golding, A.J., Finazzi, G., and Johnson, G.N.** (2004). Reduction of the thylakoid electron transport chain by stromal reductants--evidence for activation of cyclic electron transport upon dark adaptation or under drought. *Planta* **220**, 356-363.
- Granvogl, B., Reisinger, V., and Eichacker, L.A.** (2006). Mapping the proteome of thylakoid membranes by de novo sequencing of intermembrane peptide domains. *Proteomics* **6**, 3681-3695.

H

- Hansson, M., and Vener, A.V.** (2003). Identification of three previously unknown *in vivo* protein phosphorylation sites in thylakoid membranes of *Arabidopsis thaliana*. *Mol Cell Proteomics* **2**, 550-559.
- Hassidim, M., Yakir, E., Fradkin, D., Hilman, D., Kron, I., Keren, N., Harir, Y., Yerushalmi, S., and Green, R.M.** (2007). Mutations in CHLOROPLAST RNA BINDING provide evidence for the involvement of the chloroplast in the regulation of the circadian clock in *Arabidopsis*. *Plant J* **51**, 551-562.
- Hieber, A.D., Bugos, R.C., and Yamamoto, H.Y.** (2000). Plant lipocalins: violaxanthin de-epoxidase and zeaxanthin epoxidase. *Biochim Biophys Acta* **1482**, 84-91.
- Holt, N.E., Fleming, G.R., and Niyogi, K.K.** (2004). Toward an understanding of the mechanism of nonphotochemical quenching in green plants. *Biochemistry* **43**, 8281-8289.

Hoth, S., Morgante, M., Sanchez, J.P., Hanafey, M.K., Tingey, S.V., and Chua, N.H. (2002). Genome-wide gene expression profiling in *Arabidopsis thaliana* reveals new targets of abscisic acid and largely impaired gene regulation in the *abi1-1* mutant. *J Cell Sci* **115**, 4891-4900.

I

Ihnatowicz, A., Pesaresi, P., and Leister, D. (2007). The E subunit of photosystem I is not essential for linear electron flow and photoautotrophic growth in *Arabidopsis thaliana*. *Planta* **226**, 889-895.

Ihnatowicz, A., Pesaresi, P., Lohrig, K., Wolters, D., Muller, B., and Leister, D. (2008). Impaired photosystem I oxidation induces STN7-dependent phosphorylation of the light-harvesting complex I protein Lhca4 in *Arabidopsis thaliana*. *Planta* **227**, 717-722.

Ihnatowicz, A., Pesaresi, P., Varotto, C., Richly, E., Schneider, A., Jahns, P., Salamini, F., and Leister, D. (2004). Mutants for photosystem I subunit D of *Arabidopsis thaliana*: effects on photosynthesis, photosystem I stability and expression of nuclear genes for chloroplast functions. *Plant J* **37**, 839-852.

Irihimovitch, V., and Shapira, M. (2000). Glutathione redox potential modulated by reactive oxygen species regulates translation of Rubisco large subunit in the chloroplast. *J Biol Chem* **275**, 16289-16295.

J

Jach, G., Binot, E., Frings, S., Luxa, K., and Schell, J. (2001). Use of red fluorescent protein from *Discosoma* sp. (dsRED) as a reporter for plant gene expression. *Plant J* **28**, 483-491.

Jensen, P.E., Bassi, R., Boekema, E.J., Dekker, J.P., Jansson, S., Leister, D., Robinson, C., and Scheller, H.V. (2007). Structure, function and regulation of plant photosystem I. *Biochim Biophys Acta* **1767**, 335-352.

Jiang, C.Z., and Rodermel, S.R. (1995). Regulation of Photosynthesis during Leaf Development in *RbcS* Antisense DNA Mutants of Tobacco. *Plant Physiol* **107**, 215-224.

Joliot, P., and Joliot, A. (1994). Mechanism of electron transfer in the cytochrome *b/f* complex of algae: evidence for a semiquinone cycle. *Proc Natl Acad Sci* **91**, 1034-1038.

Joliot, P., Beal, D., and Joliot, A. (2004). Cyclic electron flow under saturating excitation of dark-adapted *Arabidopsis* leaves. *Biochim Biophys Acta* **1656**, 166-176.

Jornvall, H., Persson, B., Krook, M., Atrian, S., Gonzalez-Duarte, R., Jeffery, J., and Ghosh, D. (1995). Short-chain dehydrogenases/reductases (SDR). *Biochemistry* **34**, 6003-6013.

K

Kalituho, L., Grasses, T., Graf, M., Rech, J., and Jahns, P. (2006). Characterization of a nonphotochemical quenching-deficient *Arabidopsis* mutant possessing an intact PsbS protein, xanthophyll cycle and lumen acidification. *Planta* **223**, 532-541.

Kamruzzaman Munshi, M., Kobayashi, Y., and Shikanai, T. (2005). Identification of a novel protein, CRR7, required for the stabilization of the chloroplast NAD(P)H dehydrogenase complex in *Arabidopsis*. *Plant J* **44**, 1036-1044.

- Kanamaru, K., and Tanaka, K.** (2004). Roles of chloroplast RNA polymerase sigma factors in chloroplast development and stress response in higher plants. *Biosci Biotechnol Biochem* **68**, 2215-2223.
- Kanazawa, A., and Kramer, D.M.** (2002). *In vivo* modulation of nonphotochemical exciton quenching (NPQ) by regulation of the chloroplast ATP synthase. *Proc Natl Acad Sci* **99**, 12789-12794.
- Karnauchov, I., Herrmann, R.G., and Klosgen, R.B.** (1997). Transmembrane topology of the Rieske Fe/S protein of the cytochrome *b₆f* complex from spinach chloroplasts. *FEBS Lett* **408**, 206-210.
- Karszen, C.M., Brinckhorst-van der Swan, D.L.C., Breekland, A.E., and Koornneef, M.** (1983). Induction of dormancy during seed development by endogenous abscisic acid: studies on abscisic acid deficient genotype of *Arabidopsis thaliana* (L.) Heynh. *Planta* **157**, 158-165.
- Khrouchtchova, A., Hansson, M., Paakkari, V., Vainonen, J.P., Zhang, S., Jensen, P.E., Scheller, H.V., Vener, A.V., Aro, E.M., and Haldrup, A.** (2005). A previously found thylakoid membrane protein of 14kDa (TMP14) is a novel subunit of plant photosystem I and is designated PSI-P. *FEBS Lett* **579**, 4808-4812.
- Kleffmann, T., Russenberger, D., von Zychlinski, A., Christopher, W., Sjolander, K., Gruissem, W., and Baginsky, S.** (2004). The *Arabidopsis thaliana* chloroplast proteome reveals pathway abundance and novel protein functions. *Curr Biol* **14**, 354-362.
- Koncz, C., Mayerhofer, R., Koncz-Kalman, Z., Nawrath, C., Reiss, B., Redei, G.P., and Schell, J.** (1990). Isolation of a gene encoding a novel chloroplast protein by T-DNA tagging in *Arabidopsis thaliana*. *Embo J* **9**, 1337-1346.
- Koop, H.U., Steinmuller, K., Wagner, H., Rossler, C., Eibl, C., and Sacher, L.** (1996). Integration of foreign sequences into the tobacco plastome via polyethylene glycol-mediated protoplast transformation. *Planta* **199**, 193-201.
- Kouril, R., Zygadlo, A., Arteni, A.A., de Wit, C.D., Dekker, J.P., Jensen, P.E., Scheller, H.V., and Boekema, E.J.** (2005). Structural characterization of a complex of photosystem I and light-harvesting complex II of *Arabidopsis thaliana*. *Biochemistry* **44**, 10935-10940.
- Koussevitzky, S., Nott, A., Mockler, T.C., Hong, F., Sachetto-Martins, G., Surpin, M., Lim, J., Mittler, R., and Chory, J.** (2007). Signals from chloroplasts converge to regulate nuclear gene expression. *Science* **316**, 715-719.
- Kovacs, L., Damkjaer, J., Kereiche, S., Iliaia, C., Ruban, A.V., Boekema, E.J., Jansson, S., and Horton, P.** (2006). Lack of the light-harvesting complex CP24 affects the structure and function of the grana membranes of higher plant chloroplasts. *Plant Cell* **18**, 3106-3120.
- Kramer, D.M., Avenson, T.J., and Edwards, G.E.** (2004). Dynamic flexibility in the light reactions of photosynthesis governed by both electron and proton transfer reactions. *Trends Plant Sci* **9**, 349-357.
- Kyle, D.J., Ohad, I., and Arntzen, C.J.** (1984). Membrane protein damage and repair: Selective loss of a quinone-protein function in chloroplast membranes. *Proc Natl Acad Sci* **81**, 4070-4074.

L

- Laisk, A., Eichelmann, H., Oja, V., and Peterson, R.B.** (2005). Control of cytochrome *b₆* at low and high light intensity and cyclic electron transport in leaves. *Biochim Biophys Acta* **1708**, 79-90.
- Larsson, U.K., Jergil, B., and Andersson, B.** (1983). Changes in the lateral distribution of the light-harvesting chlorophyll-a/b--protein complex induced by its phosphorylation. *Eur J Biochem* **136**, 25-29.
- Leister, D.** (2003). Chloroplast research in the genomic age. *Trends Genet* **19**, 47-56.
- Leister, D.** (2005). Genomics-based dissection of the cross-talk of chloroplasts with the nucleus and mitochondria in *Arabidopsis*. *Gene* **354**, 110-116.
- Leister, D., and Schneider, A.** (2003). From genes to photosynthesis in *Arabidopsis thaliana*. *Int Rev Cytol* **228**, 31-83.
- Li, X.P., Muller-Moule, P., Gilmore, A.M., and Niyogi, K.K.** (2002). PsbS-dependent enhancement of feedback de-excitation protects photosystem II from photoinhibition. *Proc Natl Acad Sci* **99**, 15222-15227.
- Li, X.P., Bjorkman, O., Shih, C., Grossman, A.R., Rosenquist, M., Jansson, S., and Niyogi, K.K.** (2000). A pigment-binding protein essential for regulation of photosynthetic light harvesting. *Nature* **403**, 391-395.
- Li, X.P., Gilmore, A.M., Caffarri, S., Bassi, R., Golan, T., Kramer, D., and Niyogi, K.K.** (2004). Regulation of photosynthetic light harvesting involves intrathylakoid lumen pH sensing by the PsbS protein. *J Biol Chem* **279**, 22866-22874.
- Li, Y., Rosso, M.G., Strizhov, N., Viehoveer, P., and Weisshaar, B.** (2003). GABI-Kat SimpleSearch: a flanking sequence tag (FST) database for the identification of T-DNA insertion mutants in *Arabidopsis thaliana*. *Bioinformatics* **19**, 1441-1442.
- Lindgren, L.O., Stalberg, K.G., and Hoglund, A.S.** (2003). Seed-specific overexpression of an endogenous *Arabidopsis* phytoene synthase gene results in delayed germination and increased levels of carotenoids, chlorophyll, and abscisic acid. *Plant Physiol* **132**, 779-785.
- Lopez-Juez, E., and Pyke, K.A.** (2005). Plastids unleashed: their development and their integration in plant development. *Int J Dev Biol* **49**, 557-577.

M

- Magliano, T.M., Botto, J.F., Godoy, A.V., Symonds, V.V., Lloyd, A.M., and Casal, J.J.** (2005). New *Arabidopsis* recombinant inbred lines (*Landsberg erecta* x Nossen) reveal natural variation in phytochrome-mediated responses. *Plant Physiol* **138**, 1126-1135.
- Maiwald, D., Dietzmann, A., Jahns, P., Pesaresi, P., Joliot, P., Joliot, A., Levin, J.Z., Salamini, F., and Leister, D.** (2003). Knock-out of the genes coding for the Rieske protein and the ATP-synthase delta-subunit of *Arabidopsis*. Effects on photosynthesis, thylakoid protein composition, and nuclear chloroplast gene expression. *Plant Physiol* **133**, 191-202.
- Miziorko, H.M., and Lorimer, G.H.** (1983). Ribulose-1,5-bisphosphate carboxylase-oxygenase. *Annu Rev Biochem* **52**, 507-535.

- Monde, R.A., Schuster, G., and Stern, D.B.** (2000). Processing and degradation of chloroplast mRNA. *Biochimie* **82**, 573-582.
- Munekage, Y., Hojo, M., Meurer, J., Endo, T., Tasaka, M., and Shikanai, T.** (2002). PGR5 is involved in cyclic electron flow around photosystem I and is essential for photoprotection in *Arabidopsis*. *Cell* **110**, 361-371.
- Munekage, Y., Hashimoto, M., Miyake, C., Tomizawa, K., Endo, T., Tasaka, M., and Shikanai, T.** (2004). Cyclic electron flow around photosystem I is essential for photosynthesis. *Nature* **429**, 579-582.
- Munshi, M.K., Kobayashi, Y., and Shikanai, T.** (2006). Chlororespiratory reduction 6 is a novel factor required for accumulation of the chloroplast NAD(P)H dehydrogenase complex in *Arabidopsis*. *Plant Physiol* **141**, 737-744.
- Muraoka, R., Okuda, K., Kobayashi, Y., and Shikanai, T.** (2006). A eukaryotic factor required for accumulation of the chloroplast NAD(P)H dehydrogenase complex in *Arabidopsis*. *Plant Physiol* **142**, 1683-1689.

N

- Nambara, E., and Marion-Poll, A.** (2005). Abscisic acid biosynthesis and catabolism. *Annu Rev Plant Biol* **56**, 165-185.
- Nandha, B., Finazzi, G., Joliot, P., Hald, S., and Johnson, G.N.** (2007). The role of PGR5 in the redox poisoning of photosynthetic electron transport. *Biochim Biophys Acta* **1767**, 1252-1259.
- Nelson, N., and Yocum, C.F.** (2006). Structure and function of photosystems I and II. *Annu Rev Plant Biol* **57**, 521-565.
- Nishiyama, Y., Allakhverdiev, S.I., and Murata, N.** (2006). A new paradigm for the action of reactive oxygen species in the photoinhibition of photosystem II. *Biochim Biophys Acta* **1757**, 742-749.
- Niyogi, K.K.** (1999). PHOTOPROTECTION REVISITED: Genetic and Molecular Approaches. *Annu Rev Plant Physiol Plant Mol Biol* **50**, 333-359.
- Niyogi, K.K., Grossman, A.R., and Bjorkman, O.** (1998). *Arabidopsis* mutants define a central role for the xanthophyll cycle in the regulation of photosynthetic energy conversion. *Plant Cell* **10**, 1121-1134.
- Niyogi, K.K., Li, X.P., Rosenberg, V., and Jung, H.S.** (2005). Is PsbS the site of non-photochemical quenching in photosynthesis? *J Exp Bot* **56**, 375-382.

O

- Okegawa, Y., Tsuyama, M., Kobayashi, Y., and Shikanai, T.** (2005). The *pgr1* mutation in the Rieske subunit of the cytochrome *b₆f* complex does not affect PGR5-dependent cyclic electron transport around photosystem I. *J Biol Chem* **280**, 28332-28336.
- Ossenbühl, F., Hartmann, K., and Nickelsen, J.** (2002). A chloroplast RNA binding protein from stromal thylakoid membranes specifically binds to the 5' untranslated region of the *psbA* mRNA. *Eur J Biochem* **269**, 3912-3919.

P

- Parinov, S., Sevugan, M., Ye, D., Yang, W.C., Kumaran, M., and Sundaresan, V.** (1999). Analysis of flanking sequences from dissociation insertion lines: a database for reverse genetics in *Arabidopsis*. *Plant Cell* **11**, 2263-2270.
- Peltier, J.B., Cai, Y., Sun, Q., Zabrouskov, V., Giacomelli, L., Rudella, A., Ytterberg, A.J., Rutschow, H., and van Wijk, K.J.** (2006). The oligomeric stromal proteome of *Arabidopsis thaliana* chloroplasts. *Mol Cell Proteomics* **5**, 114-133.
- Perrin, R., Lange, H., Grienberger, J.M., and Gagliardi, D.** (2004). AtmtPNPase is required for multiple aspects of the 18S rRNA metabolism in *Arabidopsis thaliana* mitochondria. *Nucleic Acids Res* **32**, 5174-5182.
- Pesaresi, P., Schneider, A., Kleine, T., and Leister, D.** (2007). Interorganellar communication. *Curr Opin Plant Biol* **10**, 600-606.
- Pesaresi, P., Varotto, C., Meurer, J., Jahns, P., Salamini, F., and Leister, D.** (2001). Knock-out of the plastid ribosomal protein L11 in *Arabidopsis*: effects on mRNA translation and photosynthesis. *Plant J* **27**, 179-189.
- Pesaresi, P., Lunde, C., Jahns, P., Tarantino, D., Meurer, J., Varotto, C., Hirtz, R.D., Soave, C., Scheller, H.V., Salamini, F., and Leister, D.** (2002). A stable LHCII-PSI aggregate and suppression of photosynthetic state transitions in the *psae1-1* mutant of *Arabidopsis thaliana*. *Planta* **215**, 940-948.
- Pfannschmidt, T., Schutze, K., Brost, M., and Oelmüller, R.** (2001). A novel mechanism of nuclear photosynthesis gene regulation by redox signals from the chloroplast during photosystem stoichiometry adjustment. *J Biol Chem* **276**, 36125-36130.
- Pfannschmidt, T., Schutze, K., Fey, V., Sherameti, I., and Oelmüller, R.** (2003). Chloroplast redox control of nuclear gene expression--a new class of plastid signals in interorganellar communication. *Antioxid Redox Signal* **5**, 95-101.
- Pfannschmidt, T., Ogrzewalla, K., Baginsky, S., Sickmann, A., Meyer, H.E., and Link, G.** (2000). The multisubunit chloroplast RNA polymerase A from mustard (*Sinapis alba* L.). Integration of a prokaryotic core into a larger complex with organelle-specific functions. *Eur J Biochem* **267**, 253-261.
- Plücken, H., Müller, B., Grohmann, D., Westhoff, P., and Eichacker, L.A.** (2002). The HCF136 protein is essential for assembly of the photosystem II reaction center in *Arabidopsis thaliana*. *FEBS Lett* **532**, 85-90.
- Porra, R.J.** (2002). The chequered history of the development and use of simultaneous equations for the accurate determination of chlorophylls *a* and *b*. *Photosynth Res* **73**, 149-156.

R

- Raab, S., Toth, Z., de Groot, C., Stamminger, T., and Hoth, S.** (2006). ABA-responsive RNA-binding proteins are involved in chloroplast and stromule function in *Arabidopsis* seedlings. *Planta* **224**, 900-914.
- Renger, G., and Govindjee, M.** (1985). The mechanism of photosynthetic water oxidation. *Photosynthesis Research* **6**, 33-55.

- Richly, E., Dietzmann, A., Biehl, A., Kurth, J., Laloi, C., Apel, K., Salamini, F., and Leister, D.** (2003). Covariations in the nuclear chloroplast transcriptome reveal a regulatory master-switch. *EMBO Rep* **4**, 491-498.
- Richter, M.L., Samra, H.S., He, F., Giessel, A.J., and Kuczera, K.K.** (2005). Coupling proton movement to ATP synthesis in the chloroplast ATP synthase. *J Bioenerg Biomembr* **37**, 467-473.
- Rintamäki, E., Martinsuo, P., Pursiheimo, S., and Aro, E.M.** (2000). Cooperative regulation of light-harvesting complex II phosphorylation via the plastoquinol and ferredoxin-thioredoxin system in chloroplasts. *Proc Natl Acad Sci* **97**, 11644-11649.
- Rios, G., Lossow, A., Hertel, B., Breuer, F., Schaefer, S., Broich, M., Kleinow, T., Jasik, J., Winter, J., Ferrando, A., Farras, R., Panicot, M., Henriques, R., Mariaux, J.B., Oberschall, A., Molnar, G., Berendzen, K., Shukla, V., Lafos, M., Koncz, Z., Redei, G.P., Schell, J., and Koncz, C.** (2002). Rapid identification of *Arabidopsis* insertion mutants by non-radioactive detection of T-DNA tagged genes. *Plant J* **32**, 243-253.
- Rochaix, J.D.** (2007). Role of thylakoid protein kinases in photosynthetic acclimation. *FEBS Lett* **581**, 2768-2775.
- Rodermel, S., Haley, J., Jiang, C.Z., Tsai, C.H., and Bogorad, L.** (1996). A mechanism for intergenomic integration: abundance of ribulose biphosphate carboxylase small-subunit protein influences the translation of the large-subunit mRNA. *Proc Natl Acad Sci* **93**, 3881-3885.
- Rolland, F., Moore, B., and Sheen, J.** (2002). Sugar sensing and signaling in plants. *Plant Cell* **14 Suppl**, S185-205.
- Rosso, D., Ivanov, A.G., Fu, A., Geisler-Lee, J., Hendrickson, L., Geisler, M., Stewart, G., Krol, M., Hurry, V., Rodermel, S.R., Maxwell, D.P., and Huner, N.P.** (2006). IMMUTANS does not act as a stress-induced safety valve in the protection of the photosynthetic apparatus of *Arabidopsis* during steady-state photosynthesis. *Plant Physiol* **142**, 574-585.
- Rott, R., Liveanu, V., Drager, R.G., Stern, D.B., and Schuster, G.** (1998). The sequence and structure of the 3'-untranslated regions of chloroplast transcripts are important determinants of mRNA accumulation and stability. *Plant Mol Biol* **36**, 307-314.
- Ruban, A.V., Walters, R.G., and Horton, P.** (1992). The molecular mechanism of the control of excitation energy dissipation in chloroplast membranes. Inhibition of delta pH-dependent quenching of chlorophyll fluorescence by dicyclohexylcarbodiimide. *FEBS Lett* **309**, 175-179.
- Ruban, A.V., Berera, R., Ilioaia, C., van Stokkum, I.H., Kennis, J.T., Pascal, A.A., van Amerongen, H., Robert, B., Horton, P., and van Grondelle, R.** (2007). Identification of a mechanism of photoprotective energy dissipation in higher plants. *Nature* **450**, 575-578.

S

- Sambrook, J., Fritsch, E.F., and Maniatis, T.** (1989). *Molecular Cloning*. (New York: Cold Spring Harbor Laboratory Press).

- Samson, F., Brunaud, V., Balzergue, S., Dubreucq, B., Lepiniec, L., Pelletier, G., Caboche, M., and Lecharny, A.** (2002). FLAGdb/FST: a database of mapped flanking insertion sites (FSTs) of *Arabidopsis thaliana* T-DNA transformants. *Nucleic Acids Res* **30**, 94-97.
- Schagger, H., and von Jagow, G.** (1987). Tricine-sodium dodecyl sulfate-polyacrylamide gel electrophoresis for the separation of proteins in the range from 1 to 100 kDa. *Anal Biochem* **166**, 368-379.
- Schagger, H., and von Jagow, G.** (1991). Blue native electrophoresis for isolation of membrane protein complexes in enzymatically active form. *Anal Biochem* **199**, 223-231.
- Schmidt, G.W., and Mishkind, M.L.** (1983). Rapid degradation of unassembled ribulose 1,5-bisphosphate carboxylase small subunits in chloroplasts. *Proc Natl Acad Sci* **80**, 2632-2636.
- Schmitz-Linneweber, C., Williams-Carrier, R., and Barkan, A.** (2005). RNA immunoprecipitation and microarray analysis show a chloroplast Pentatricopeptide repeat protein to be associated with the 5' region of mRNAs whose translation it activates. *Plant Cell* **17**, 2791-2804.
- Schreiber, U., Schliwa, U., and Bilger, W.** (1986). Continuous recording of photochemical and non-photochemical chlorophyll fluorescence quenching with a new type of modulation fluorometer. *Photosynth Res* **10**, 51-62.
- Schreiber, U., Klughammer, C., and Neubauer, C.** (1988). Measuring P700 absorbance changes around 830 nm with a new type of pulse modulation system. *Z. Naturforsch.* **43c**, 686-698.
- Schwartz, S.H., Tan, B.C., McCarty, D.R., Welch, W., and Zeevaart, J.A.** (2003). Substrate specificity and kinetics for VP14, a carotenoid cleavage dioxygenase in the ABA biosynthetic pathway. *Biochim Biophys Acta* **1619**, 9-14.
- Schwenkert, S., Legen, J., Takami, T., Shikanai, T., Herrmann, R.G., and Meurer, J.** (2007). Role of the low-molecular-weight subunits PetL, PetG, and PetN in assembly, stability, and dimerization of the cytochrome *b₆f* complex in tobacco. *Plant Physiol* **144**, 1924-1935.
- Schwenkert, S., Umate, P., Dal Bosco, C., Volz, S., Mlcochova, L., Zoryan, M., Eichacker, L.A., Ohad, I., Herrmann, R.G., and Meurer, J.** (2006). PsbI affects the stability, function, and phosphorylation patterns of photosystem II assemblies in tobacco. *J Biol Chem* **281**, 34227-34238.
- Seelert, H., Poetsch, A., Rohlf, M., and Dencher, N.A.** (2000). Dye-ligand chromatographic purification of intact multisubunit membrane protein complexes: application to the chloroplast H⁺-FoF1-ATP synthase. *Biochem J* **346 Pt 1**, 41-44.
- Seki, M., Ishida, J., Narusaka, M., Fujita, M., Nanjo, T., Umezawa, T., Kamiya, A., Nakajima, M., Enju, A., Sakurai, T., Satou, M., Akiyama, K., Yamaguchi-Shinozaki, K., Carninci, P., Kawai, J., Hayashizaki, Y., and Shinozaki, K.** (2002). Monitoring the expression pattern of around 7,000 *Arabidopsis* genes under ABA treatments using a full-length cDNA microarray. *Funct Integr Genomics* **2**, 282-291.
- Seo, M., and Koshiba, T.** (2002). Complex regulation of ABA biosynthesis in plants. *Trends Plant Sci* **7**, 41-48.

- Sessions, A., Burke, E., Presting, G., Aux, G., McElver, J., Patton, D., Dietrich, B., Ho, P., Bacwaden, J., Ko, C., Clarke, J.D., Cotton, D., Bullis, D., Snell, J., Miguel, T., Hutchison, D., Kimmerly, B., Mitzel, T., Katagiri, F., Glazebrook, J., Law, M., and Goff, S.A.** (2002). A high-throughput *Arabidopsis* reverse genetics system. *Plant Cell* **14**, 2985-2994.
- Shi, L.X., and Schroder, W.P.** (2004). The low molecular mass subunits of the photosynthetic supracomplex, photosystem II. *Biochim Biophys Acta* **1608**, 75-96.
- Shikanai, T.** (2006). RNA editing in plant organelles: machinery, physiological function and evolution. *Cell Mol Life Sci* **63**, 698-708.
- Shikanai, T.** (2007). Cyclic electron transport around photosystem I: genetic approaches. *Annu Rev Plant Biol* **58**, 199-217.
- Smeeckens, S.** (2000). Sugar-Induced Signal Transduction in Plants. *Annu Rev Plant Physiol Plant Mol Biol* **51**, 49-81.
- Strand, A.** (2004). Plastid-to-nucleus signalling. *Curr Opin Plant Biol* **7**, 621-625.
- Stroebel, D., Choquet, Y., Popot, J.L., and Picot, D.** (2003). An atypical haem in the cytochrome *b₆f* complex. *Nature* **426**, 413-418.
- Suorsa, M., Sirpio, S., Allahverdiyeva, Y., Paakkarinen, V., Mamedov, F., Styring, S., and Aro, E.M.** (2006). PsbR, a missing link in the assembly of the oxygen-evolving complex of plant photosystem II. *J Biol Chem* **281**, 145-150.
- Szabo, I., Bergantino, E., and Giacometti, G.M.** (2005). Light and oxygenic photosynthesis: energy dissipation as a protection mechanism against photo-oxidation. *EMBO Rep* **6**, 629-634.

T

- Taiz, L., and Zeiger, E.** (1998). *Plant Physiology*. (Sinauer Associates, Inc).
- Takizawa, K., Kanazawa, A., and Kramer, D.M.** (2008). Depletion of stromal P(i) induces high 'energy-dependent' antenna exciton quenching (q(E)) by decreasing proton conductivity at CF(O)-CF(1) ATP synthase. *Plant Cell Environ* **31**, 235-243.
- Tatusova, T.A., and Madden, T.L.** (1999). BLAST 2 Sequences, a new tool for comparing protein and nucleotide sequences. *FEMS Microbiol Lett* **174**, 247-250.
- Terzaghi, W.B., and Cashmore, A.R.** (1995). Photomorphogenesis. Seeing the light in plant development. *Curr Biol* **5**, 466-468.
- Timmis, J.N., Ayliffe, M.A., Huang, C.Y., and Martin, W.** (2004). Endosymbiotic gene transfer: organelle genomes forge eukaryotic chromosomes. *Nat Rev Genet* **5**, 123-135.
- Towbin, H., Staehelin, T., and Gordon, J.** (1979). Electrophoretic transfer of proteins from polyacrylamide gels to nitrocellulose sheets: procedure and some applications. *Proc Natl Acad Sci U S A* **76**, 4350-4354.
- Trissl, H.W., and Wilhelm, C.** (1993). Why do thylakoid membranes from higher plants form grana stacks? *Trends Biochem Sci* **18**, 415-419.

U

Umate, P., Schwenkert, S., Karbat, I., Dal Bosco, C., Mlcochova, L., Volz, S., Zer, H., Herrmann, R.G., Ohad, I., and Meurer, J. (2007). Deletion of PsbM in tobacco alters the QB site properties and the electron flow within photosystem II. *J Biol Chem* **282**, 9758-9767.

V

Vallon, O., Bulte, L., Dainese, P., Olive, J., Bassi, R., and Wollman, F.A. (1991). Lateral redistribution of cytochrome *b₆f* complexes along thylakoid membranes upon state transitions. *Proc Natl Acad Sci* **88**, 8262-8266.

van Roon, H., van Breemen, J.F., de Weerd, F.L., Dekker, J.P., and Boekema, E.J. (2000). Solubilization of green plant thylakoid membranes with n-dodecyl-alpha,D-maltoside. Implications for the structural organization of the Photosystem II, Photosystem I, ATP synthase and cytochrome *b₆f* complexes. *Photosynth Res* **64**, 155-166.

Varotto, C., Pesaresi, P., Meurer, J., Oelmuller, R., Steiner-Lange, S., Salamini, F., and Leister, D. (2000). Disruption of the *Arabidopsis* photosystem I gene *psaE1* affects photosynthesis and impairs growth. *Plant J* **22**, 115-124.

W

Walker, M.G., Volkmuth, G., Sprinzak, E., Hodgson, D., and Klingler, T. (1999). Prediction of gene function by genome-scale expression analysis: prostate cancer-associated genes. *Genome Research* **9**, 1198-1203.

Wollman, F.A. (2001). State transitions reveal the dynamics and flexibility of the photosynthetic apparatus. *Embo J* **20**, 3623-3630.

Wostrikoff, K., and Stern, D. (2007). Rubisco large-subunit translation is autoregulated in response to its assembly state in tobacco chloroplasts. *Proc Natl Acad Sci* **104**, 6466-6471.

Y

Yakushevskaya, A.E., Jensen, P.E., Keegstra, W., van Roon, H., Scheller, H.V., Boekema, E.J., and Dekker, J.P. (2001). Supermolecular organization of photosystem II and its associated light-harvesting antenna in *Arabidopsis thaliana*. *Eur J Biochem* **268**, 6020-6028.

Yamaguchi, K., Beligni, M.V., Prieto, S., Haynes, P.A., McDonald, W.H., Yates, J.R., 3rd, and Mayfield, S.P. (2003). Proteomic characterization of the *Chlamydomonas reinhardtii* chloroplast ribosome. Identification of proteins unique to the 70 S ribosome. *J Biol Chem* **278**, 33774-33785.

Yang, J., and Stern, D.B. (1997). The spinach chloroplast endoribonuclease CSP41 cleaves the 3'-untranslated region of *petD* mRNA primarily within its terminal stem-loop structure. *J Biol Chem* **272**, 12874-12880.

Yang, J., Usack, L., Monde, R.A., and Stern, D.B. (1995). The 41 kDa protein component of the spinach chloroplast *petD* mRNA 3' stem-loop:protein complex is a nuclear encoded chloroplast RNA-binding protein. *Nucleic Acids Symp Ser*, 237-239.

Yi, X., Hargett, S.R., Frankel, L.K., and Bricker, T.M. (2006). The PsbQ protein is required in *Arabidopsis* for photosystem II assembly/stability and photoautotrophy under low light conditions. *J Biol Chem* **281**, 26260-26267.

Ytterberg, A.J., Peltier, J.B., and van Wijk, K.J. (2006). Protein profiling of plastoglobules in chloroplasts and chromoplasts. A surprising site for differential accumulation of metabolic enzymes. *Plant Physiol* **140**, 984-997.

Z

Zhang, H., Whitelegge, J.P., and Cramer, W.A. (2001). Ferredoxin:NADP⁺ oxidoreductase is a subunit of the chloroplast cytochrome *b₆f* complex. *J Biol Chem* **276**, 38159-38165.

Zhang, S., and Scheller, H.V. (2004). Light-harvesting complex II binds to several small subunits of photosystem I. *J Biol Chem* **279**, 3180-3187.

Zimmermann, P., Hirsch-Hoffmann, M., Hennig, L., and Gruissem, W. (2004). GENEVESTIGATOR. *Arabidopsis* microarray database and analysis toolbox. *Plant Physiol* **136**, 2621-2632.

Zito, F., Finazzi, G., Joliot, P., and Wollman, F.A. (1998). Glu78, from the conserved PEWY sequence of subunit IV, has a key function in cytochrome *b₆f* turnover. *Biochemistry* **37**, 10395-10403.

Zygadlo, A., Jensen, P.E., Leister, D., and Scheller, H.V. (2005). Photosystem I lacking the PSI-G subunit has a higher affinity for plastocyanin and is sensitive to photodamage. *Biochim Biophys Acta* **1708**, 154-163.

6 Supplementary Data

6.1 Mass spectrometry fragmentation spectra

6.1.1 PPP4

#12750-12750 RT:75.32-75.32 NL: 2.11E4

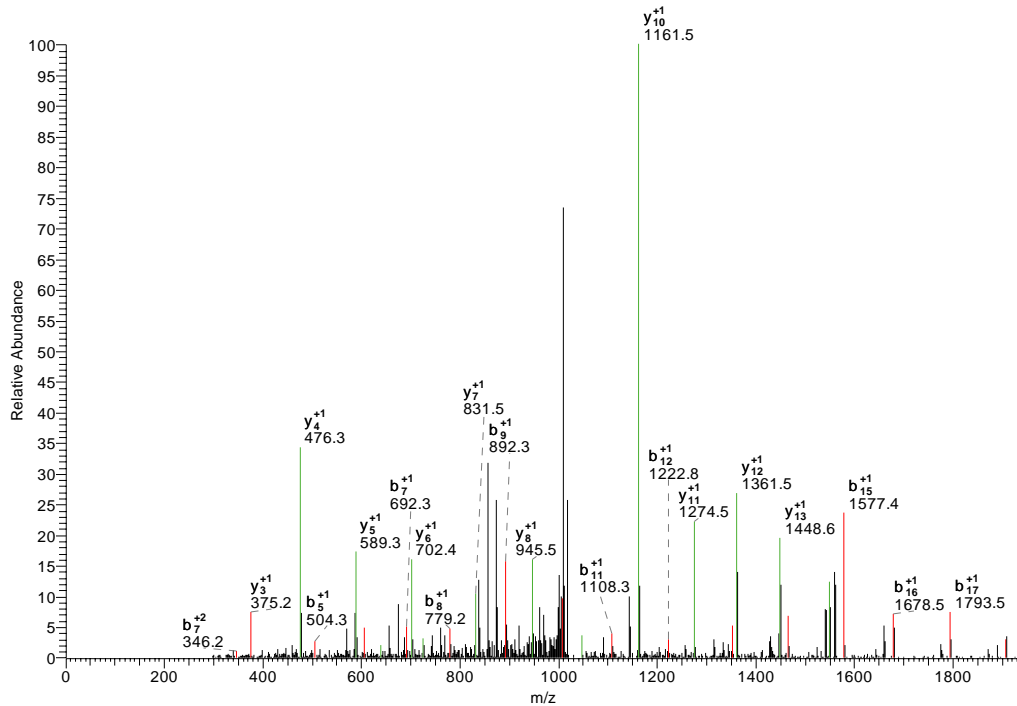


Fig 6.1.1 Fragmentation spectrum of the identified tryptic peptide ASSEETSSID of PPP4

#10751-10751 RT:63.65-63.65 NL: 8.43E3

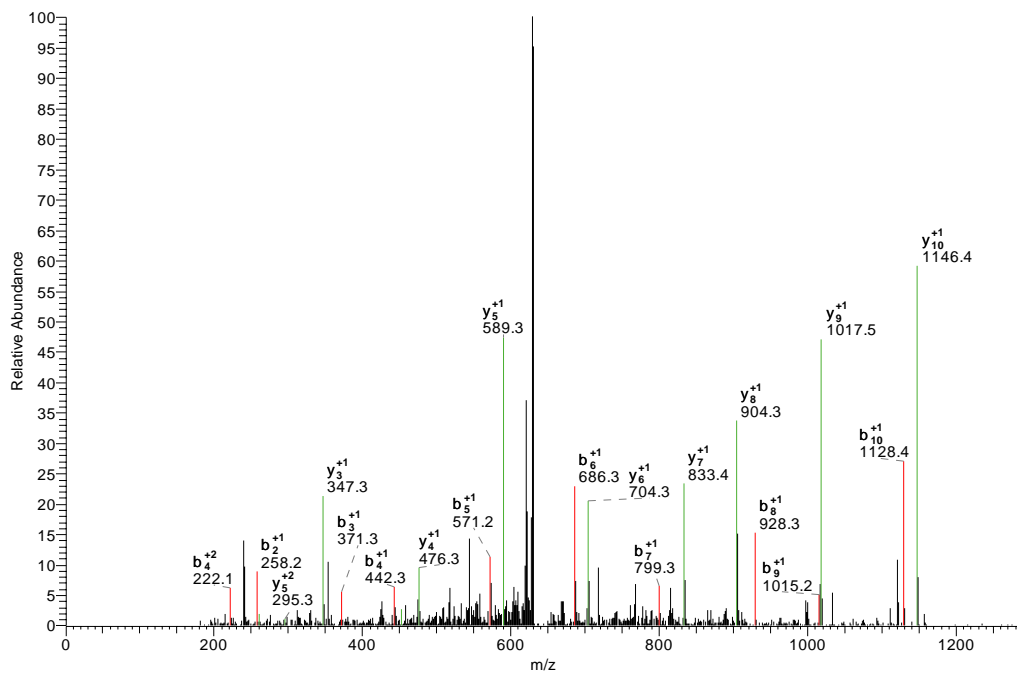
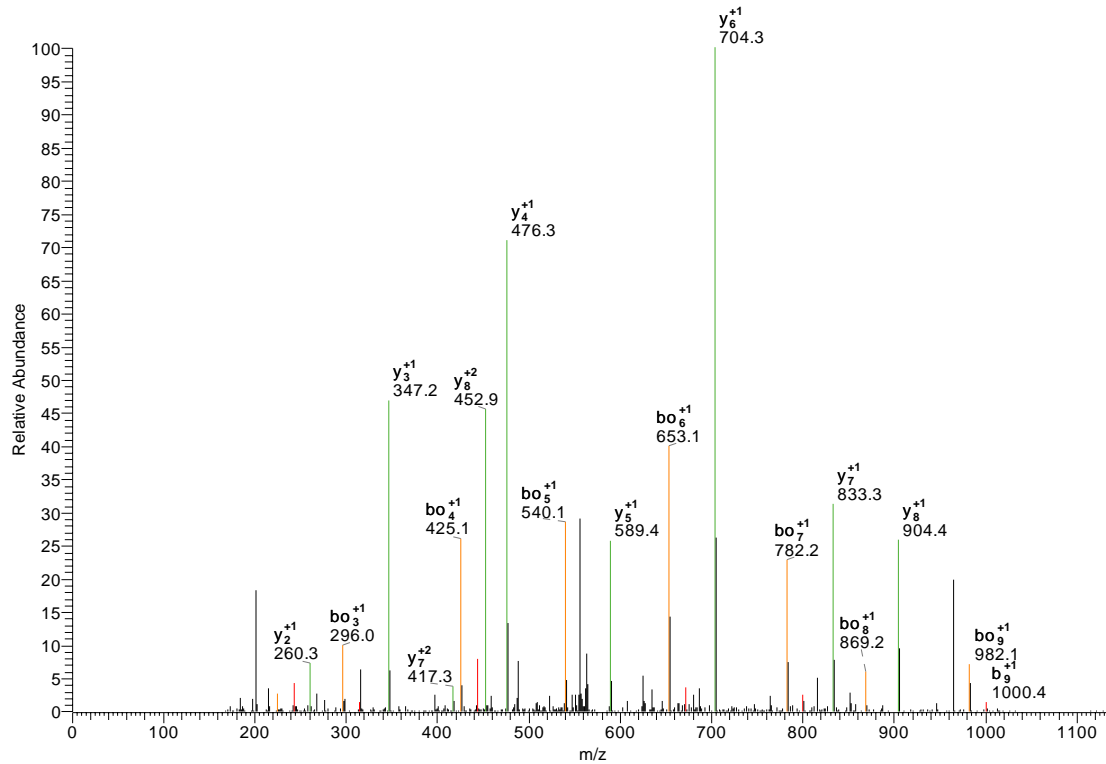
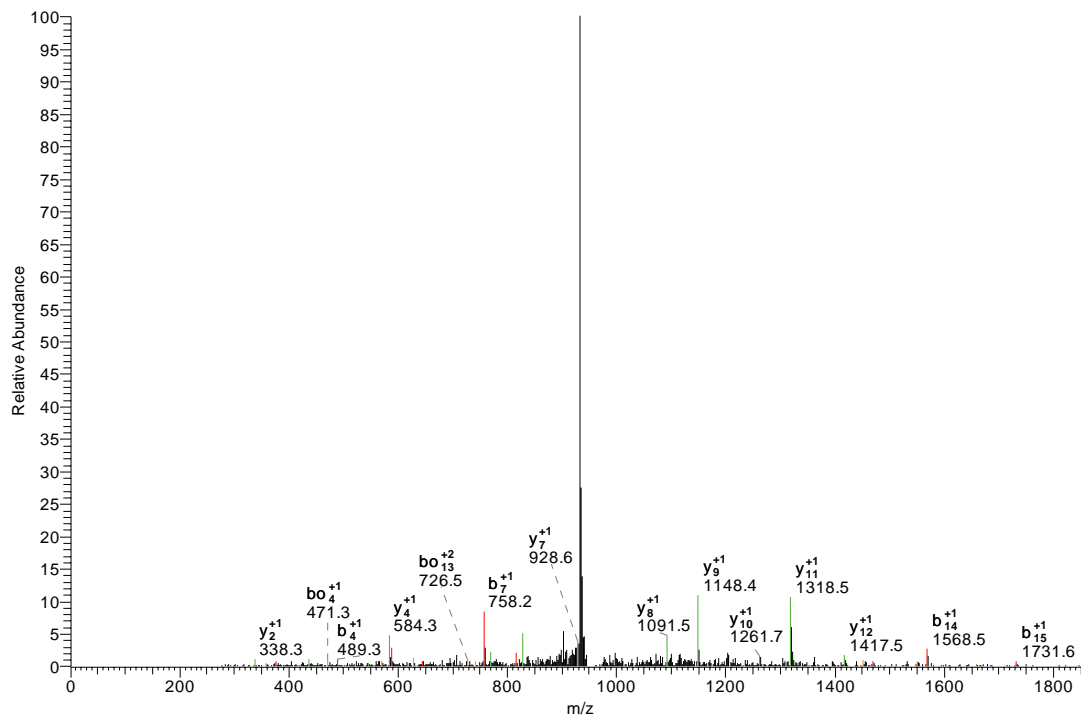


Fig 6.1.2 Fragmentation spectrum of the identified tryptic peptide KELAEDIESLK of PPP4

#11634-11634 RT:68.56-68.56 NL: 5.90E4

**Fig 6.1.3** Fragmentation spectrum of the identified tryptic peptide ELAEDIESLK of PPP4

#14734-14734 RT:89.97-89.97 NL: 7.67E3

**Fig 6.1.4** Fragmentation spectrum of the identified tryptic peptide VMELVGLGYTGWFVYR of PPP4

6.1.2 TMP14

#11428-11428 RT:72.15-72.15 NL: 4.05E4

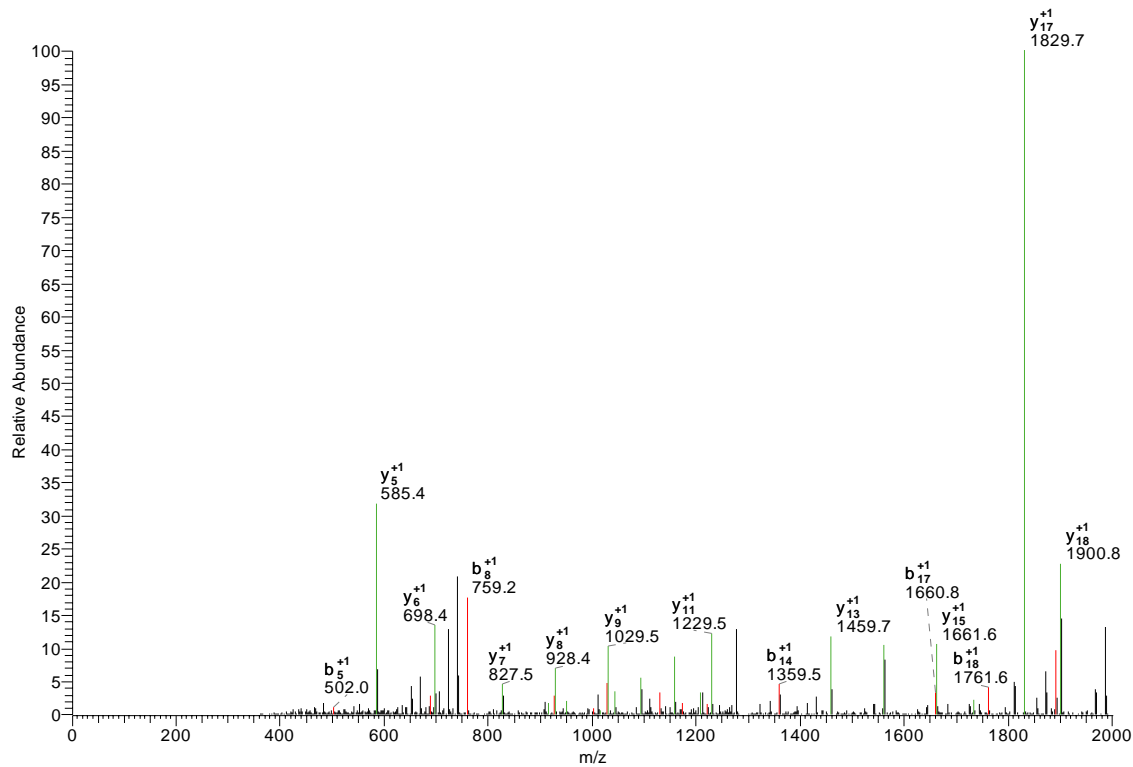


Fig 6.1.5 Fragmentation spectrum of the identified tryptic peptide ATTEVGEPATTTTEAETTELPEIVK of TMP14

#12560-12560 RT:79.23-79.23 NL: 4.81E3

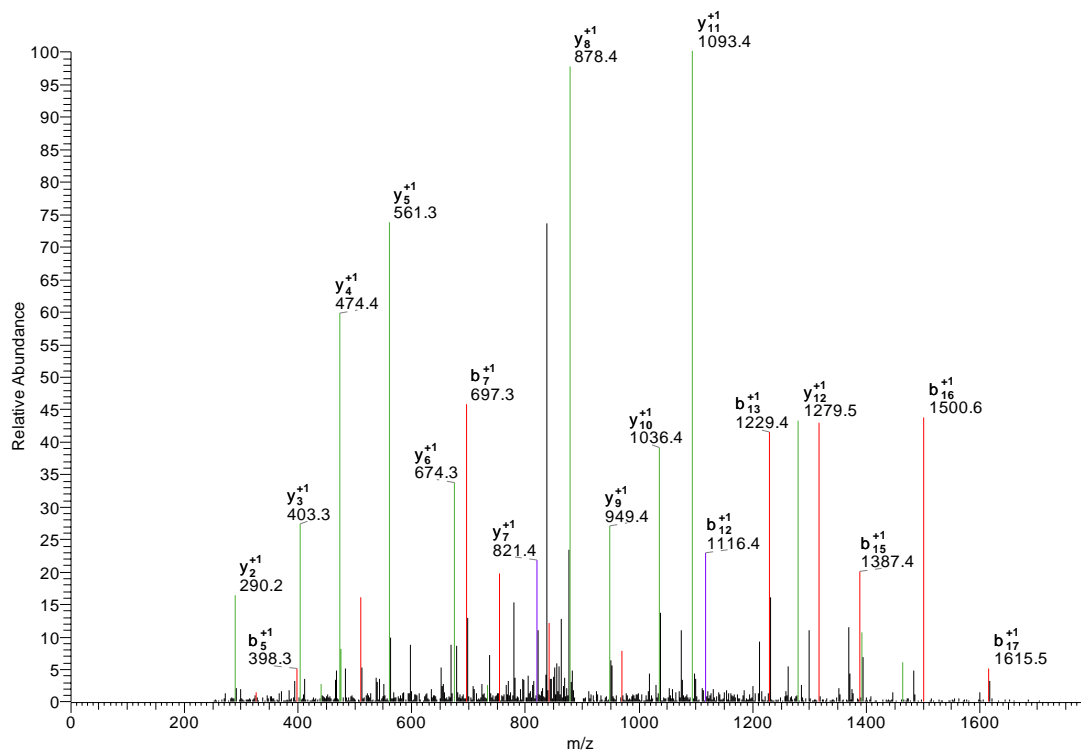


Fig 6.1.6 Fragmentation spectrum of the identified tryptic peptide AGVVALWGSAGMISAIDR of TMP14

6.1.3 TMP14-like

#10455-10455 RT:62.11-62.11 NL: 1.48E4

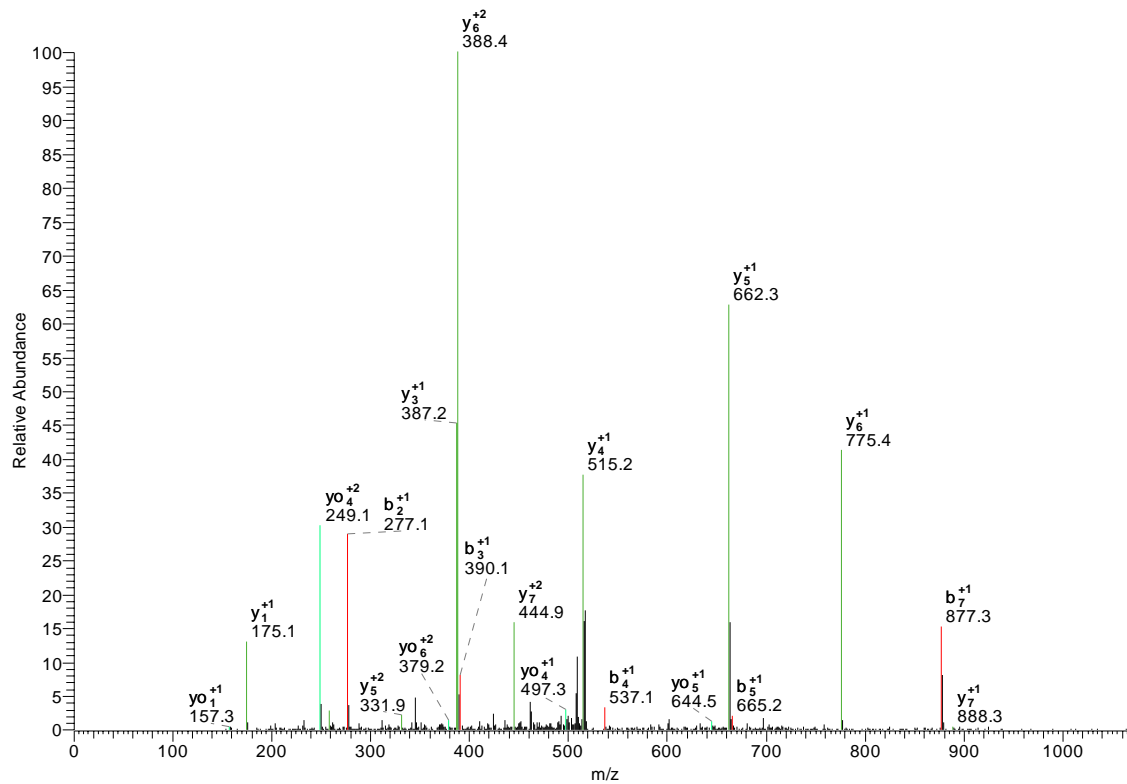


Fig 6.1.7 Fragmentation spectrum of the identified tryptic peptide YLLFKPDR of TMP14-like

#10995-10995 RT:64.99-64.99 NL: 9.98E2

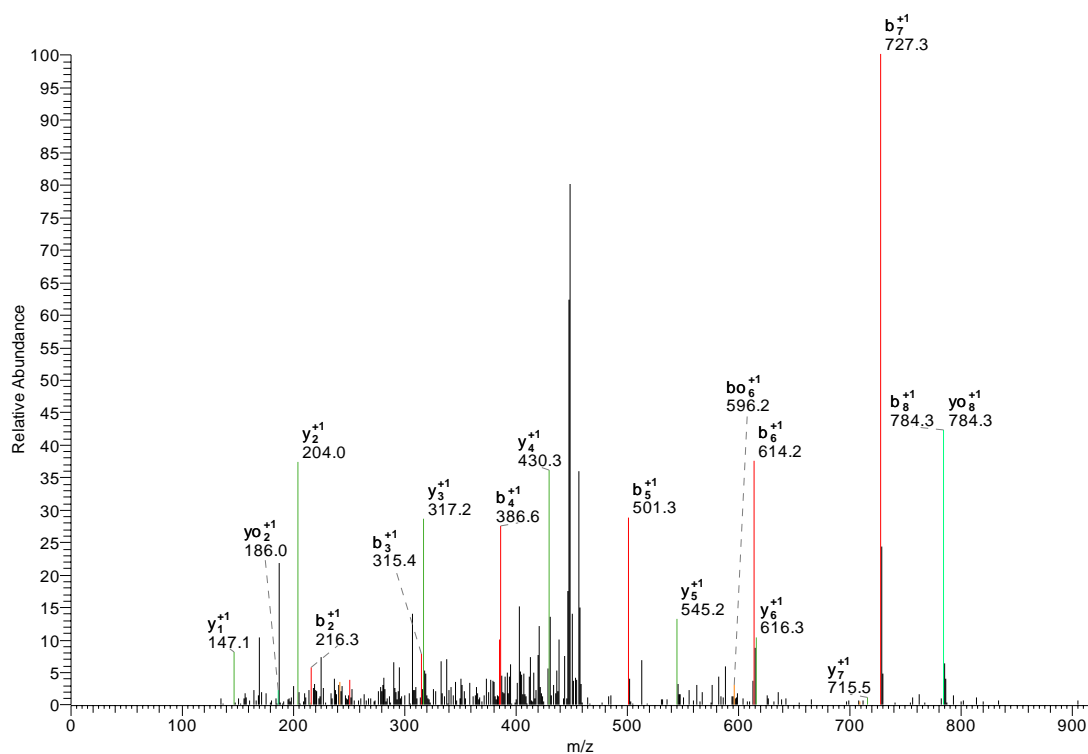


Fig 6.1.9 Fragmentation spectrum of the identified tryptic peptide KSVADILGQ of TMP14-like

6.2 Plastome expression analysis of *ppp1* mutants

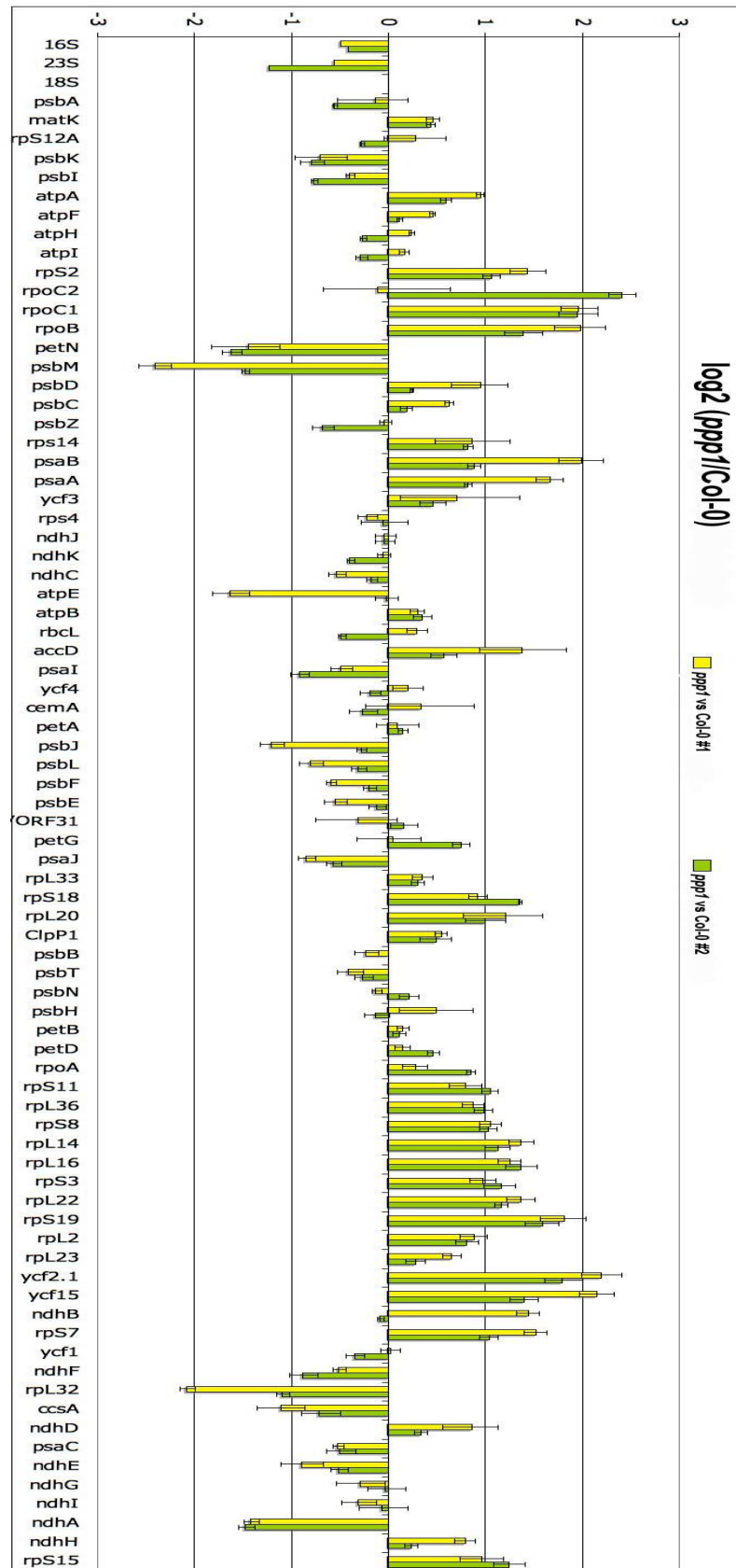


Fig 6.2.1 Plastome expression analysis by qRT-PCR

Carried out by Andreol Falcon De Longvialle (ARC Centre of Excellence, Perth, Australia) with RNA from *ppp1-1* and Col-0 plants grown in the greenhouse using gene specific primers. Two independent experiments were performed and are plotted. For each experiment three repetitions were made and error bars represent standard deviation.

Acknowledgements

First of all, I would like to thank Prof. Dr. Dario Leister for giving me the opportunity to carry out my Ph.D. research under his supervision.

Additionally, I would like to thank everyone, who contributed to the experimental outcome of this thesis: Dr. Bernd Müller and Youlia Davidova for performing the MS analyses, Prof. Dr. Peter Jahns for the pigment analyses, Agata Kazmierczak for the transcript end mappings, Sabine Raab and Dr. Peter Hoth for the germination assays, Prof. Dr. Christian Schmitz-Linneweber for trial RIP-Chip analyses and Dr. Andreol Falcon De Longevialle for plastome expression analyses.

Moreover I would like to thank Alexander Hertle, Dr. Elena Aseeva and Dr. Tatjana Kleine for critically reading and correcting my thesis.

I would like to express my gratefulness to the other members of the team, who were always willing to discuss experimental problems or novel hypotheses.

Last but not least, I would like to thank my family and friends, especially my parents and Alex for supporting and helping me throughout stressful times.

Curriculum vitae

PERSONAL DATA

Date of birth: 19.08.1978

Place of Birth: Kleve, NRW, Germany

Nationality: German

RESEARCH EXPERIENCES

October 2005 - now

Ludwig-Maximilians-Universität München

Department Biology I, Botany

- PhD continuation. Supervisor Prof. Dr. Dario Leister

July 2004 – September 2005

Max Planck Institut für Züchtungsforschung (Köln)

- PhD in “Characterization of three novel photosynthetic proteins in *Arabidopsis thaliana*”.

Supervisor Prof. Dr. Dario Leister

February 2004 - April 2004

School of Biological Sciences, University of Auckland (New Zealand)

- Technical Assistant

November 2002 – December 2003

School of Biological Sciences, University of Auckland (New Zealand)

- Diploma thesis “Epitope tagging of the flowering time gene *GIGANTEA*”

September 2001 - March 2002

Scion (formerly Forest Research Institute), Rotorua (New Zealand)

- Internship at the department of Molecular Biology

EDUCATION

2000 - 2004

Universität zu Köln

- Main diploma studies in Biology with graduation in March 2004 (Grade: 1.0)

1998 - 2000

Rheinische Friedrich-Wilhelms-Universität Bonn

-Pre-diploma studies in Biology (Grade: 1.0)

August 1995- February 1996

Eastlake High school, Redmond, Washington, USA

1989 - 1998

Konrad-Adenauer Gymnasium in Kleve

- Abitur (Grade: 2.6)

PUBLICATIONS

Noutsos, C., Kleine, T., Armbruster, U., DalCorso, G., and Leister, D. (2007). Nuclear insertions of organellar DNA can create novel patches of functional exon sequences. *Trends Genet* **23**, 597-601.

David, K.M., Armbruster, U., Tama, N., and Putterill, J. (2006). *Arabidopsis* GIGANTEA protein is post-transcriptionally regulated by light and dark. *FEBS Lett* **580**, 1193-1197.

POSTERS

Armbruster, U. and Leister, D.: PPP4: Identifizierung von photosynthetischen Proteinen mittels Expressionsanalysen. 21. Tagung Molekularbiologie der Pflanzen, Dabringhausen 2008

Armbruster, U. and Leister, D.: PPP4: A putative photosynthetic protein. 10th International Colloquium on Endocytobiology and Symbiosis 2007, Gmunden, Austria

Armbruster, U., David, K.M. and Putterill, J.: Epitope tagging of the *Arabidopsis* flowering time gene *GIGANTEA*. Queenstown Molecular Biology Meeting 2003 (New Zealand)

SCHOLARSHIPS and PRIZES

International Colloquium on Endocytobiology and Symbiosis 2007, Gmunden, Austria
- Poster prize

Queenstown Molecular Biology Meeting 2003, New Zealand
-Poster prize

2001-2004

- Scholarship of the „Studienstiftung des deutschen Volkes“, additionally financing internship and diploma thesis in New Zealand

LANGUAGES

German, mother tongue

English, fluent

French, basic

Ehrenwörtliche Versicherung

Hiermit versichere ich, dass ich die vorliegende Arbeit selbständig und nur unter Verwendung der angegebenen Hilfsmittel und Quellen angefertigt habe. Die Autorin hat zuvor nicht versucht, anderweitig eine Dissertation einzureichen oder sich einer Doktorprüfung zu unterziehen. Die Dissertation wurde keiner weiteren Prüfungskommission weder in Teilen noch als Ganzes vorgelegt.

München,

Mai 2008

Ute Armbruster